MICROMACHINING AND SURFACE BUILD-UP ON BOROSILICATE GLASS USING EXCIMER LASER

By

SURYA JILLUDIMUDI

Bachelor of Technology

JAWAHARLAL NEHRU TECHNOLOGICAL UNIVERSITY

Visakhapatnam, India 2002

Submitted to the Faculty of the
Graduate College of the
Oklahoma State University
in partial fulfillment of
the requirements for
the Degree of
MASTER OF SCIENCE
Dec, 2005

MICROMACHINING AND SURFACE BUILD-UP ON

BOROSILICATE GLASS USING EXCIMER LASER

Thesis Approved:

Dr. Ranga Komanduri

Thesis Advisor

Dr. Delahoussaye

Dr. H. B. Lu

Dr. A. Gordon Emslie

Dean of the Graduate College

SUMMARY

Micromachining is advancing rapidly for numerous nanotechnology applications. It is an enabling technology for the production of micro-electro-mechanical-systems (MEMS). Borosilicate glass, owing to its several desirable properties, such as electrical insulation, resistance to many chemicals, and transparency at certain wavelengths finds a number of applications in microsensor and microactuator technologies. The main feature this glass requires now is ability to be shaped for MEMS components to the required size and surface finish. Since conventional machining techniques result in microcracks in such brittle materials as borosilicate glasses, in this investigation, laser micromachining is used. Material build-up and material removal result when an excimer laser beam impinges a borosilicate glass surface. The material build up features are studied by systematic investigating various input parameters, such as input energy, size of the mask and the media used to obtain desirable shape and quality. Good material built up, in the order of 25 to 35nm was observed for 1mm mask when tests were conducted in air, distilled water and methanol. Surface machining (material removal) of borosilicate glass was conducted such that microcracks formed on the periphery of the machined surface were minimal. Micromachining of borosilicate glass was done in air, distilled water and polymer to asses the role of the media in minimizing crack formation. It is found that borosilicate glass results in lesser number of cracks when machining under a polymer compared to machining in air, and under water.

ACKNOWLEDGEMENTS

I would like to express my sincere appreciation to my advisor, Dr. Ranga Komanduri for his intelligent supervision, constructive guidance, financial support, inspiration, motivation and friendship. I would like to thank Dr. Delahoussaye and Dr. Hongbing Lu for being in my committee. I would also like to thank Ganesh, Choo, Sony and Kyoshi for their help and suggestions. I wish to extend my gratitude to Anand, Hari and Raju for their encouragement and friendship.

I wish to express my sincere thanks to my parents for their confidence in me. I would like to thank them for their encouragement at times of difficulty, love and understanding.

This project is funded by a grant from the National Science Foundation (EPS-9977830) through a subcontract from the University of Arkansas. The principal investigator at the University of Arkansas is Dr. Ajay Malshe.

Finally, I would like to thank the Department of Mechanical and Aerospace Engineering for providing me with the opportunity to pursue M.S. at Oklahoma State University.

TABLE OF CONTENTS

LIST OF FIGURES

LIST OF TABLES

CHAPTER 1

INTRODUCTION TO LASERS

1.1 Introduction

From the invention of the first working laser by Theodore Maiman in 1960 [1], significant progress took place in the form of inventions and industrial developments. Now lasers are available with more versatility than ever before, with their operation simplified and their applications multiplied to an innumerable extent. Since machining is the most dominant process for shaping materials in manufacturing industry, the application of laser on micromachining triggered an immediate rise in the manufacturing of micro and nano materials. Manufacturing industry now uses laser micromachining in many high-tech application areas for which microfabrication is an enabling technology. Thus, this chapter will give an introduction to lasers and the next two chapters discuss micromachining and laser material interactions.

1.2 Laser

The word laser, is an acronym for **L**ight **A**mplification by **S**timulated **E**mission of **R**adiation and is synonymous with the most significant feature of laser action. In other words, it is a device that uses a quantum mechanical effect, called, stimulated emission in order to generate a narrow, intense beam of coherent light with its wavelength ranging

from UV to infrared. The output of a laser may be a continuous or pulsed wave depending on the technique used.

1.3 History

The history of the laser dates back to the year 1916 when Albert Einstein [3] published "Sources of Quantum Mechanics" explaining spontaneous and stimulated emission. Although he did not invent the laser, his work laid the foundation for it. In 1951 Charles H. Townes [2], a physicist at Columbia University and his students built a MASER (**M**icrowave **A**mplification by the **S**timulated **E**mission of **R**adiation) using ammonia gas and microwave radiation by following Albert Einstein's theoretical prediction of the "stimulated emission" process. The word “laser” was coined in 1957 by Gordon Gould. The first working laser was a ruby laser built by Theodore H. Maiman [1] in 1960 at Hughes Research Laboratories in Malibu, CA. Maiman used a solid-state flash lamp-pumped synthetic ruby crystal to produce red laser beam at 694-nanometres wavelength. In the same year, an Iranian physicist, Ali Javan, invented the gas laser made of helium and neon and it generated a continuous beam of light at 1.15 μm wavelength. This was followed by the first continuous operation of an optically pumped solid-state laser, namely Nd: $CaWO_4$ laser at 1.06 μm wavelength. The first high power laser was a 10.6 μm wavelength carbon dioxide laser developed in 1964 by C.K.N. Patel of Bell Laboratories in Princeton, NJ. In the same year, J.F. Geusic and R.G. Smith of Bell Labs invented the first Nd: YAG (neodymium-doped yttrium aluminum garnet) laser. Thus with each passing year more powerful and more efficient lasers were being introduced.

1.4 Working Principle of Lasers

Lasers work on the central concept of converting electrical energy into a high energy density beam of light through stimulation and amplification. Atoms and molecules have determinate energetic levels, which can be low or high. The low energetic levels can be excited to higher levels by different techniques, such as heating. Once they reach the higher energetic superior levels, they go back to the original state and in return this energy is converted to photon energy.

Under normal conditions, the proportion of atoms at low energetic levels in a body is higher than that of the atoms that are found in higher levels. By this reason, any luminous beam that crosses a body loses energy since part of its photons are absorbed when crossing. Fig. 1.1 shows schematically the emission of light.

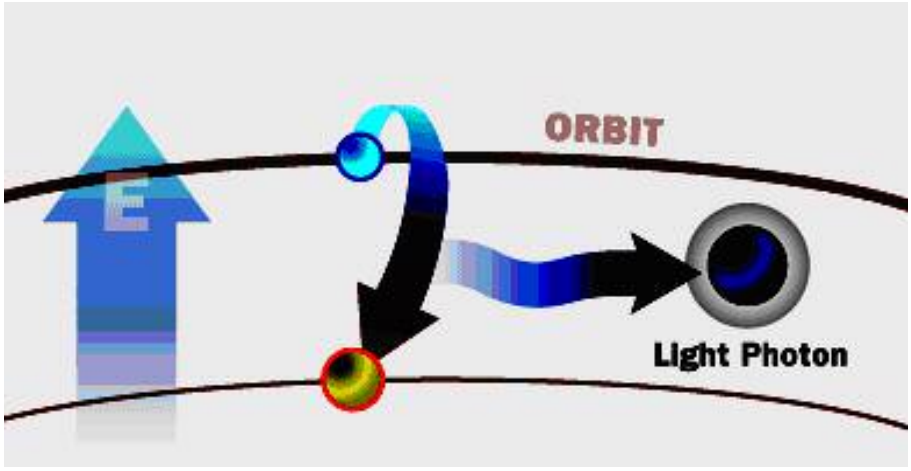

Fig. 1.1 Emission of light

In most cases the sources of ordinary light which comes from atoms and excited molecules and the light emission comes in various wavelengths (and frequencies). But, if

during the short instant, an atom is excited, that atom is influenced by light of a certain wavelength. This atom can be stimulated to launch radiation that is in phase with the wavelength that has stimulated it.

The increase of the new emission amplifies the wave. If the phenomenon can be multiplied, we arrive at a condition that where percentage of atoms with high energy levels will be significantly more than the percentage of atoms in the normal state. This phenomenon is known as population inversion. Then, the resulting beam is a coherent light beam and high-powered.

1.5 Types of Lasers

Lasers are of many different types. The laser medium can be a solid, gas, liquid or semiconductor. Lasers are commonly designated by the type of lasing material employed. All of these types of lasers are available in continuous or pulsed modes. Figure 1.2 shows different kinds of lasers available.

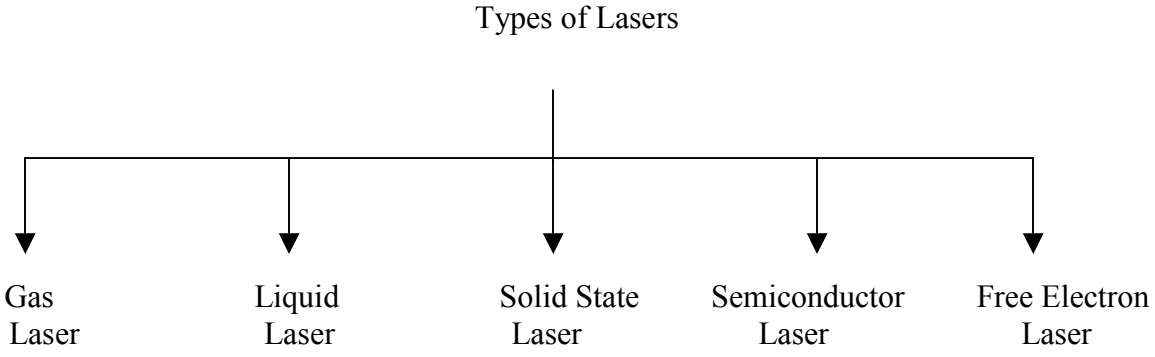

Fig. 1.2 Different types of lasers

1.5.1 Gas Laser:

A gas laser is a laser in which an electric current is discharged through a gas to produce light. They can be classified further depending on the compilation of the gas as neutral atom, ion, or molecular. Though neutral atoms and ions find many applications, molecular gas lasers are the lasers that have their uses in machining applications. These lasers can be further classified as: helium neon laser, argon or krypton laser and CO_2 laser. These will be briefly described in the following.

1. **Helium Neon Laser**

This laser is called a He-Ne laser and it is a small gas laser. Figure 1.3 is a schematic diagram of the helium-neon laser. The medium of the laser is a mixture of helium and neon gases, approximately in the ratio 5:1, contained at low pressure (300 Pa) in a glass envelope.

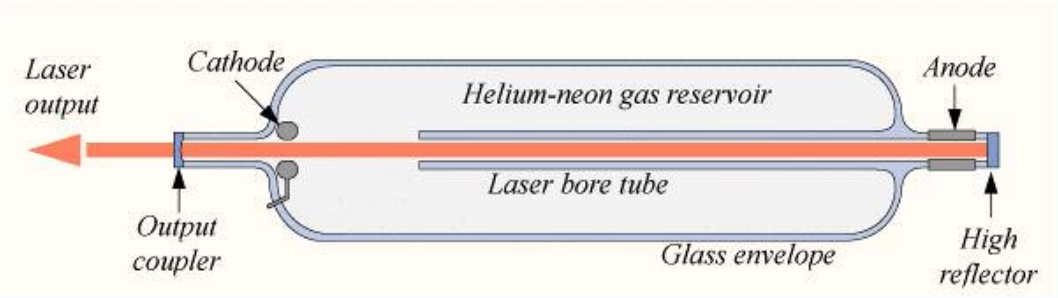

Fig. 1.3 Helium-Neon laser

The energy or pumping source of the laser is provided by an electrical discharge of ~ 1000 V through an anode and a cathode at each end of the glass tube. The cavity of the laser typically consists of a plane, high-reflecting mirror at one end of the laser tube

and a concave output coupler mirror of ~ 1% transmission at the other end. These lasers are typically small, with cavity lengths of ~ 15 cm and up to 0.5 m. The optical output power ranges from 1 to 100 mW. They have many industrial and scientific applications, and often used in laboratory demonstrations of optics. Its usual operational wavelength is 632.8 nm in the red portion of the visible spectrum.

2. Ion laser (Argon or Krypton)

An ion laser is a gas laser which uses an ionized gas as its lasing medium. Like other gas lasers, ion lasers feature a sealed cavity containing the lasing medium and mirrors forming a resonator. Unlike He-Ne lasers, the energy level transitions that contribute to lasing action come from ions. Because of the large amount of energy required to excite the ionic transitions used in ion lasers, the required current is much higher, and as a result all but the smallest ion lasers are water cooled. A small air cooled ion laser can produce, for example, 130 mW of laser beam with a tube current of 10 A. The two gases that are used in ion lasers are argon and krypton. Figure 1.4 shows the diagram of the ion laser.

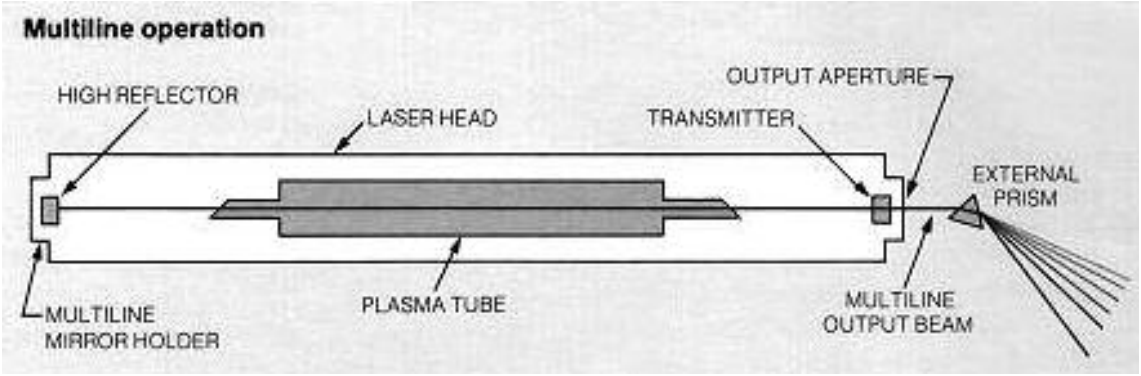

Fig. 1.4 Ion laser

3. Carbon Dioxide Laser

CO_2 lasers operate in the infrared region and require materials for their construction. The most basic form of a CO_2 laser consists of a gas discharge with a total reflector at one end, and an output coupler (usually a semi-reflective coated zinc selenide mirror) at the output end. The reflectivity of the output coupler is typically ~ 5-15%. The laser output may also be edge-coupled in higher power systems to reduce optical heating problems. The CO_2 laser can be constructed with powers ranging from milli watts (mW) to giga watts (GW).

1.5.2 Liquid Laser

The most common liquid laser media are inorganic dyes contained in glass vessels. They are pumped by intense flash lamps in the pulse mode or by a separate gas laser in the continuous wave mode. Some dye lasers are tunable, meaning that the color of the laser light they emit can be adjusted with the help of a prism located inside the laser cavity.

1.5.3 Solid State Laser

Solid-state lasers produce a laser beam by means of a solid medium. The most common solid laser media are rods of ruby crystals and neodymium-doped glasses and crystals. The ends of the rods are fashioned into two parallel surfaces coated with a highly reflecting nonmetallic film. Solid-state lasers offer the highest power output. They are usually pulsed to generate a very brief burst of laser beam. Bursts as short as 12×10^{-15} sec have been achieved. These short bursts are useful for studying

physical phenomena of very brief duration. One method of exciting the atoms in a laser is to illuminate the solid laser material with higher-energy beam than the laser produces. This procedure, called pumping, is achieved with brilliant strobe light from xenon flash tubes, arc lamps, or metal-vapor lamps. Figure 1.5 shows a Neodymium -YAG solid state laser.

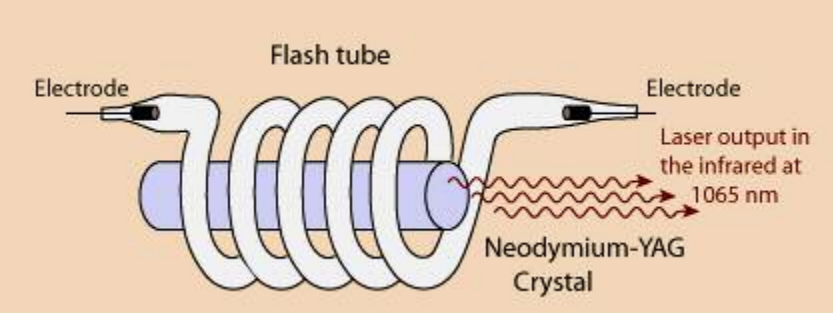

Fig. 1.5 Solid state laser

1.5.4 Semiconductor Laser

Semiconductor lasers are the most compact lasers. Gallium arsenide is the most common semiconductor used with applications involving rectifiers and transistors. A typical semiconductor laser consists of a junction between two flat layers of gallium arsenide. One layer is treated with an impurity atom providing an extra electron and the other with an impurity atom one electron short. Semiconductor lasers are pumped by the direct application of electric current across the junction. They can be operated in the continuous wave mode with better than 50 % efficiency. Only a small percentage of the energy is used for excitation.

Scientists have developed extremely tiny semiconductor lasers, called quantum-dot vertical-cavity surface-emitting lasers. These lasers are so tiny that more than a million of them can fit on a chip, which is the size of a fingernail. Common uses for semiconductor lasers include compact disc (CD) players and laser printers. Semiconductor lasers also form the heart of fiber-optics communication systems.

1.5.5 Free Electron Lasers

Free electron lasers employ an array of magnets to excite free electrons (electrons not bound to atoms). They are first developed in 1977, and are becoming an important research tools. Free electron lasers are tunable over a broad range of energies than dye lasers. The devices become more difficult to operate at higher energies but generally work successfully from infrared through ultraviolet wavelengths. Theoretically, electron lasers can function even in the X-ray range. Figure 1.6 is a schematic showing a free electron laser.

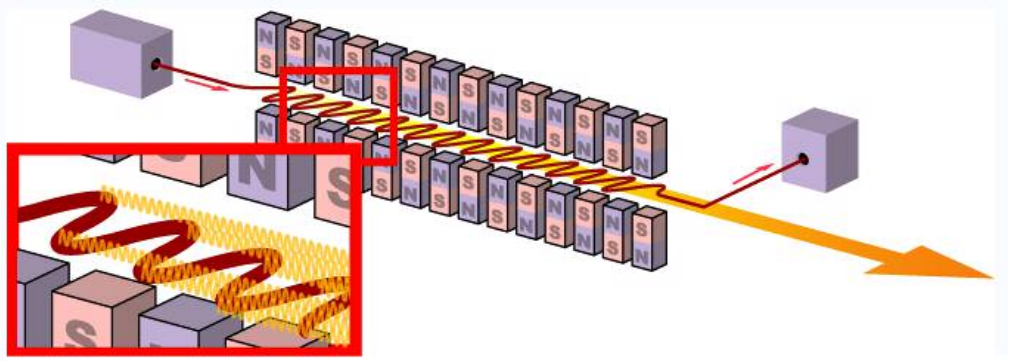

Fig.1.6 Free electron laser

It has been reported that free electron laser facility in the University of California at Santa Barbara uses an intense far-infrared light to investigate mutations in DNA

molecules and to study the properties of semiconductor materials. Free electron lasers should also eventually become capable of producing very high-power radiation that is currently too expensive to produce. At high power, near-infrared beams from a free electron laser can defend against a missile attack.

1.6 Classification of lasers

The principle mechanism for laser injury is thermal. As a result, there is a threshold for the amount of thermal energy transferred to the exposed tissue below which there will be no injury. Based on this lasers are classified into four major types. All lasers are labeled and should be in one of the following four designations:

Class I (depends on wavelength)

Any laser or laser system which has a nominal power output ≤ 0.5 mW is a Class I laser. There is no hazard using this class of lasers.

Class II (≤ 1 mW average power and if applicable, a pulse duration of < 0.25 secs)

These are low power lasers emitting in the visible wavelengths (0.4 to 0.7 μm). They could result in exposure, if intentionally viewed for more than 0.25 secs. An example of a Class II laser is a He-Ne pointer laser of 1 mW or less.

Class IIIa

These lasers emit light in the visible wavelengths (0.4 to 0.7 μm) and are not intended for prolonged viewing. Most pen like pointing lasers are in this class. They are hazardous only for intra beam viewing.

Class IIIb (excess of IIIa power levels but typically ≤ 0.5 W average power)

The hazard for class IIIb lasers is potentially greater than that for IIIa. The hazard, however is still limited to direct viewing of the laser beam. These are lasers with output ≤ 0.5 Watt. These lasers do not produce hazardous diffuse reflections or represent a skin exposure hazard.

Class IV (≥ 0.5 W)

These are high powered lasers that represent hazards (eye damage, skin injury, and or potential flammable material ignition source) for direct viewing, viewing of diffuse reflections, and skin exposure. The power levels for Class IV lasers are ≥ 0.5 W.

1.7 Characteristics of a laser beam

1. Coherence. Different parts of the laser beam are related to each other in phase. This phase relationship is maintained over long enough time that interference effects may be seen or recorded photographically. This coherence property is what makes holograms possible.

2. Monochromatism. Laser light consists of essentially one wavelength having its origin in stimulated emission from one set of atomic energy levels.

3. Collimator. Because of bouncing back between mirrored ends of a laser cavity, those paths which sustain amplification must pass between the mirrors many times and be very nearly perpendicular to the mirrors. As a result, laser beams are very narrow and do not spread very much.

CHAPTER 2

EXCIMER LASER AND MICROMACHINING

2.1 Excimer laser

An excimer laser is a form of ultraviolet chemical laser which found applications in eye surgery and semiconductor manufacturing. This laser emits very concentrated beam of light in the ultraviolet (UV) region of the spectrum. The term *excimer* is short for excited dimer, and refers to the chemical gain medium of the laser.

The first excimer laser was invented in 1971 by Nikolai Basov, V. A. Danilychev and Yu. M. Popov, at the P. N. Lebedev Physical Institute in Moscow. They used a xenon dimer (Xe_2) excited by an electron beam to give stimulated emission at 172 nm wavelength. A later improvement was the use of noble gas halides (originally XeBr), invented in 1975 by George Hart and Stuart Searles of the Naval Research Laboratory.

Laser action in an excimer molecule occurs because it has a bound (associative) excited state and a repulsive (disassociate) ground state. This is because noble gases such as xenon and krypton are highly inert and do not usually form chemical compounds. However, when in an excited state (induced by an electrical discharge), they can form temporarily-bound molecules with themselves or with halides (complexes), such as fluorine and chlorine. The excited compound can give up its excess energy by undergoing

spontaneous or stimulated emission, resulting in a strongly-repulsive ground state molecule which very quickly (on the order of a picosecond) disassociates back into two unbound atoms. This forms a population inversion between the two states.

Excimer lasers are usually operated with a pulse rate of ~ 100 Hz and pulse duration of ~ 10 ns, although some operate as high as 200 Hz and 30 ns. Their high-power ultraviolet output makes them useful for surgery (particularly eye surgery), for lithography for semiconductor manufacturing, and for dermatological treatment. They are quite large and bulky devices, which is a disadvantage in their medical applications, although their size is rapidly decreasing with ongoing developments. Table 2.1 gives different kinds of excimer laser with their wavelengths.

Table 2.1 Different kinds of excimer lasers and wavelengths

Excimer	F_2	ArF	KrF	XeBr	XeCl
Wave length	157	193	248	282	308

The Excimer laser is a cool laser, which means that it does not heat up the surrounding air or surfaces. Instead, a very tightly-focused beam of ultraviolet light is emitted. The ultraviolet light is absorbed by the upper layer of the surface that it contacts. The sheer amount of ultraviolet light is too much for most organic materials (such as the cornea of the eye) to absorb, resulting in the breakdown of the molecular bonds of the material.

2.2 Laser Micromachining

Laser machining is a material removing process that is achieved through interactions between the laser and the target material. Laser machining is different processes grouped into one; those being one, two and three dimensional laser machining, which are, drilling, cutting, and shaping respectively. Additionally, laser machining includes the subcategories of laser grooving, marking and scribing. It is accomplished by transporting photon energy from the laser into the target material in the form of thermal or photochemical energy to remove material by melting and blow away, or by direct vaporization and ablation. Regular machining processes, conversely, rely on mechanical stresses on the target material inputted by the cutting element to break the chemical bonds of the material. This is the major difference between laser machining and conventional machining.

When this machining is considered at micrometer level it becomes micromachining. The continuing trend towards miniaturization and the use of advanced materials in medical devices has increased the need for new micromachining technologies. Laser is able to play a major role in micromachining industry because of the development of systems with smaller wavelengths and shorter pulses, with smaller spot sizes and reduced heat input. Machining with excimer laser results in the absence of thermal damage, thus enabling the living tissue to heal with no scarring. Because of this ability excimer lasers found major applications in medical devices especially in eye surgery. Figure 2.1 is a photograph of an excimer laser used in eye surgeries.

Fig. 2.1 VISX Star S4 excimer laser used in eye surgery

Apart from the applications in medical devices, laser micromachining has applications in the manufacturing of micro orifices, micro features and micro structures, down to 5 μm in size, in metals, polymers, glasses, and crystalline materials. With more efficient and powerful lasers lining up in the market their applications are increasing very rapidly. Figure 2.2 is a photograph of excimer laser used in micromachining.

Fig. 2.2 Excimer laser used in micromachining

CHAPTER 3

LASER - MATERIAL INTERACTIONS

3.1 Introduction

Excimer laser ablation is an effective method for machining polymeric materials in biomedical devices. Application of this technique, however, requires knowledge of laser-material interactions. Process viability is strongly influenced by such ablation characteristics as the removal rate and the presence of thermally affected zones surrounding an ablated area. Furthermore, the selection of laser parameters can significantly influence debris generation and the extent of downstream cleaning which is needed. This creates a need for the study of this phenomenon. For more than 25 years, the interaction of materials with intense laser beams has been a topic of great interest. The improvement of industrial excimers has contributed much to the evolution of these processes. These lasers operate at repetition rates and pulse energies which have made the use of ablation economically competitive, particularly for the ablation of organic polymers.

3.2 Material Interaction

A laser beam striking a material can be reflected, transmitted, or absorbed. In practice, all three occur to some degree. In order for laser machining to be practical, the laser beam must be absorbed by the material. Reflected and transmitted light are lost

during processing. So only absorbed light is able to do the work of material removal. Figure 3.1 is a schematic showing different kinds of laser beam incident on glass.

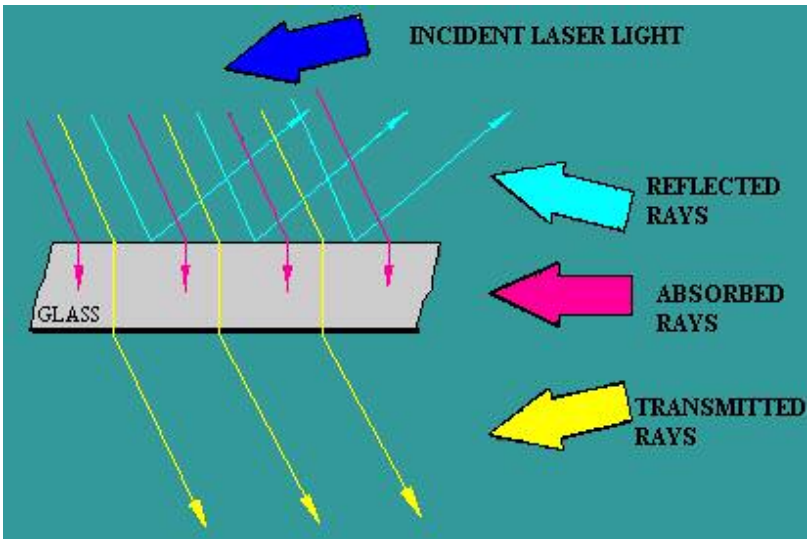

Fig. 3.1 Different kinds of light

At the interaction region where the radiation strikes the surface, the roughness and conductivity of the material will determine what fraction of the power is reflected and transmitted into the material. The transmitted portion of the power will then be absorbed within a certain depth of the surface determined by the conductivity of the material. As the material is heated by the absorbed portion of the transmitted radiation, absorbed gases, material vapor, and sputtered material can be ejected from the surface into the oncoming beam. This causes further interaction where coupling of the beam into the material is affected by scattering off the ejected material or by shielding of radiation from the surface with a plasma plume, which is created by the beam in the ejected vapor. In addition to creating emission of the material from the surface, the absorbed energy may also create thermal, mechanical, and phase changes which propagate into the material.

This entire process depends on “ablation threshold energy”. It can be defined as the minimum energy required for the ablation process to take place. Figure 3.2 shows a "typical" ablation curve for a pulsed excimer laser.

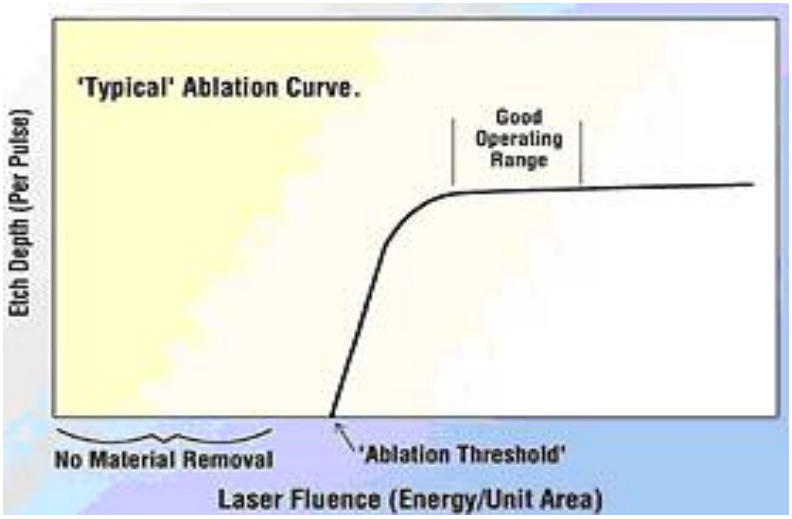

Fig. 3.2 Ablation threshold curve

At energy densities below the "ablation threshold" no material removal occurs. In this case, the energy from absorbed photons is converted into thermal energy and the part heats up but no material removal occurs. At energy densities above the ablation threshold, material removal occurs, and the etch depth per pulse increases asymptotically until it reaches the plateau where further increase of the energy density does not greatly affect the material removal rate. Typically, lasers are best utilized in the range marked as a "good processing range," where the flatness of the curve keeps power density constant over a fairly large dynamic range and the photons are used most effectively in this range. Figure 3.3 shows the material removal rates by XeCl Excimer laser [4] for different polymers.

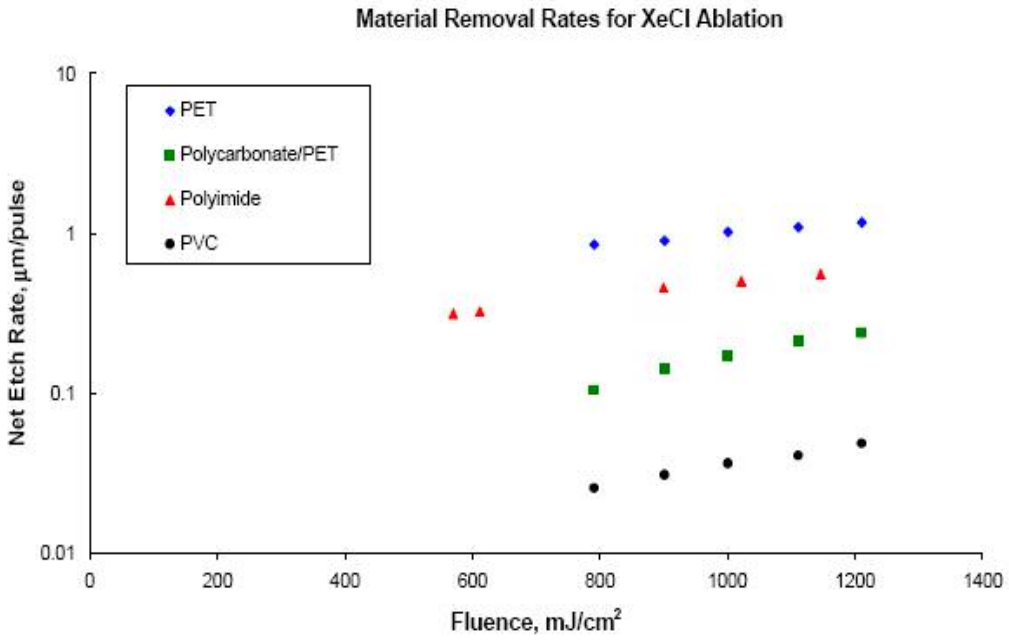

Fig. 3.3 Material removal rates for different polymers [4]

The most important factor affecting good material processing is the wavelength of the laser beam used. Different materials absorb light at different parts of the electromagnetic spectrum. The first thing that must be done is to choose the correct laser wavelength so that absorption of the photons can occur. On a molecular level, infrared photons, like those emitted from a CO_2 or Nd:YAG laser, interact with materials by influencing the way the molecules vibrate internally. The infrared photon energies are matched very closely to quantized vibrational energy levels. Ultraviolet photons on the other hand have a much shorter wavelength and therefore higher photon energy.

These UV photons can interact with the electronic bonds directly and therefore the material removal mechanism is not a first-order thermal one. It is also important to note that when a material has a very high absorption, the penetration depth and, therefore,

the interaction volume is generally small, slowing the material removal process. The result is that, unless secondary thermal effects are observed, much cleaner and more precise processing can be done with shorter wavelength light, but at the expense of speed.

Lim *et al*. [7] investigated the cause for turbulence, oscillations in the substrate and multi stable biological systems during laser-material interaction and predicted the optimal laser machining control parameters. A one dimensional heat transfer model was used and the condition for the beginning of non-linear motion was verified by the variations in the cutting rates. The cutting rates were predicted using the isoclines approach and it was found that experimental results agree very well with the actual cutting rates.

Another important consideration is the taper associated with laser-machined features. In general, the entry side of the hole will be slightly larger than the exit side (or hole bottom for a blind hole). Normally the exit hole is specified as the hole diameter in laser processing. The taper is usually on the order of 5 to 10º, and increases as the aspect ratio (hole depth to hole diameter) increases. For instance, while it is possible to drill a 1μm exit hole in some materials, the entrance hole would be much larger. Still, when considering some competitive technologies, such as etching, even a 2:1 aspect ratio is better than can be obtained with the best chemical etchants, and 10:1 is unthinkable. For lasers, 10:1 is routine and up to 100:1 can be realized. Taper is caused by several factors including diffraction, reflection off of the hole walls, and absorption of incoming photons by the escaping plasma.

Secondary, thermal effects also play an important role in the final results of laser processing. The process of using UV light to process a plastic like polyamide is discussed below. Though there is a very high absorption coefficient, much of the photon energy gets converted to heat. These secondary thermal processes may cause undesirable effects on the part, such as charring, burning, delaminating, or marking. This is especially true as the pulse length of the laser increases or as the repetition rate of the laser gets higher as there is not sufficient recovery time for the material ejected on the previous pulse to escape. New studies with very short pulse length lasers, on the order of a few hundred femtoseconds show extremely clean processing results in almost all materials. Unfortunately, these very short pulse lasers are presently confined to research laboratories in view of their high cost.

In the case of laser drilling, the materials used are copper and some type of dielectric. Copper is more than 99.9% reflective of CO_2 laser beam at 10μm wavelength. Therefore, copper drilling in general must be done at a different wavelength. Normally the tripled YAG laser at 355 nm wavelength is chosen for copper drilling. There is a technique by which an absorptive coating is applied to copper to stimulate absorption of the CO_2 photons, thereby, thermally overloading copper and allowing holes to be "drilled." However, this material removal process is a second-order mechanism and not a true interaction of the copper with photons.

The 355 nm YAG laser is also perfectly capable of drilling dielectrics, but the removal rate, while potentially cleaner than using a CO_2 laser, is much slower. For this reason several companies are offering a dual-laser system as a product to take advantage

of the selectivity and positive aspects of both lasers. The dual laser approach can end up an accepted method for the production of most micro devices at least until such time as the CO_2 laser can no longer be used to drill the dielectric because the holes are too small. This will occur when the sizes of the holes are 50 μm or less.

3.3 Heat Affected Zone (HAZ)

During laser cutting of steel considerable amount of energy is conducted through the workpiece and this results in change in the material properties and the microstructure of steel. This also results in a narrow zone of material adjacent to the laser cut, which experiences changes in material properties. For example, in stainless steel 304, the changes occur either as grain refinement, or as precipitation of carbides (which are harmful for corrosion resistance properties of the steel) and other impurities, such as sulfides and phosphides. This entire region, which differs from the base material in properties, can be defined as the heat affected zone (HAZ). Figure 3.4 is an illustration showing the heat affected zone by a pulsed laser beam.

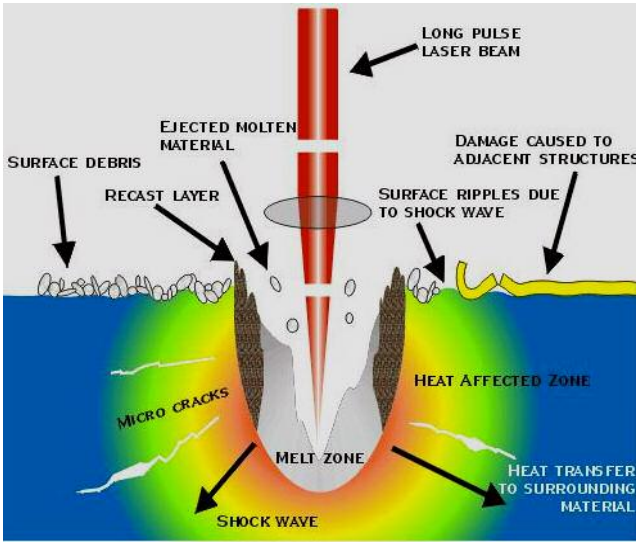

Fig. 3.4 Heat affected zone by a pulsed laser beam

To determine the extent of this heat affected zone, two parameters are important. The first is the maximum temperature any particular point reaches in the material and the second is the rate of heating or cooling of the material. Both these parameters depend on the laser cutting parameters, namely, the laser power and the laser cutting speed. The higher the cutting speed, the smaller is the thickness of the heat-affected zone.

CHAPTER 4

LITERATURE REVIEW

4.1 Introduction

Prior to the invention of excimer lasers, the field of micro electro mechanical systems (MEMS) was extremely narrow. Excimer laser with its ability to micromachine suddenly triggered the development of MEMS. It turned out to be of immense value where mechanical methods are not adequate or the etching-based methods too slow. A further advantage of excimer laser micromachining is its remarkable ability to cause little or no apparent thermal damage to the surrounding unirradiated portions of the material. It is this inbuilt feature that enabled it to machine a wider range of materials, such as glass, polymers, silicon and ceramics. Prior to laser micromachining, borosilicate glass had very limited use in micromachining industry. With the developments in laser micromachining and its ability to machine materials inspite of their brittleness with little or no residual stresses resulted in a sudden escalation in borosilicate glass applications.

Machining with a laser beam is quite different from other machining techniques in that the effectiveness of the process depends on many material properties, some of which the user has no control over then. The workpiece surface and subsurface characteristics depend on how well the incident beam is absorbed and what type of thermal and

photochemical effect there may be. Thus excimer laser machining is divided into two broad categories, ablation (material removal) and polymerization (material build-up).

When a laser beam interacts with metals, the photons will "couple" with the free electrons. The efficiency of how well the photonic energy can be transferred to vibrational energy is a measure of this coupling. As the electrons are excited, they will collide with the crystal lattice of the metal thus raising the temperature. If the temperature is high enough, melting or vaporization will occur. If the coupling is low, the metal is said to be reflective and the temperature will not be raised significantly for material removal to take place.

This effect is somewhat different in polymers than in metals. Ultraviolet light will excite bound electrons. If there is sufficient energy, some bonds will break however, some energy will also be converted to molecular vibration and heat. Since this is a lower percentage than in metals, it is said that ultraviolet produces a cooler excitation in polymers. Infrared, on the other hand, causes mostly molecular vibration and material change comes about by mostly thermal processes. Whereby coupling efficiency in metals is quantified by lack of reflectivity, in polymers, it is quantified by lack of transmission (absorption).

Clean ablative etching can also be achieved using pulsed laser sources at wavelengths other than ultraviolet. Provided photons are absorbed strongly to submicro meter depths in timescales less than the time it takes for the heat to diffuse away from the irradiated region, then pulsed lasers, such as copper vapor laser (CVL), CO_2 and Nd and its harmonics can be effective for ablative micromachining. Thus, for a particular

micromachining application the choice of laser is now judged by such criteria as process speed, part throughput, reliability, service intervals, capital, and operating costs of the overall machine tool rather than solely by the quality of the processed part.

Dyer *et al*. [5] investigated etching techniques using 308 nm and 248 nm excimer laser as a means of micromachining thin, free-standing polymer films. The technique is interesting because it allows potentially disruptive mechanisms, such as ablation pressure, melting, and stress relaxation. Dyer *et al*. [5] observed that by carefully controlling the operating parameters, such as wavelength and fluence, high quality grid patterns can be produced on free standing polymer films with a thickness down to 1.5μm.

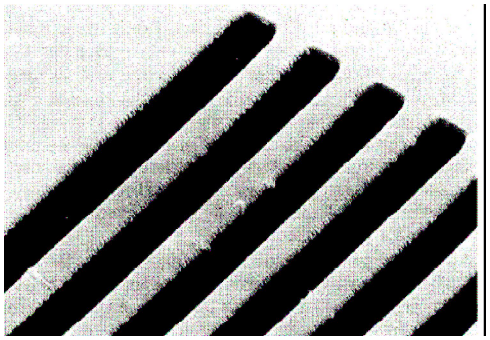

Fig. 4.1 Polymer film etched to 1.5 μm [5]

Fujii *et al*, [12] developed a newly structured microdiaphragm which has a pressure inlet port bored perpendicularly from the reverse surface of the silicon wafer. A XeCl excimer laser with a wavelength of 308 nm, a pulse period of 50 ns and a pulse frequency of 100 Hz has been used for this purpose. When this laser irradiated the silicon substrate, it instantly evaporated, allowing highly preferential machining to occur, since the laser affected only the surface layer. Holes were bored to varying sizes of 20 x 20, 30

x 30 and 40 x 40 μm^2 under laser irradiation energy densities of 10, 14, and 24 J/cm^2. When the relationship between the number of excimer laser pulse shots and the hole depth are determined, they observed that boring speed is almost unchanged irrespective of large changes in irradiation energy density ranging from 10 to 24 J/cm^2. This demonstrated that boring can be controlled by the number of laser shots despite slight variations in laser power.

Lutz *et al.* [6] investigated the possibilities of micromachining ceramic materials using a XeCl excimer laser with a wavelength of 308 nm. The influence of the optical setup and laser parameters on the processing quality has been determined as well as the behavior of various ceramic materials during the machining process. The machining results and the structural quality are discussed concerning the shape of the holes, break outs in the structure and homogeneity in the hole, depth, and size. They observed that a structure size of 25 x 75 μm^2 at 300 µm can be reached. They also found that deposits, which caused the shallow areas, can be reduced resulting in the improvement of the surface.

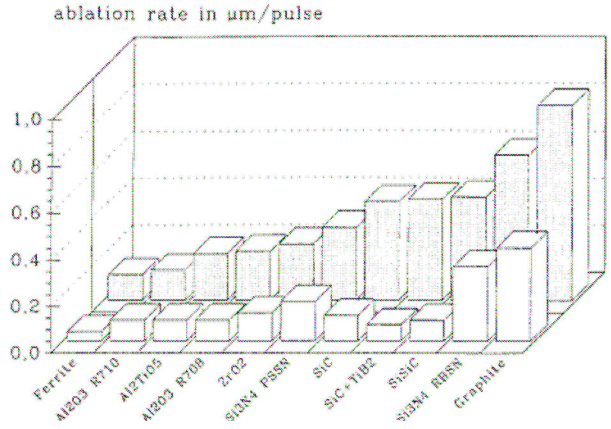

Fig. 4.2 Ablation rates for different ceramic materials [6]

Choo *et al.* [35] conducted micromachining of silicon in air and water using a short pulse excimer laser that generates energy in the range of 100-480 mJ. The excimer laser used is KrF (248 nm). They conducted drilling tests and characterized using conventional optical and scanning electron microscope. They observed that once the laser fluence exceeds a certain threshold value (1.7 J/cm^2), the ablation depth was found to increase rapidly with respect to the laser fluence of pulses. They also found that the ablation depth depends on the number of pulses, increasing with increasing number of pulses.

Seddon *et al.* [8] presented a method for the fabrication of carbon ink micro electrodes in a composite membrane or a thin laminate arrangement. It utilizes UV excimer laser photo ablation of nanosecond pulse duration at a wavelength of 248 nm to generate the required microhole in 12 μm PET film. They observed that at laser fluences of the order of 1.0 $mJcm^{-2}$, film ablation rates were controlled to 0.4 μm per pulse without thermal deformation of the micro-hole.

Lutz *et al.* [9] carried out experiments using a 50 W CO_2 laser and a 308 nm XeCl excimer laser to study the topography and the surface modification of glass. They used a beam cross section of 45 x 55 mm^2 and a pulse length of 50 ns. They found that lower temperatures were present for glasses of smaller absorption coefficients. They observed that a maximum of 150°C was reached for 2000 pulses and ablation starts once the threshold value of the energy density is reached. They observed that for borosilicate and vitreous glasses, material is removed from the rear of the sample. Figure 4.3 shows the

relationship between the energy density and the removal rate per pulse. It shows that glasses with higher absorption coefficients have lower ablation rates.

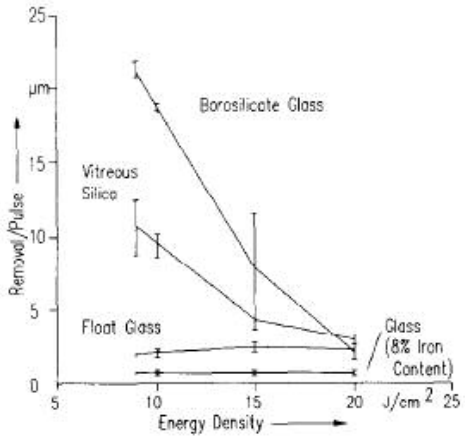

Fig. 4.3 Energy density and removal rate per pulse [9]

Lutz *et al.* [9] developed mathematical models to simulate laser treatment of fused silica and soda lime glass. They used a 308 nm XeCl excimer laser to investigate melting, softening and ablation effects of the glasses. They found that XeCl laser ablation takes place from 2000 laser pulses due to better coupling of the laser beam energy to the modified surfaces by reduced bond energy or surface roughness. They found that fused silica reacts differently due to its optical properties when irradiated at various wavelengths. At 10.6 μm, the glass heats up rapidly due to strong absorption. Holes of ~ 100 μm in diameter were produced by the evaporation of the material. Surface reactions are negligible because of its high transmission rate. High ablation rates of ~ 10μm/pulse were obtained above the ablation threshold of 7 J/cm^2 and results in roughened surfaces.

Soda lime silicate glass absorbs strongly at all wavelengths due to high iron-oxide content. At both 10.6 μm and 1.06 μm, it is possible to drill holes into glass. At lower

frequencies, holes with roughly parallel sides are drilled and the removed liquid material solidifies right at the edge of the hole. The ablation threshold for 308 nm irradiation lies at 3 J/cm^2. Due to small interaction depth, cracks are observed only in the solidified thin molten layers.

Zimmer *et al.* [10] investigated new machining techniques for the fabrication of 3D structures with analogous topology by excimer laser ablation. Polymers are used because of their low ablation threshold, smooth etching behavior, and ablation rates of tenths of micrometers per pulse at very modest energy fluences. They found that the energy density distribution and the displacement of the substrate between subsequent laser pulses have an important influence on the accuracy of the surface topology and the roughness. Therefore, they improved the mask design of the gray scale mask technique to achieve adequate structures. With these techniques micro-spherical and cylinder lenses and lens arrays were fabricated with lateral dimensions in the range from 10 µm to some millimeter and a large structure depth. Figure 4.4 shows an atomic force microscope image of a micro lens array.

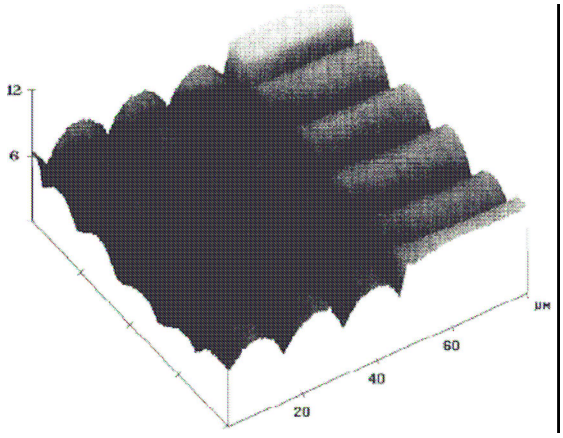

Fig. 4.4 AFM image of micro lens array machined in polyamide [10]

Ihlemann [11] investigated the ablation process of fused silica using a standard nanosecond excimer laser pulses at 193, 248 and 308 nm and 500 femtosecond pulses at 248 nm. He found that using nanosecond pulses, ablation appears like a controlled continuous surface damage process whereas with femtosecond pulses volume absorption causes ablation. Nanosecond treatment of polished samples at 248 and 308 nm exhibits two phase ablation consisting of a surface modifying smooth etching at low rate and etching at high rate producing more rugged structures. At 193 nm, the rear side of the sample can be ablated cleanly without alteration of the front side and also drilling of the deep channels is possible.

Ihlemann *et al.* [14] investigated the photo ablation behavior of glasses and ceramic oxides. An ArF excimer laser, wavelength of 193 nm and KrF excimer laser have been used to test the ablation rates of fused silica for nanosecond pulses and sub-picoseconds pulses. They found that in case of fused silica for nanosecond pulses two ablation phases are observed. Ablation starts at a low rate and after 20 to 40 pulses ablation continues at a rather high rate of 2 μm/pulse. This ablation continues even at 5 J/cm^2 even though the fluence is far below the threshold of the untreated surface. They found that the property of optical avalanche breakdown which could be supported by surface defects is much lower for sub-picoseconds pulses.

In the case of ablation rates for fused silica and borosilicate glass at 193 nm, Ihlemann *et al.* [14] found, for fused silica, ablation occurs at the rear side of a thin

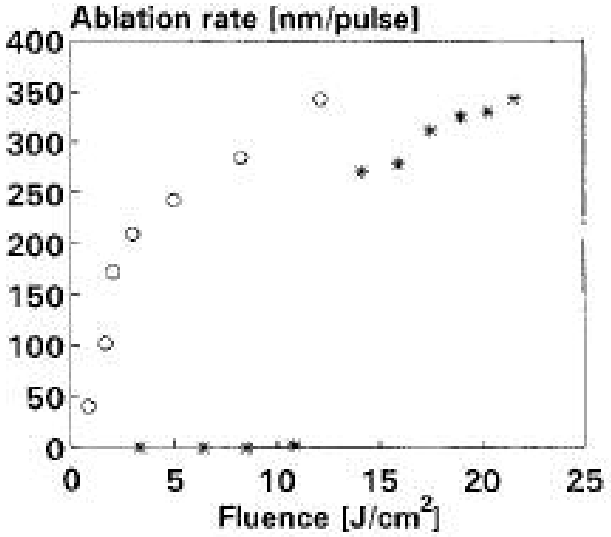

Fig. 4.5 (a) Ablation rates of fused silica at 248 nm for different pulse durations.* - 24 ns; 0- 0.5 ps [14]

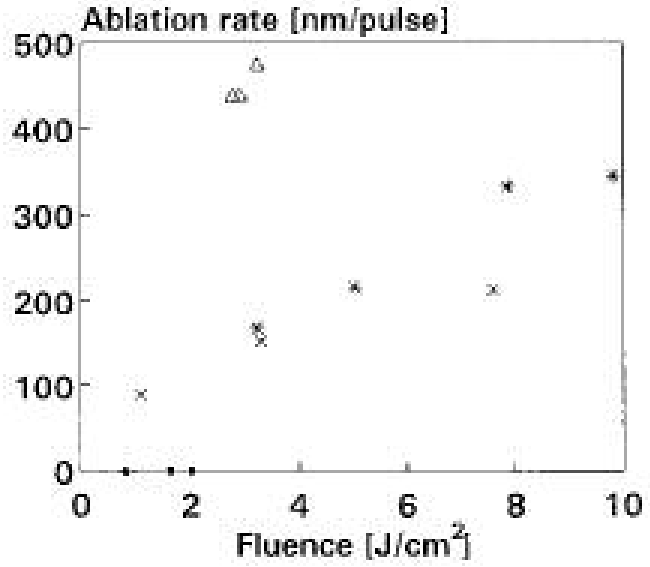

Fig. 4.5 (b) Ablation rates of fused silica at 193 nm, 18ns. * - fused silica (front side); Δ - fused silica (rear side); × - borosilicate glass [14]

sample (1mm). This indicates that at 193 nm optical breakdown effects play an important role due to the interference of incoming and reflected waves. The electric field strength is higher at the rear side of a weakly absorbing slab so that the break down threshold is

lower at the rear side. The absorptivity even of highly transparent materials like fused silica is sufficient to achieve clean ablation with nanosecond pulses. By testing for different wavelengths, Ihlemann *et al.* [14] concluded that for all practical micromachining purposes the ArF excimer laser is most suitable. Figures 4.5 (a) and (b) show ablation rates for fused silica at different wavelengths for pulse durations of 24 ns and 0.5 ps.

Tseng *et al.* [15] developed an excimer laser micromachining system to study ablation of high aspect ratio microstructures by examining the ablation efficiency, specifically, the impact of changing major laser operating parameters. Primary materials for their study were glasses. They observed that in ablating grooved structures, the ablation depth has been observed to be linearly proportional to the operating parameters, such as the pulse number and the fluence. The results from these experiments indicate that ablation at low fluence and high repetition rates tend to form a V shaped cross section or profile, while a U shaped profile is obtained at high fluence and low repetition rate. The experiments show that increasing the repetition rate favors the morphology of ablated surfaces, though the effect of repetition rate on ablation depth is insignificant.

Zimmer *et al.* [17] studied etching of solid surfaces at the interface with liquids as a new promising method for micromachining of transparent materials. A XeF excimer laser was used for different types of glasses to study the etch rates of these materials. They found that etch rates of the materials investigated increase almost linear at low laser fluences. They determined low threshold fluences (0.5 J/cm^2) and etch rates 6 to 10 nm per pulse for glass. They found that the etch rate and the threshold fluence depends also

on the liquid used, consisting of a solvent (acetone, toluene) and a certain concentration of dissolved pyrene, but only little on the glass type. Extremely smooth surfaces are achieved because of the low etch rate. When surface roughness is measured Pyrex glass has high surface roughness and is dominated by pits of micrometer dimensions. Best results are obtained on Corning 7059 with the roughness of the etched glass surface of 4 nm at an etch depth of 3.7 μm. When compared to the etch rate of fused silica at a wavelengths of 248 and 351 nm, the used solution influences both the etch threshold and the etch rate. These results indicate that this technique may be suitable for future precision micromachining applications.

In excimer laser ablation of glass fiber reinforced polymer, Yue *et al*. [33] found that fibers act as refocusing lens and cause partial fiber removal. They developed an analysis to calculate the laser intensity within the fiber and concluded that fibers were sticking out of the hole and thus providing a shielding effect to the material underneath. This is due to insufficient intensity of the laser beam to ablate the glass fibers.

Ben-Yakar *et al*. [32] studied the morphology of borosilicate glass surface machined by femtosecond laser pulses. They found a thin rim formed around the ablated craters after a single laser pulse. They also found that craters overlap and produce surface roughness when multiple laser pulses are overlapped. They concluded that rim appears to be a resolidified splash from a molten layer during the ablation process.

Ben-Yakar *et al*. [31] studied femtosecond laser (200 fs duration at 700 nm wavelength) ablation properties of borosilicate glass using atomic force microscopy. They showed that both single-shot and multi-shot ablation threshold fluence can be

determined by studying the diameter and depth of single shot ablated craters. They found a linear relationship between square of the crater diameter and logarithm of the laser fluence. This can provide a single shot ablation threshold and the linear relationship between the ablation depth and the logarithm of the laser fluence provides multishot ablation threshold. They found the multishot ablation threshold value to be 1.7 J/cm^2 and independent of the atmospheric conditions.

Vanagas *et al*. [29] investigated cutting of quartz and other glasses by a lateral scanning of femtosecond pulses (150 fs at 1 kHz repetition rate) of 800 nm wavelength. They found that cutting of 0.1-0.5 mm thickness can be successfully achieved without any heat affected zone. They observed that by optimizing the process conditions, such as pulse energy and scanning speed microcracks and redeposition of ablated material can be reduced considerably.

Zhang *et al*. [34] reported precision micromachining of fused quartz and Pyrex glass by laser induced plasma assisted ablation (LIPAA) using a nanosecond ultraviolet laser (248 nm). They fabricated high quality micrograting structures with periods of 1.06 and 20 μm. They produced a fresnel zone pattern in fused quartz and drilled a hole of 700 μm in fused quartz and Pyrex glass. The investigation on LIPAA indicated that either energetic species in the plasma or thin metal film can induce the laser ablation of glass.

Keiper *et al*. [30] investigated drilling of anodically bonded Pyrex glass by laser micro processing using the excimer laser mask projection technique. The excimer lasers used for this purpose are 248 nm and 193 nm wavelength, pulse duration of 10 ns, pulse energy of 8 mJ and pulse repetition rate of 500 Hz. They observed the crack formation in

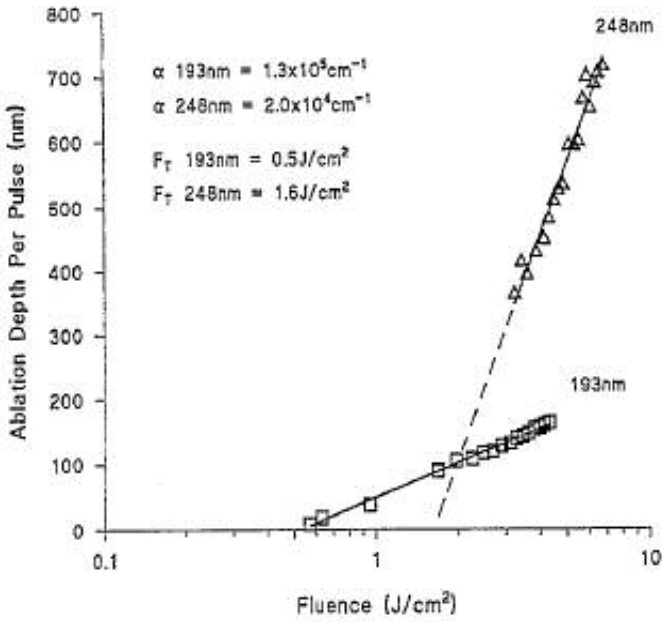

Fig. 4.6 (a) Ablation depth per pulse as a function of fluence for irradiation of Nd: glass by 193 and 248 nm lasers [21]

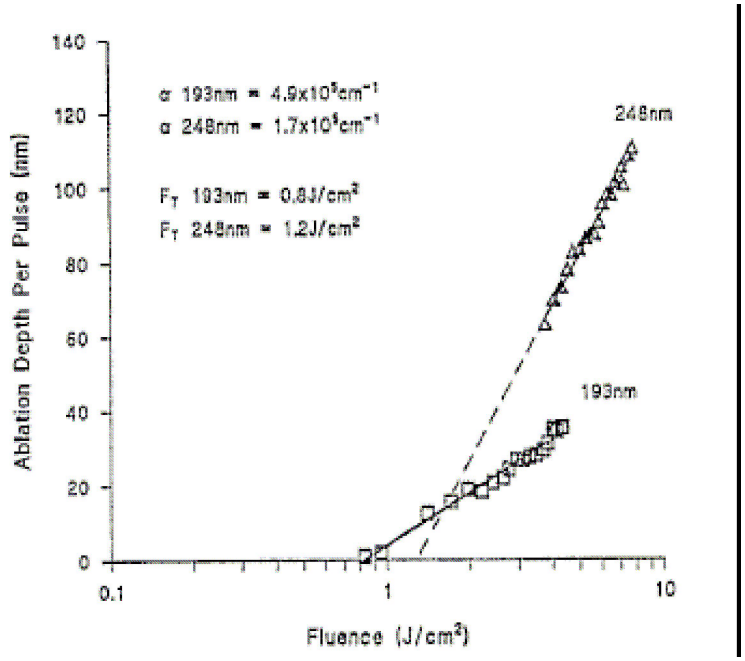

Fig. 4.6 (b) Ablation depth per pulse as a function of fluence for irradiation of Nd: YAG by 193 and 248 nm lasers [21]

the laser processed region and found distinct relationships between the process parameters and the quality of the walls of the drilled holes. They found the change from 248 nm to 193 nm wavelength led to a decrease in crack formation.

Jackson *et al*. [21] investigated the performance of Nd doped glass and Nd-doped YAG crystals using 193 and 248 nm radiation. When the resulting etch rate versus fluence (energy per unit area) is plotted, it shows the ablation thresholds be in the range of 0.5-1.6 J/cm^2 range. The measured values of the effective absorption coefficients were found to be on the order of 10^4-10^5 cm^{-1}, two or three orders of magnitude greater than the smallest absorption coefficient. When the results between the ArF (193nm) and KrF (248nm) are compared, it is found that ablation at 193 nm produced etch pits of superior quality and can be easily cleaned to those at 248 nm laser exposure. Thus ArF laser is potentially more attractive for fabricating microstructures in these laser active materials. Figures 4.1(a) and (b) show the ablation depth per pulse as a function of fluence for irradiation by 193 and 248 nm lasers.

Sanchez *et al*. [24] studied ablation rate, surface morphology, and deposition rate on quartz crystals and emission analysis when an yttria stabilized zirconia (YSZ) has been irradiated with ArF (193nm) and KrF (248nm) excimer lasers. The results obtained from the characterization equipment indicated that the ablation process of YSZ took place at two different processes. The first is a non thermal process which originates a laser plume and expands during the first few microseconds. The second process causes large and slow particulates to be ejected after some hundreds of microseconds.

Laurens *et al*. [25] investigated the modifications induced by excimer laser radiation on different types of polymer surfaces [polyetheretherketone (PEEK), polycarbonate (PC) and epoxy resin] performed at fluences below the material ablation threshold. They observed the laser wavelength to influence the characteristic of the treated surfaces. They also found that treatment with 193 nm increases the surface wettability for all the polymers forming hydroxyl, carboxyl, and peroxide groups.

Laude *et al*. [26] studied ablation of a polymer (polyethyleneterephtalate) under excimer laser irradiation of polyethyleneterephtalate with a 248 nm wavelength excimer laser. They observed the ablation threshold to take place at and above a given value of the pulse energy density. Above this threshold, ablation at first increases with fluence at a constant rate and then saturates with further increase in fluence thus fixing the maximum ablation depth per pulse.

Suzuki *et al*. [27] investigated the effects of cooling target, heating substrate, and the addition of polysilanes to control the film structure and properties of silicon based polymer films synthesized by laser ablation and deposition of hexaphenyldisilane. They observed that cooling target reduces the thermal effect and film structure was changed by heating substrate and exhibited significant increase in microhardness. They found the addition of polysilanes (polydimethylsilanes) to be very effective in developing the Si-C network structure in the resultant films.

Kruger *et al*. [28] studied the KrF excimer laser ablation of polyethylene terephthalate (PET), polyamide (PI), and polycarbonate (PC) in *situ* monitoring technique. The short acoustic pulse generates a microphone signal which represents the

etch rate of laser ablation depending on the laser fluence. By drawing a linear relationship between the microphone output voltage and the laser fluence, the single pulse ablation thresholds were found to be 30 mJ/cm^2 for PET, 37 mJ/cm^2 for PI, 51 mJ/cm^2 for PC. They found the ablation thresholds of PET and PI not to be influenced by the number of pulses.

Chen *et al*. [23] studied ablation of single and arrayed microstructures using an excimer laser. The purpose for fabricating these microstructures is to evaluate the ablation mechanism, threshold fluence, and associated material removal rate. Various changes observed during ablation are investigated with importance given to ablation defects, debris, or recast layers. The materials to be concentrated are borosilicate glass, polyamide, and silicon. Thus, the arrayed microstructures are ablated to show that, by repetition of a simple-patterned mask associated with synchronized laser pulses and substrate movement, arrayed and more complex structures can be cost-effectively manufactured.

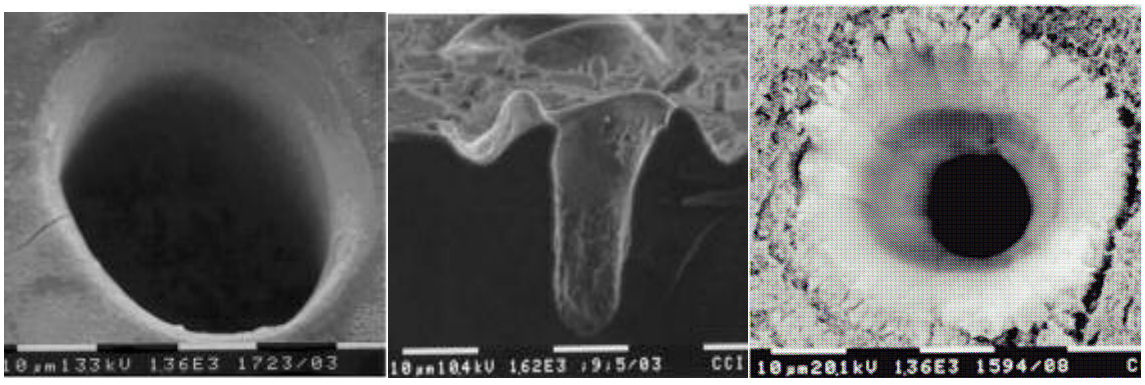

Fig. 4.7 Surface morphology at 2.4 J/cm^2 with 2000 shots [23]

Dyer *et al*. [20] studied laser ablation of bulk samples of Upilex polyamide and low density polyethylene. Three techniques, namely, high speed shadow photography (HSSP), probe beam deflection (PBD), and time resolved interferometry (TRI) were used to provide information about the ablation process. They observed that high speed shadow photography and time resolved interferometry are effective for measurements of the formation and development of the shock front. Probe beam deflection provides information about ablation over a large range of conditions, even in those when no visible plume is observed. This third technique is complemented by the other two techniques.

Dyer *et al*. [22] studied the formation of gratings for optoelectronics applications using 248 nm and 193 nm excimer lasers which also include studies of ablation of various glasses. They found remarkable wavelength dependence in the preparation of reorganized polymer films from polyacrylonitrile (PAN) using 308, 248, and 193 nm wavelength excimer lasers. At 193 nm, they found the nature of the ablation-deposition process is much distinct from the other two wavelengths.

Zimmer *et al*. [17] investigated etching of solid surfaces at the surface by liquids as a new promising method for micromachining of transparent materials. They used a XeF (351 nm) excimer laser for etching different types of glasses and fused silica. They found the etch rates to increase almost linearly at low laser fluences. They determined the threshold fluences for glass to be as low as 0.5 J/cm^2 and etch rates from 6 to 10 nm per pulse at 1 J/cm^2. They found the etch rate and threshold fluence to depend on the liquid used, consisting of a solvent (acetone, toluene) and a certain concentration of dissolved pyrene, and not significantly on the glass type. The resulting surface is usually round and

the surface roughness measured by AFM at an etch depth of 3.7 μm is 4 nm. They found that Pyrex of all the glasses, exhibits high surface roughness.

Kopitkovas *et al*. [36] investigated the fabrication of micro-optical elements in quartz by laser induced backside wet etching where the quartz plate is in contact with an organic solution. They observed that this allows microstructuring of quartz with an XeCl or KrF excimer laser at laser fluences below the damage threshold of quartz. They showed different types of structures in quartz varying from simple binary structures to complex 3D structures can be fabricated. Laser fluence and substrate play a role in the amount of surface roughness and the roughness varies from 50 to 500 nm.

Figure 4.8 show a Siemens star in quartz fabricated by KrF laser with a fluence of 0.7 J/cm^2 and 800 pulses irradiation. It shows clean etching without any pronounced cracking on the quartz.

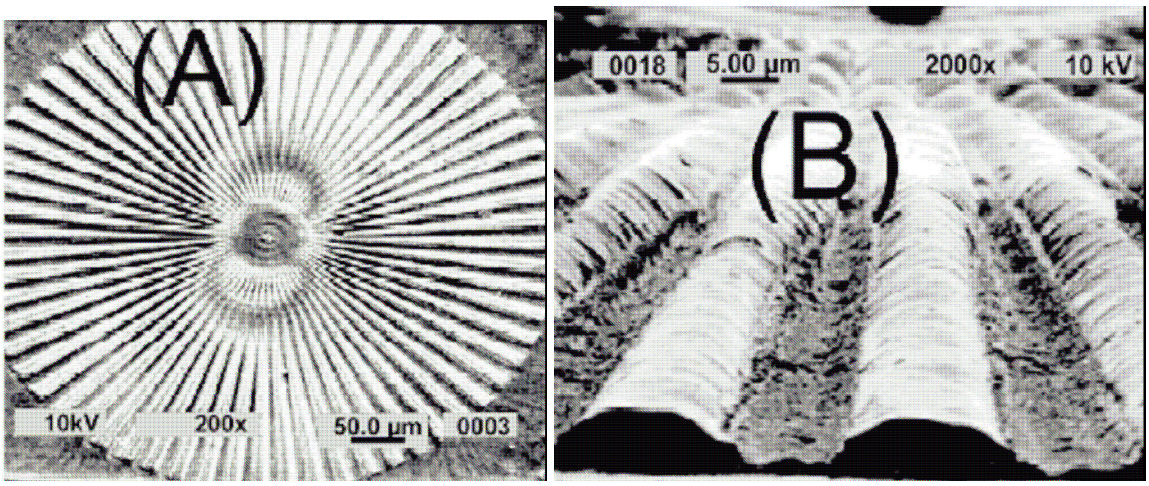

Fig. 4.8 SEM picture of Siemens star etched in quartz by LIBWE [17]

Ding *et al.* [16] investigated laser-induced backside wet etching (LIBWE) by nanosecond pulsed KrF excimer laser irradiation. They fabricated microstructures with well defined 1 μm-scale grating and grid patterns on the surfaces of silica glass through a mask projection system. This method is based on the deposition of laser energy onto a thin layer at the glass-liquid interface during ablation of a liquid substance. Transient shockwaves and vapor micro-bubbles were observed following laser

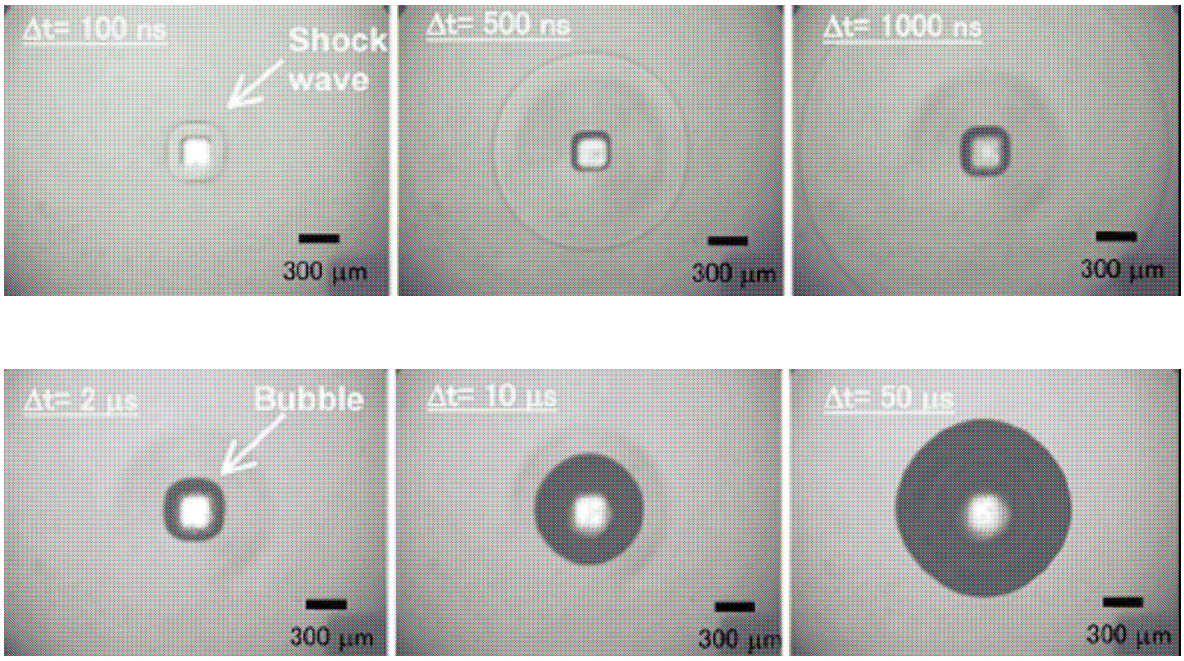

Fig. 4.9 Front view images of toluene ablation [15]

irradiation, indicating the generation of high pressures and temperatures on the surface of glass by laser irradiations. Well defined microfabrications were successfully performed on the glass surface without any crack or debris formation. Figures 4.9 show the front view images of toluene ablation using time resolved shadowgraph.

Zimmer *et al*. [17] investigated the influence of the laser spot size and applied pulse number to the etch rate for fused silica and two different liquids during laser induced backside wet etching (LIBWE) of transparent solids. They observed a significant increase in etch rate with spot size and considerable incubation effects at low laser fluences and pulse numbers. They explained the influence of the laser spot size on the etch rate by the formation of laser induced bubbles. They concluded that etch rate depends on the bubble life time, the maximum radius of the bubble and consequently the laser spot size.

CHAPTER 5

PROBLEM STATEMENT

The main problem that arises with conventional micromachining of brittle materials is the formation of cracks on the substrate. Micromachining is achieved by means of an excimer lasers because of its various favorable features, such as high ablation rate and short wavelengths. Applications of micromachining increase on once hard materials and the process can be performed without the formation of ridges or cracks. This increases the life of the MEMS devices. Borosilicate glass though has many applications in the MEMS industry, it is still not very widely used because of its brittle nature. Micromachining of borosilicate glass results in considerable cracking and ridges around the ablated surface. Thus, one objective of this work is to conduct experiments using excimer laser for different test conditions and trying to obtain the final ablated or micromachined surface with fewer cracks.

In case of micromachining with lower laser energy, a material build up is formed on the substrate. This surface acts as a microchip breaker and needs to be smooth and uniform and as high as possible. Thus, another objective of the work is to conduct experiments at different test conditions to obtain a smooth and uniformly built up surface. In other words, the various parameters involved in the process are to be optimized in order to obtain a good built up surface of high surface finish. The optimizing parameters

or the test conditions include laser energy, size of the mask, number of loops and different media. In the case of built up formation, the input laser energy is varied from 376 mJ in air to 480 mJ in solutions for 1mm mask and from 550 mJ to 672 mJ in air for 0.3 mm mask. The media used are air, water, sugar, salt, polymer and methanol solutions. The number of loops is limited to 4 or till cracks begin to appear. In case of micromachining (material removal) the input energy used was 536 mJ for 1mm mask.

These micromachined or built up surfaces are observed using an optical microscope and Micro XAM laser interference microscope.

CHAPTER 6

EXPERIMENTAL SETUP

6.1 Introduction

The Excimer laser micromachining apparatus comprises of three major units. They are (i) excimer laser generator system, (ii) stage and motion controller and (iii) optical or laser beam delivery system. A computer station interfaces the excimer laser generator system with the stage and motion controller.

6.2 Excimer Laser Generator System

This excimer laser generator produces a high power laser beam. It consists of a short pulse (FWHM= 25 ns) Lambda Physik COMPex205i excimer laser. It is connected to a 115V (10%), 25A power supply. This generator system has two triggers (a) Internal Trigger where the control panel is connected to the trigger and (b) connected to a computer station to which the stage and the motion control are interfaced. This laser is provided with Lambda Physik's NovaTube technology which provides stable laser performance, reduced maintenance, and minimum cost. The gas used for the laser system is KrF with a wavelength of 248 nm. The life time of the gas used is $\sim 10^6$ laser pulses. Tables 6.1 and 6.2 gives the specifications of the LAMBDA PHYSIK COMPEX 205i EXCIMER LASER, and specification of the gases used in the excimer laser.

Table 6.1 Specifications of LAMBDA PHYSIK COMPEX 205i Excimer Laser

COMPEX 205i Excimer Laser	KrF
Wavelength (λ)	248nm
Energy	650mJ
Maximum average power	30W
Maximum pulse repetition rate	10 Hz
Nominal pulse duration	25ns
Orientation of the laser beam	horizontal
Type of the homogenizer	dual axis
Beam Divergence	3 x 1 mrad
Beam Dimensions	24×6^{-12} mm^2

Table 6.2 Specification of the gases used in the Excimer Laser

	Type of Gas	Purity
Buffer	Ne	99.995%
Rare	Kr	99.99%
Halogen	5% F_2, 95% He	99.995%
Inert	He	99.995%

6.3 Stage and Motion Controller System

The stage and motion control system is a UNIDEX 500 (U 500) system or a combination of the U500 PC bus-based motion control card, the Windows-based Toolkit or MMI interface software, and any various optional accessories. The U500 system integrates with amplifiers, positioning stages, and the accessories to form a complete programmable customized control system that is suitable for a range of motion control applications. The UNIDEX 500 control card is available in three models (Base, Plus, and Ultra) to provide a level of motion control to match any application. The Base model contains the basic version of the UNIDEX 500 family whereas the ultra version consists of the most versatile version of the U500 family of controllers.

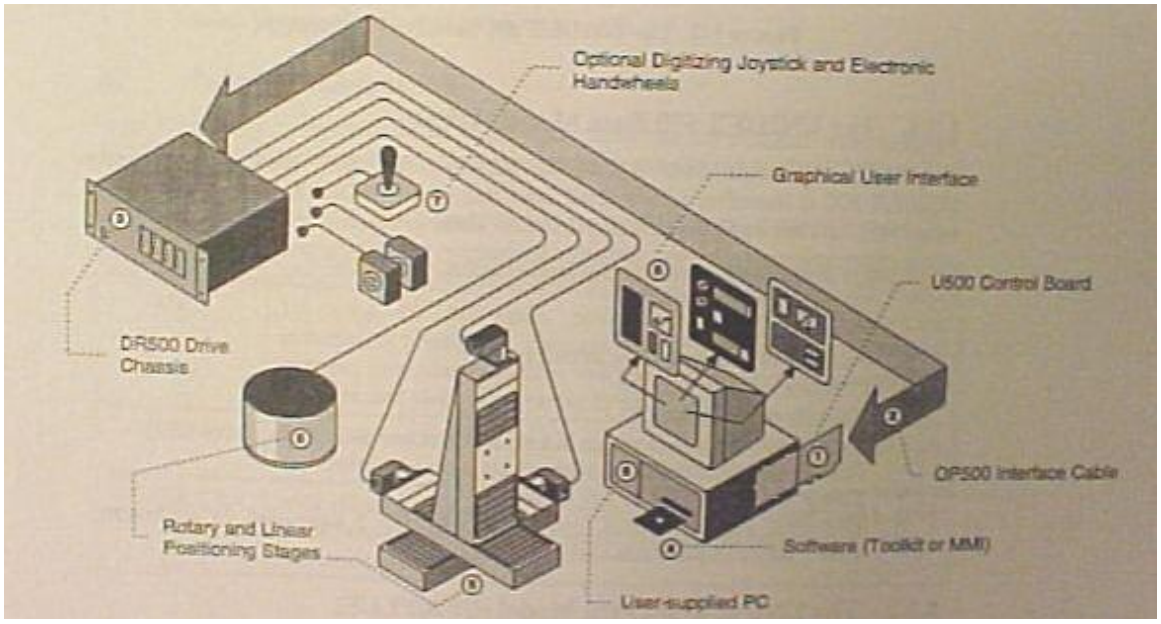

Fig. 6.1 UNIDEX 500 system diagram [39].

6.4 Optical or Laser beam delivery system

The optics system consists of five main parts: (1) attenuator module, (2) homogenizer (3) field lens, (4) mask, and (5) doublet. Figure 6.2 shows the optical delivery system.

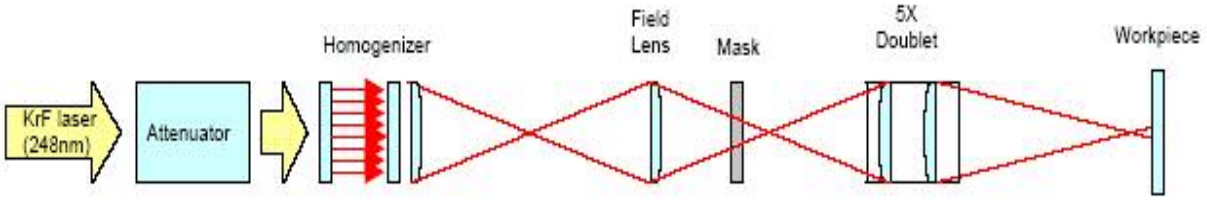

Fig.6.2 Optical delivery system used for laser micromachining [50]

Attenuator: The main purpose of the attenuator is to control the intensity of the laser beam. The optical attenuator uses a specially coated attenuating element and a counterrotating compensator plate. The compensator plate compensates the beam displacement. The elements are coated for a specific excimer laser wavelength. The angle of the elements can be varied using a hand-driven dial on the front panel of the attenuator housing. The optical transmission changes from 10 to 90%.

Homogenizer: The purpose of the homogenizer is to divide the incoming excimer laser beam into segments and overlay the segments at the object plane to create a homogenous intensity profile. In other words, this homogenizer forces a plane of homogenous illumination at the location of the mask. It consists of two arrays of cylindrical lens and a condenser lens. The arrays can be single axis arrays or crossed arrays.

Field Lens: The field lens gathers the laser beam and converges it onto a doublet. Thus this field lens facilitate in obtaining a clear and uniform intensity laser beam.

Mask: The main function of the mask is to control the shape of the structures formed on the substrate. Thus the final shape formed on the substrate can be controlled by the type of mask used. There are three different kinds of mask used. They are (a) free standing metal mask. (b) metal film on quartz substrate (c) dielectric mask.

Doublet: The doublet is used to demagnify the mask. It is composed of 2 spherical lenses, each with a radius of curvature, r = 50 mm. These lenses are mounted with a separation of about 7 mm of the curved surface. The doublet should be pointed with the curved sides of the lens both pointing towards the object (mask or aperture) in order to get the lowest amount of aberration.

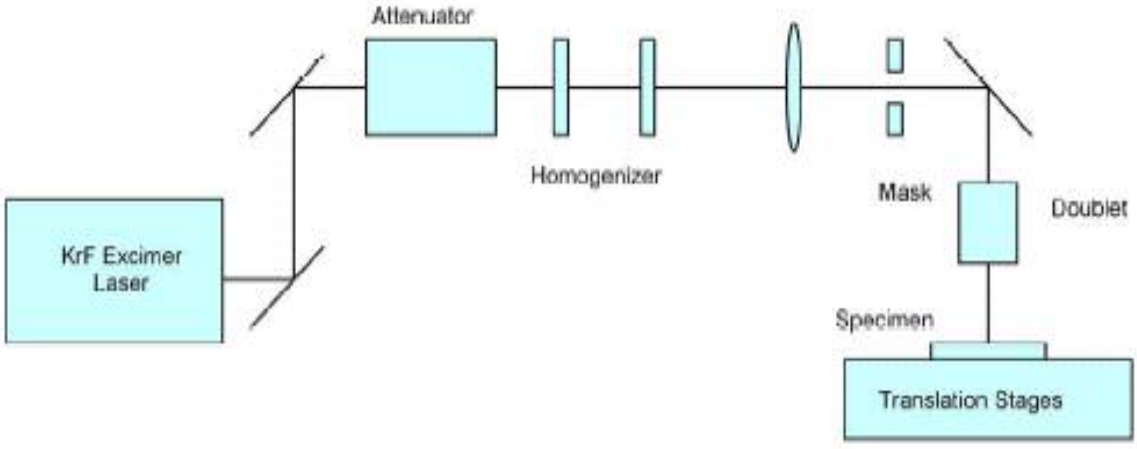

Fig.6.3 Schematic of the experimental setup used for laser micromachining [50]

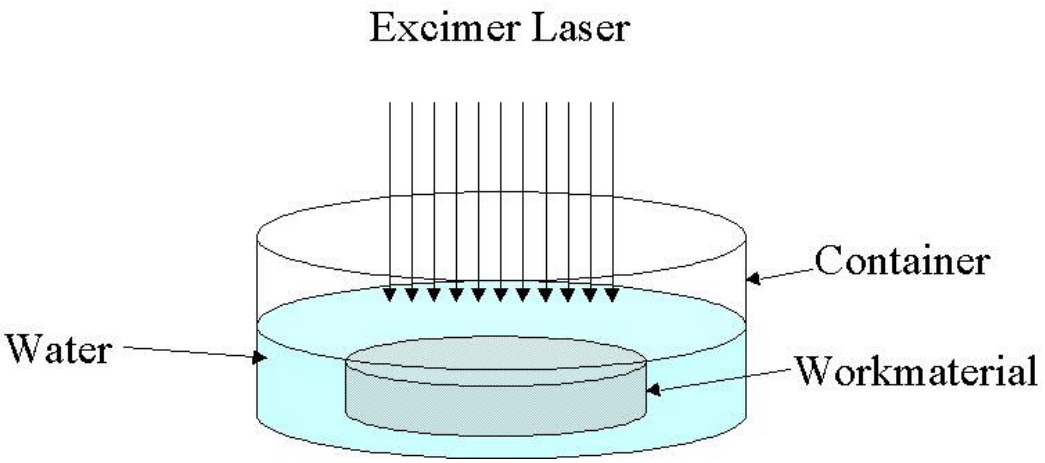

Fig 6.4 Schematic of the setup used for underwater micromachining [50]

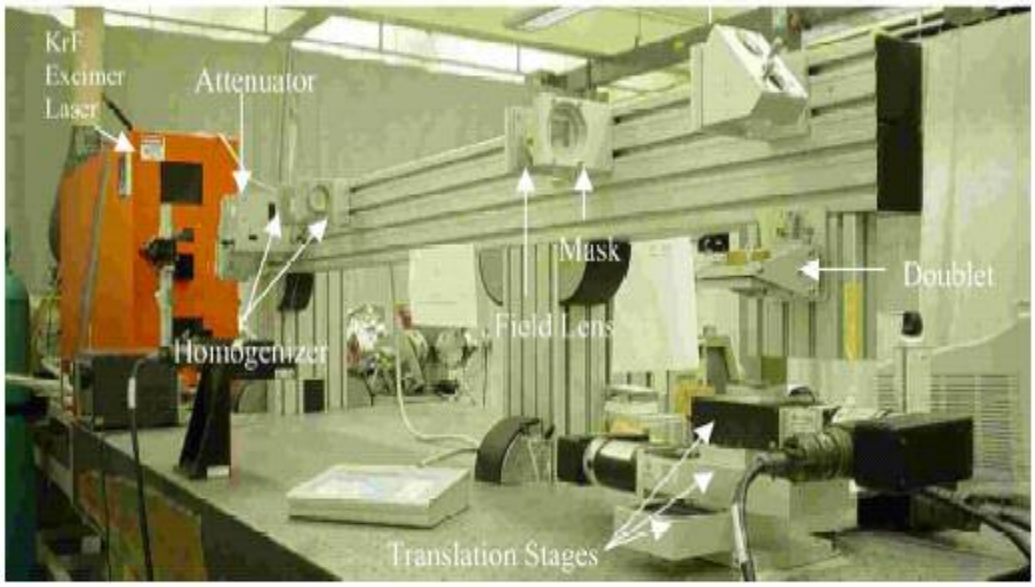

Fig.6.5 Photograph of the experimental setup used for laser micromachining [50].

CHAPTER 7

METHODOLOGY

7.1 Introduction

The standard test procedures used for laser micromachining are the following (1) sample preparation, (2) determination of laser fluence, (3) input energy, (4) laser micromachining in air and different media (5) optical microscopy and characterization using MicroXam laser interference microscopy.

7.2 Sample Preparation

1. The sample is placed in a beaker with a detergent solution and subjected to an ultrasonic treatment for 2-3minutes.
2. The sample is then rinsed with distilled water.
3. The sample is placed in a beaker containing distilled water and subjected to an ultrasonic treatment for 2-3 minutes.
4. The sample is rinsed with methanol.
5. The sample is placed in a beaker containing methanol and subjected to ultrasonic treatment for 2 minutes.
6. Finally, compressed air is used to dry up the sample.

7.3 Determination of Laser Fluence

The pulse energy decreases as the life time of the gas in the cylinder is reduced. Hence, it is important to determine the fluence before carrying out the experiments. Laser fluence is defined as the energy per unit area. A Melectron M400 energy detector is used to measure the laser energy. The fluence is calculated using the following equation:

$$f = \frac{\text{Eavg}}{\pi.(\text{D}/4)^2}$$

where E_{avg} is the average of the single pulse energy and D is the diameter of the mask.

7.4 Input Energy

The input energy is varied using the control terminal of the excimer laser. For a fixed mask, fluence is directly proportional to input energy which can be viewed from the control terminal display.

7.5 Laser Micromachining in Air and Different Media

In air, an excimer laser with 25ns FWHM is used to machine different materials. Different media implies a liquid media placed on top of the glass substrate to reduce thermal damage. The results obtained carrying these experiments are discussed in Chapters 8 and 9.

7.6 Optical Microscopy

An optical microscope is used to observe the surface profiles of the machined surfaces. The intensity of the thermal damage resulting from laser ablation under different conditions are observed and compared.

7.7 MicroXam laser interference microscopy

This microscope is used for examining the surface profiles. It uses different wavelengths of light to scan through the irradiated area and gives a three dimensional profile of the surface. Thus the depth and height for the ablated surface can be observed without disturbing it.

CHAPTER 8

MATERIAL BUILD-UP ON BOROSILICATE GLASS USING EXCIMER LASER

8.1 Introduction

Excimer lasers are high-pressure gas lasers, which emit short-pulse (a few nanoseconds) radiation in the ultraviolet range of the electromagnetic spectrum. The material of the workpiece is removed by the process solid-vapor ablation i.e. when an excimer laser beam of extremely short wavelength impinges on the workpiece material, high energy photons coming from the laser beam fall on the substrate and breaks the bonds between the atoms/molecules in the material. Thus this process results in ablation of the material and the depth of this ablation depends on the ability of the material to absorb laser energy. In other words, an excimer laser provides sufficiently high photonic energy to ablate the required material by a process called micromachining.

The micromachining process involving material removal (described above) takes place only if the energy is above a certain threshold value. If the energy emitted by the laser is below the threshold value (different for different materials), then it results in built up of the material. This energy is not sufficient to cause solid-vapor ablation and no material is removed. The height of the new surface formed on the material is on the order

LOOP–1 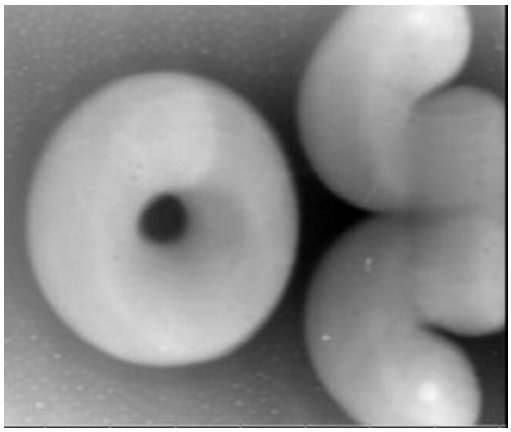	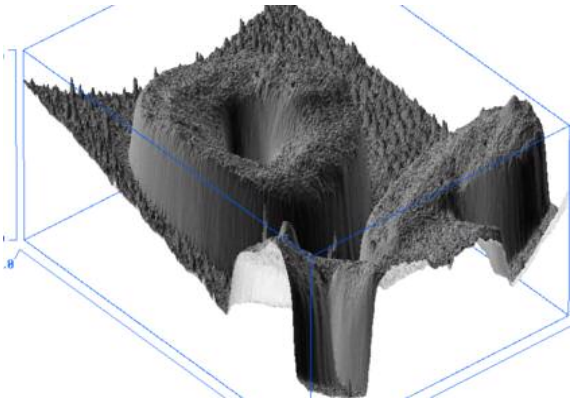
LOOP–2 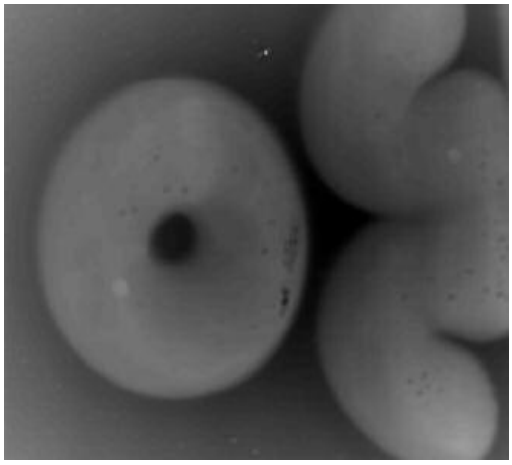	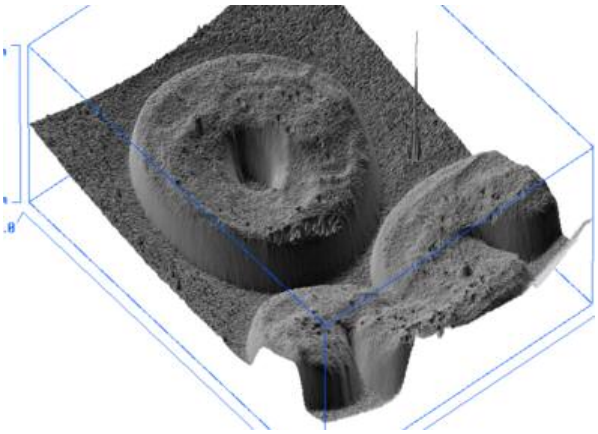
LOOP–3 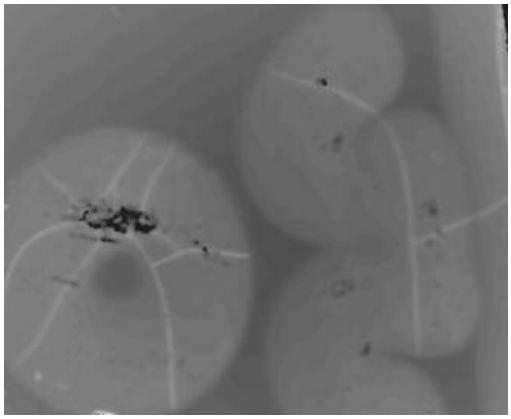	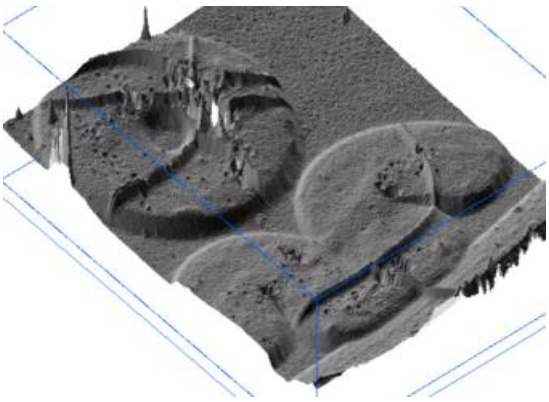

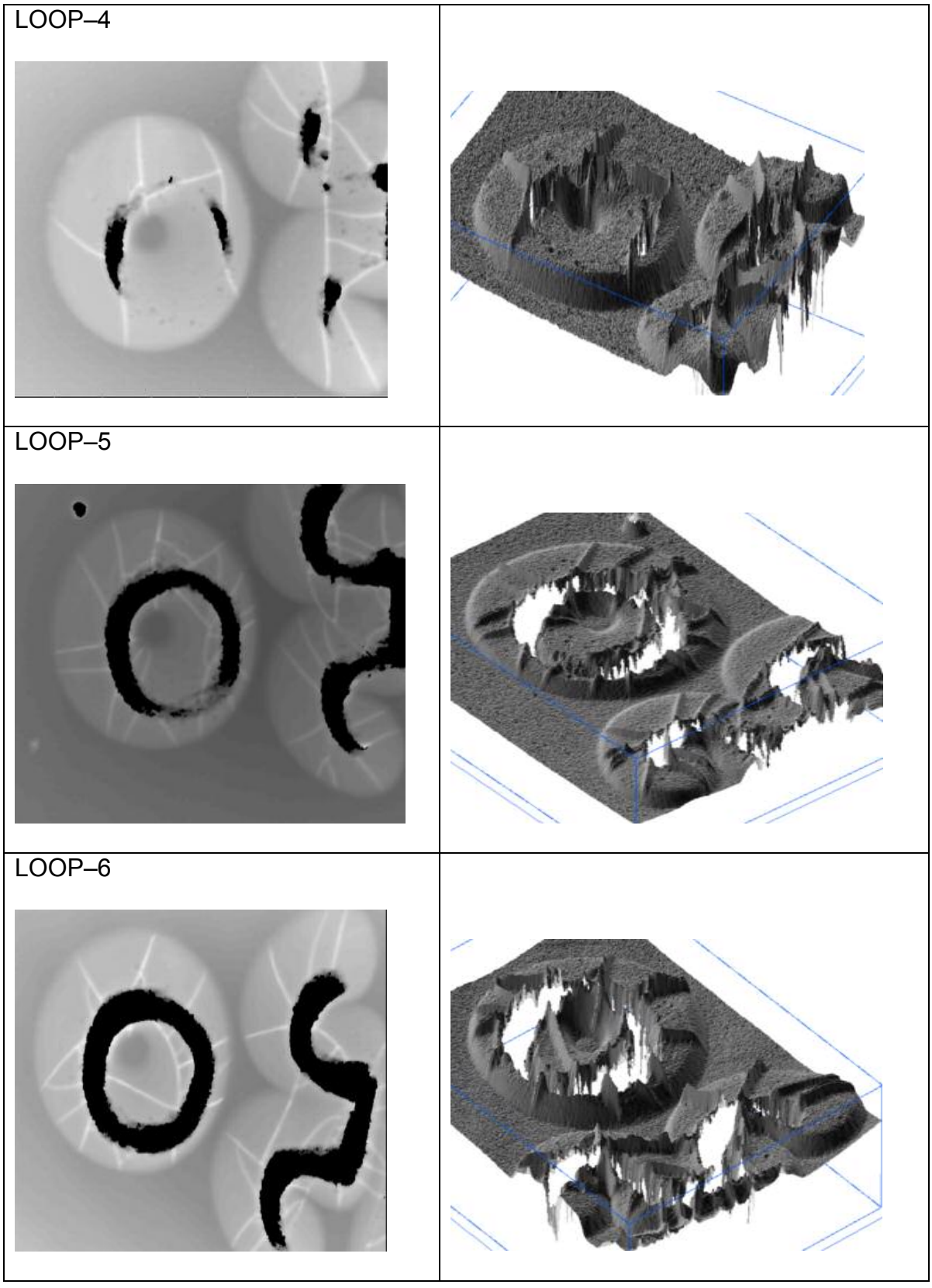

Fig 8.1 Transformation process from material build-up to material removal at 356 mJ energy

of a few nanometers. Figure 8.1 shows the transformation from material build-up to material removal for borosilicate glass as the number of loops is increased.

The main reason for this process is the deposition of the matter from a resultant chemical interaction between the photons emitted by the laser beam and the workpiece. When the energy of the photons is not high enough, it does not have the strength to ablate the material. Its energy is still high enough to break the resultant chemical bonds in the workpiece. Thus, the chemical bonds are broken within the workpiece till the effect of the energy is subsided. These photons then react in air or under water with the individual elements of the material and the resultant substance formed by the chemical reaction are deposited on the surface. The height of this new surface ranges from 5 to 35 nm. This nanometrically built up surface can be used in MEMS devices and in many circuit devices. Different design patterns can be achieved using this method. This chapter summarizes different experiments conducted and results obtained using this process. A much detailed study of this process can take us closer to nanotechnology. These nanosurfaces are made of extremely small sized particles and find a number of applications. The build up surfaces can be used for breaking the circuits in the microchips.

8.2 Experimental Procedure

A borosilicate glass slide is used as the work material. Two masks 300 μm and 1000 μm diameter are used for this purpose. The surface of the glass is then exposed to a laser beam in air with fluences varying from 1.8 to 2.4 J/cm^2 (energy from 375 mJ to 650 mJ). The reason for this is to generate surfaces of different heights at nanometer level.

Another important thing is to obtain a build up surface which is smooth and devoid of surface irregularities and cracks. This experiment is repeated for different number of loops ranging from one to four. After this series of tests are conducted, the conditions are changed from air to other media, such as under water, salt solution, sugar solution, and methanol solution and the above procedure repeated. When the experiment is repeated with different solutions, the height of the lower meniscus of the liquid is fixed at 3 mm. When using either sugar or salt solutions care is taken such that the all the sugar or salt added is completely dissolved. The methanol solution is formed by mixing methanol and water in the ratio 1:4. The sample subjected to laser energy is then ultrasonically cleaned. The material build up is examined using MicroXam laser interference microscope for surface mapping and for the determination of the build up height. The results obtained from these solutions are observed and necessary relations are plotted.

8.3 Results and Discussion

1. Initially this surface material build-up process is compared with material removal. Figures 8.2 (a) and (b) show two similar samples tested at different energies using a 1mm mask. Figure 8.2 (a) shows a sample (borosilicate glass) tested at 500 mJ and Figure 8.2 (b) shows a similar one tested at 420 mJ. At 500 mJ, the material is ablated or removed and micromachining process takes place but at energy of 420 mJ, a material build up is observed. Further reduction of energy results in no influence of laser on glass. A number of differences can be noted between the two processes as given in the following.

The first and the most obvious difference between the two processes is that in micromachining the surface is removed in micrometers where as in material build up, the built up surface is on the order of nanometers. In the micromachining process, the machined surface is non-uniform with cracks and ridges formed due to thermal damage on the material. Contrary to it, the built up surface is much smoother and the surface is devoid of any cracks or ridges. Figures 8.3 and 8.4 show different patterns obtained on the surface of borosilicate glass by material built up using both the masks. The thickness of the built up surface is $1/5^{th}$ of the mask used, i.e. 200 µm for 1000 µm mask and 60 µm for 300 µm mask. Since the area of the figures is 544,000 μm^2 with length 890 µm and breadth 612 µm, only a part of the built up surface can be seen in case of 1000 µm mask whereas in the case of 300 µm mask greater details of the surface due to laser impingement is visible.

Front View

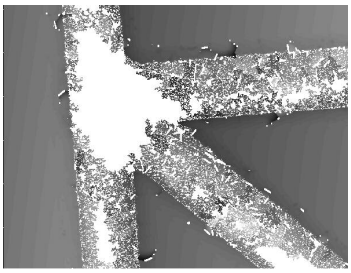

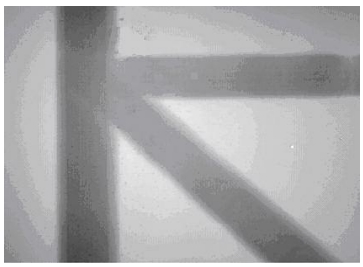

3Dimensional view

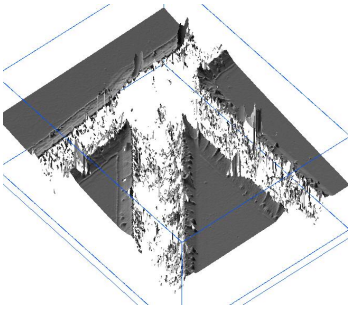

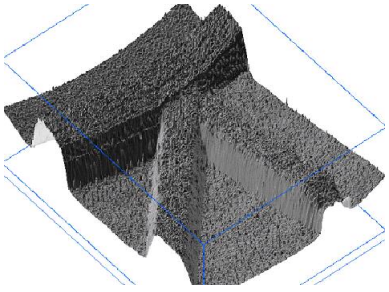

(a) Material removal, Energy 500 mJ (b) Material build up, Energy 420 mJ

Figs. 8.2 (a) and (b) Comparison of material removal and build up using 1000 µm mask.

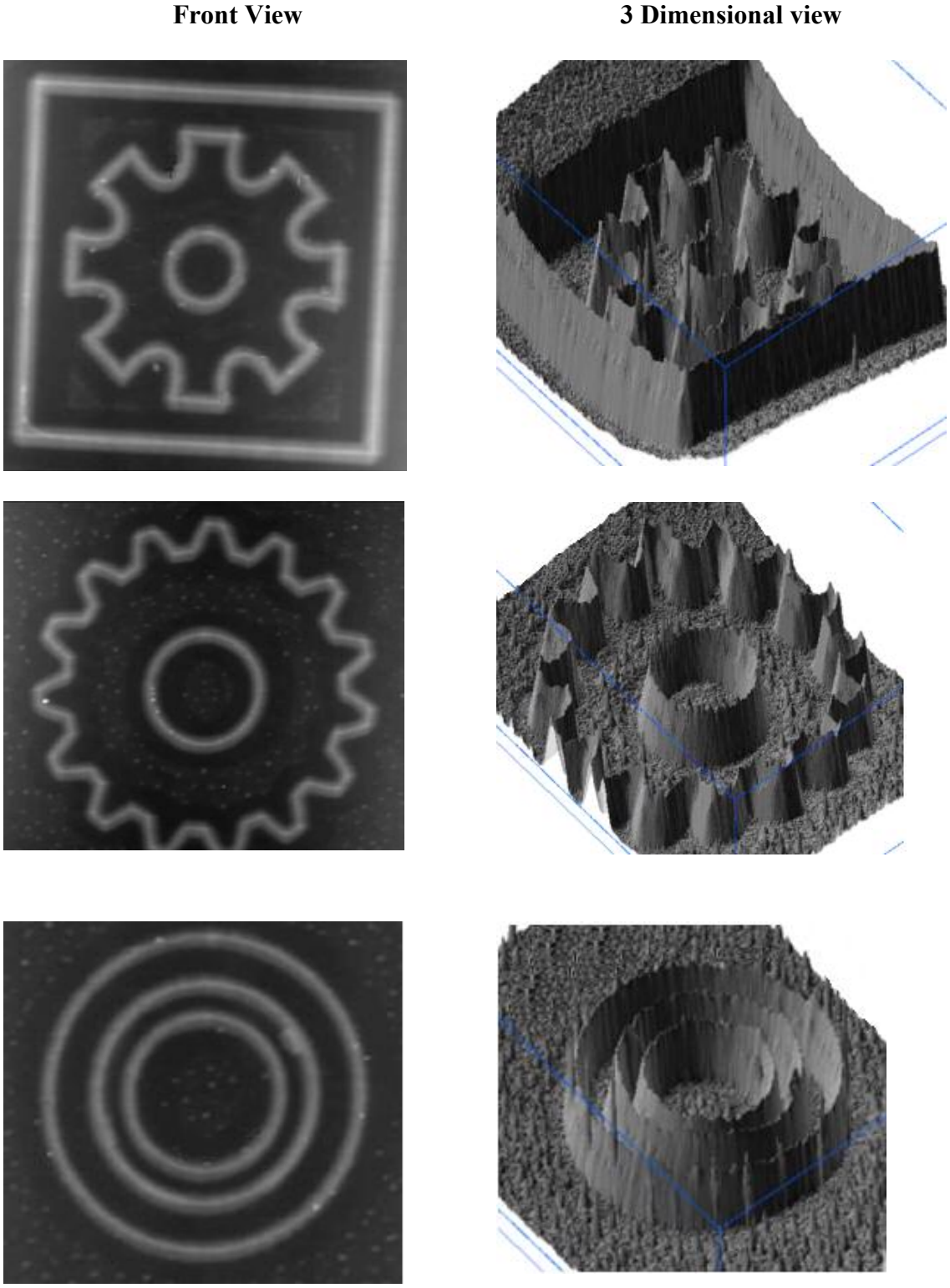

Fig. 8.3 Different surface patterns formed at 550 mJ energy using a 300 μm mask.

Front View **3 Dimensional View**

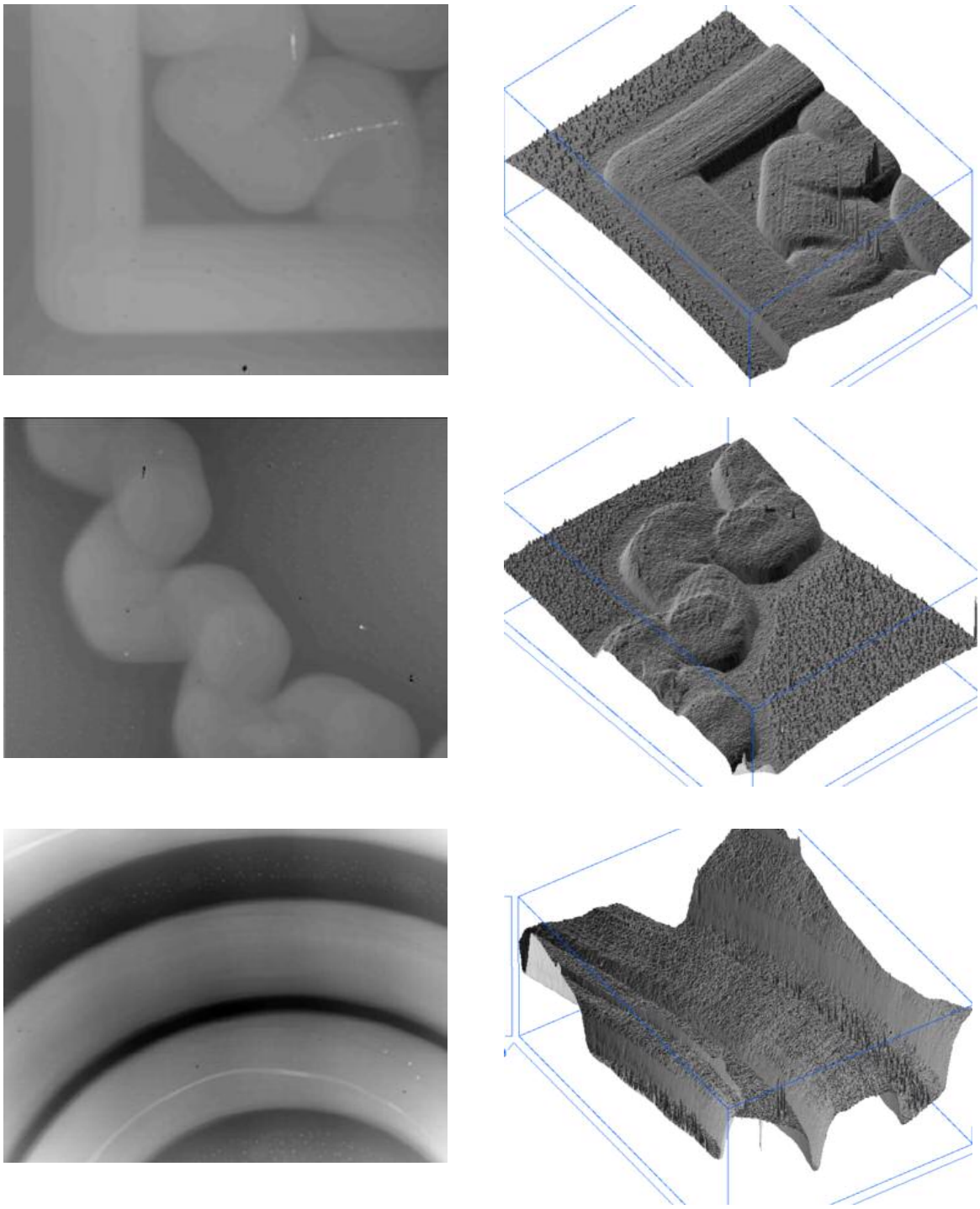

Fig. 8.4 Different surface patterns formed at 400 mJ energy using a 1000 µm mask.

2. An interesting feature observed in the material built upprocess is the change in height of the built up surface when energy is increased. The change in the height of the glass substrate is observed in nanometers and is directly proportional to the increase in energy i.e. with increase in energy, the height also increases. The built up height is calculated using the line segment profile present in the Micro XAM interference microscope. The height obtained is the difference between the average of points (equidistant from each other) taken at ground level and the average of points taken at elevated level.

The height obtained at 556 mJ energy in dry micromachining of borosilicate glass with a 300 μm mask is 14 nm. As the energy is increased to 600 mJ the height measured is 20 nm. Also, with increase in energy, the inverted V-shaped profile changed to inverted U-shaped profile. Thus the sharp profile of the built up surface gets reduced. This process (increase of height with increase in energy) is observed irrespective of the mask and the medium used. When different media were used, the initial minimum energy needed for the material built up varied accordingly. For any given mask, air requires minimum energy for material built up followed by distilled water, salt water, sugar water, and methanol solution in that order. This increase in height with increase in energy takes place till certain threshold energy is reached. This is the energy at which the surface starts to get removed instead of built up. Hence, it can be defined as the minimum required energy for a material to get ablated. At this stage, cracks start to appear and the substrate get ablated or micromachining takes place.

The reason for the material built upcan be given as the formation of a plasma cloud which acts as a barrier between the laser beam and the final substrate. In other words, it absorbs most of the energy thus reducing the final energy reaching the glass surface. Thus, the material built up is also dependant on the plasma cloud intensity. A plasma cloud of higher intensity will be formed when different solutions are used thus causing higher energy for material built up.

Based on various observations, the energy required for the formation of the surface depends on various properties of the medium. It also depends on the thickness of the mask and the reactive nature of the medium with the substance used. This built up surface is directly proportional to the energy of the laser beam, i.e. the height of the built up material increases with increase in energy. Figures 8.5 to 8.8 show the process of dry machining with a 300 μm mask where the built up height starts from 14 nm at energy of 556 mJ in Figure 8.5 and increases to a height of 32 nm for energy of 672 mJ in Figure 8.8. When the mask is changed to 1000 μm, the built up height is observed to be 15nm at energy of 376 mJ in Figure 8.9 and is 27 nm for energy of 424 mJ in Figure 8.12. Also, the surface finish increases with the increase in energy. Therefore, the built up surface for 424 mJ energy has a better surface finish compared to 376 mJ.

Figures 8.5 to 8.8 show top view and the 3D model of a borosilicate glass when subjected to different energies in air for a 300 μm mask and Figures 8.9 to 8.12 for 1000 μm mask.

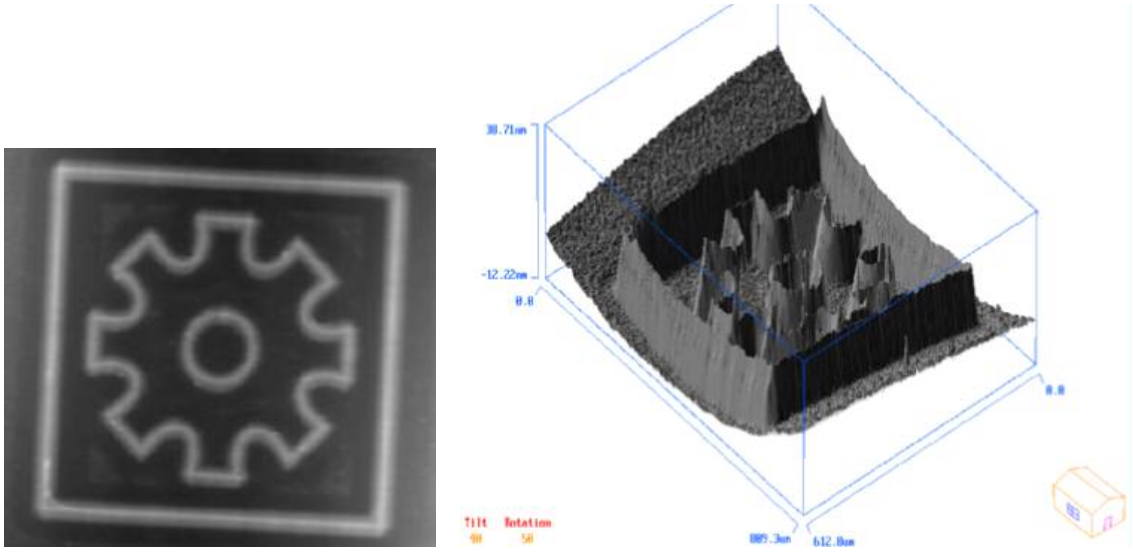

(a) (b)

Fig 8.5 (a) Top view (b) 3 D solid model of borosilicate glass subjected to energy of 556 mJ in air using 300 µm mask. Height formed is 14 nm.

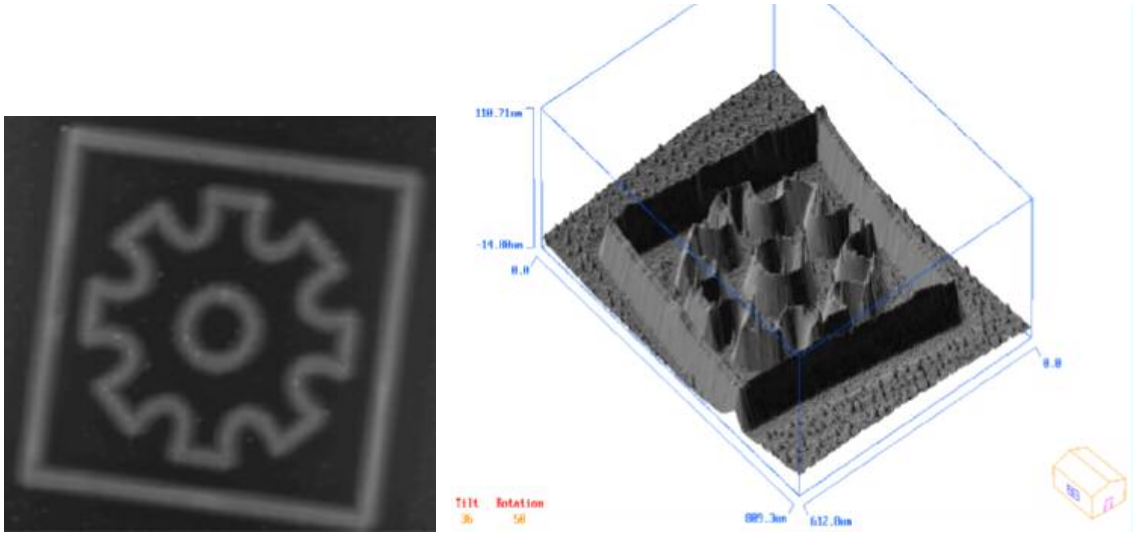

(a) (b)

Fig 8.6 (a) Top view (b) 3 D solid model of borosilicate glass subjected to energy of 600 mJ in air using 300 µm mask. Height formed is 20 nm.

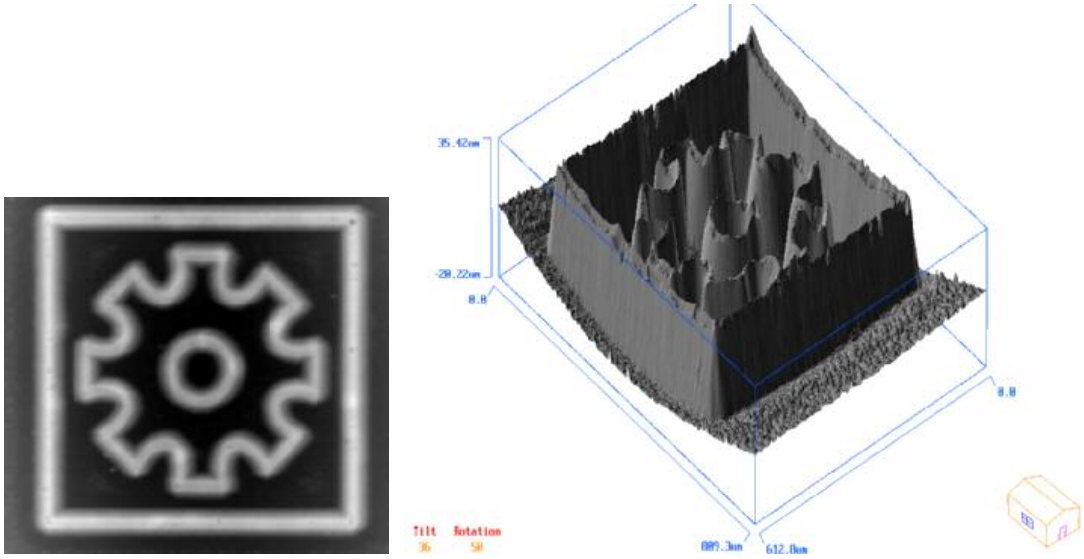

(a) (b)

Fig 8.7 (a) Top view (b) 3 D solid model of borosilicate glass subjected to energy of 638 mJ in air using 300 µm mask. Height formed is 26 nm.

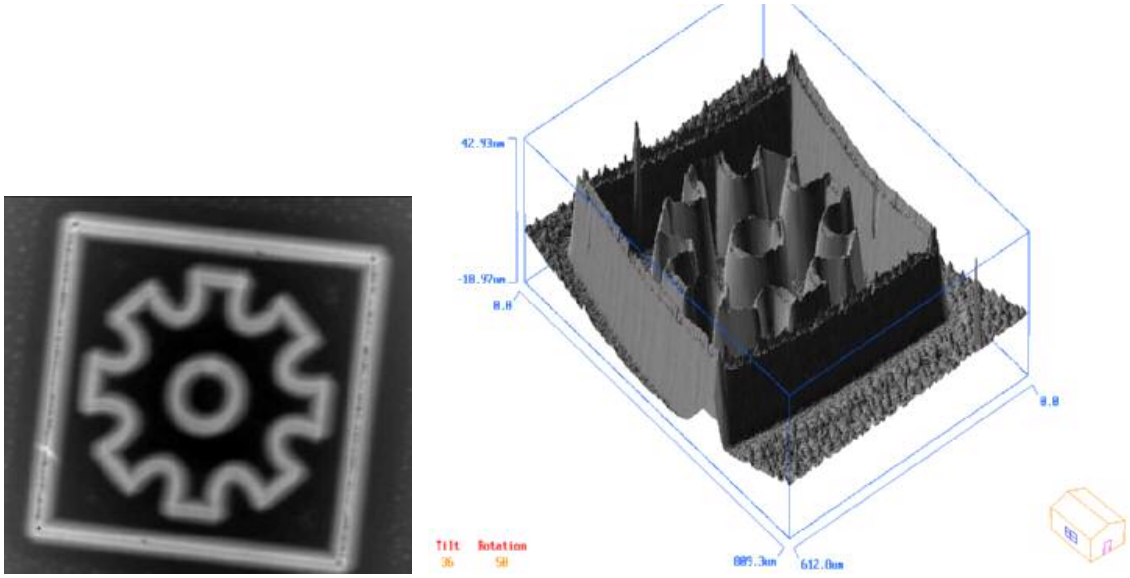

(a) (b)

Fig 8.8 (a) Top view (b) 3 D solid model of borosilicate glass subjected to energy of 672 mJ in air using 300 µm mask. Height formed is 32 nm.

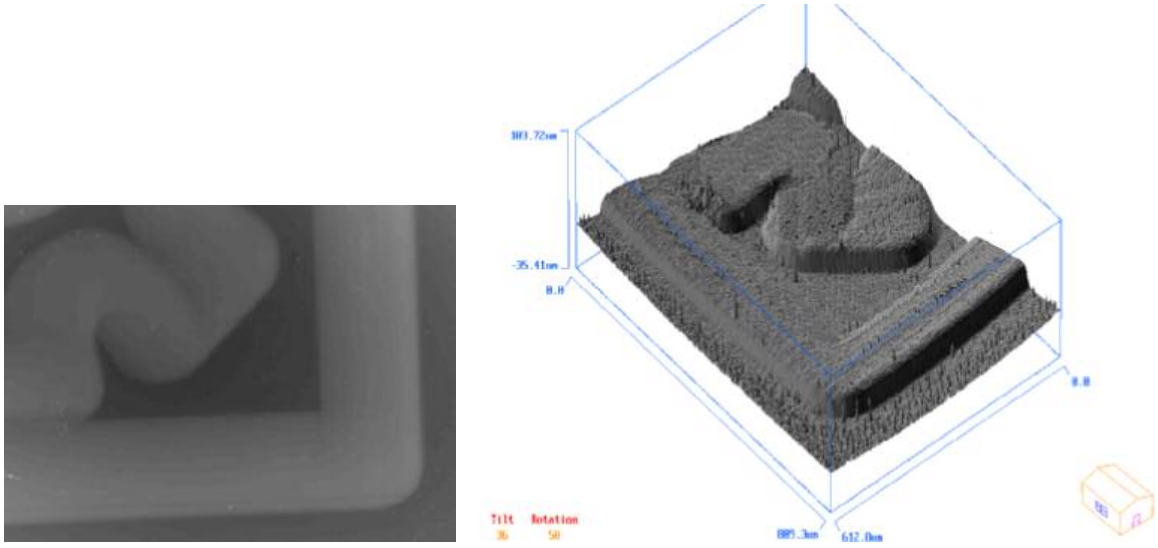

(a) (b)

Fig 8.9 (a) Top view (b) 3 D solid model of borosilicate glass subjected to energy of 376 mJ in air using 1000 µm mask. Height formed is 15 nm.

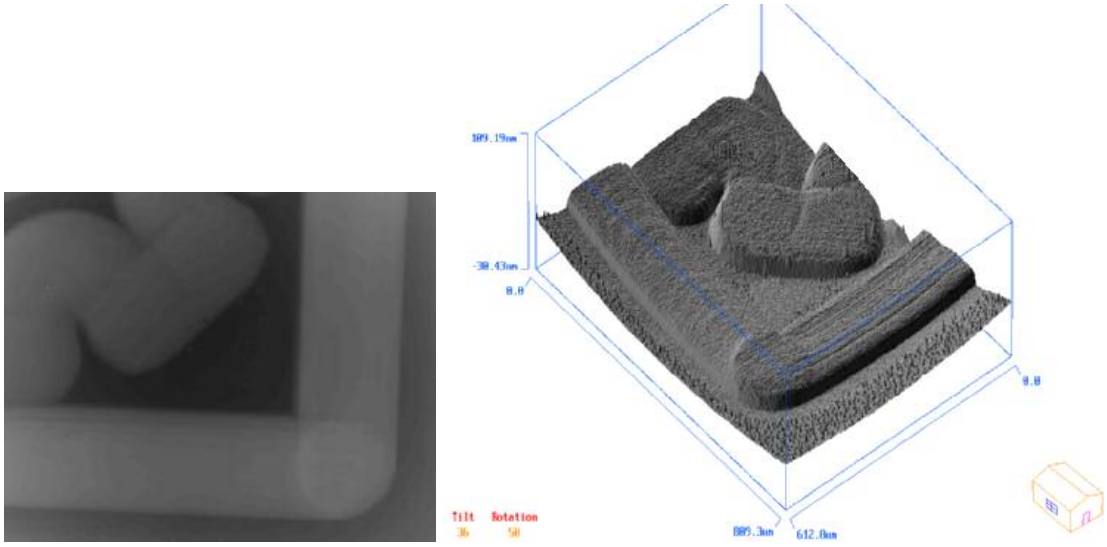

(a) (b)

Fig 8.10 (a) Top view (b) 3 D solid model of borosilicate glass subjected to energy of 400 mJ in air using 1000 µm mask. Height formed is 21 nm.

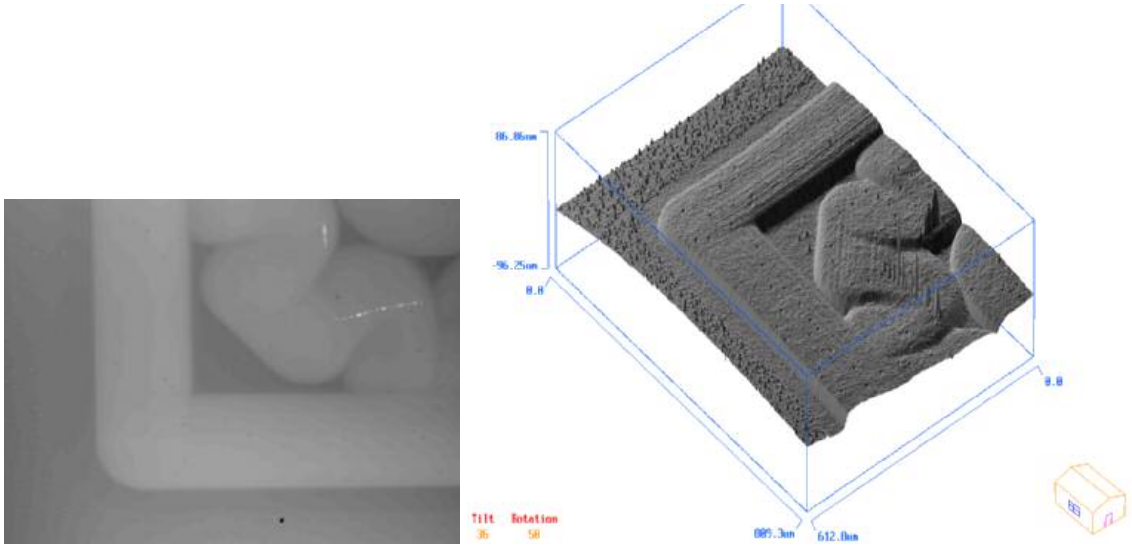

(a) (b)

Fig 8.11 (a) Top view (b) 3 D solid model of borosilicate glass subjected to energy of 412 mJ in air using 1000 µm mask. Height formed is 24 nm.

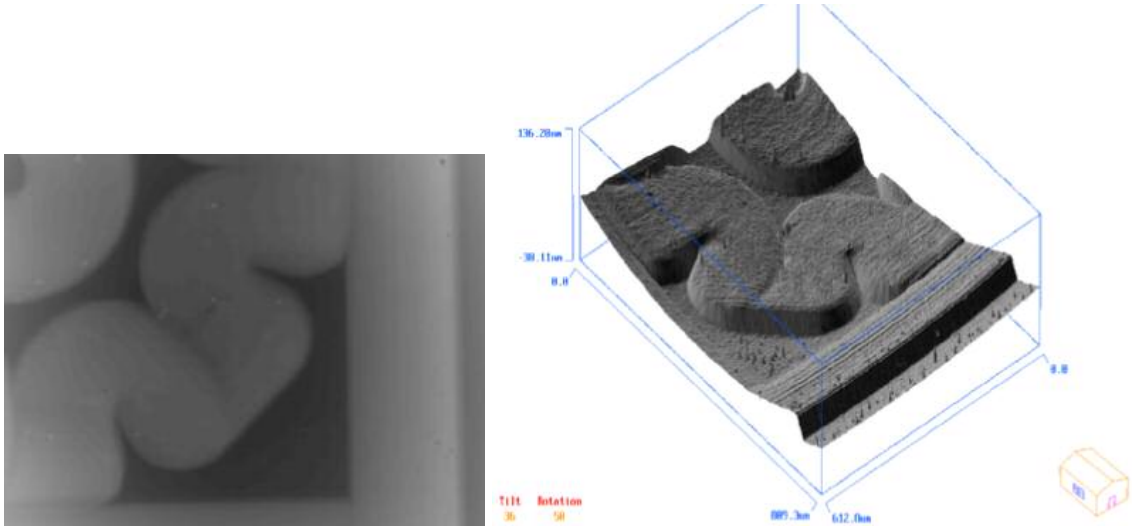

(a) (b)

Fig 8.12 (a) Top view (b) 3 D solid model of borosilicate glass subjected to energy of 424 mJ in air using 1000 µm mask. Height formed is 27 nm.

Figure 8.13 shows the variation of height with energy for two different masks in air. It consists of a graph drawn with energy supplied (in mJ) in the X-axis and the built up height is (in nm) on the Y-axis. The heights obtained at four different levels of energy (lesser than threshold energy) for these masks are plotted on the graph. It shows that the built up height increases linearly. However, if the graph is plotted beyond the threshold energy, then there will be a steep drop of the curve because of the material removal.

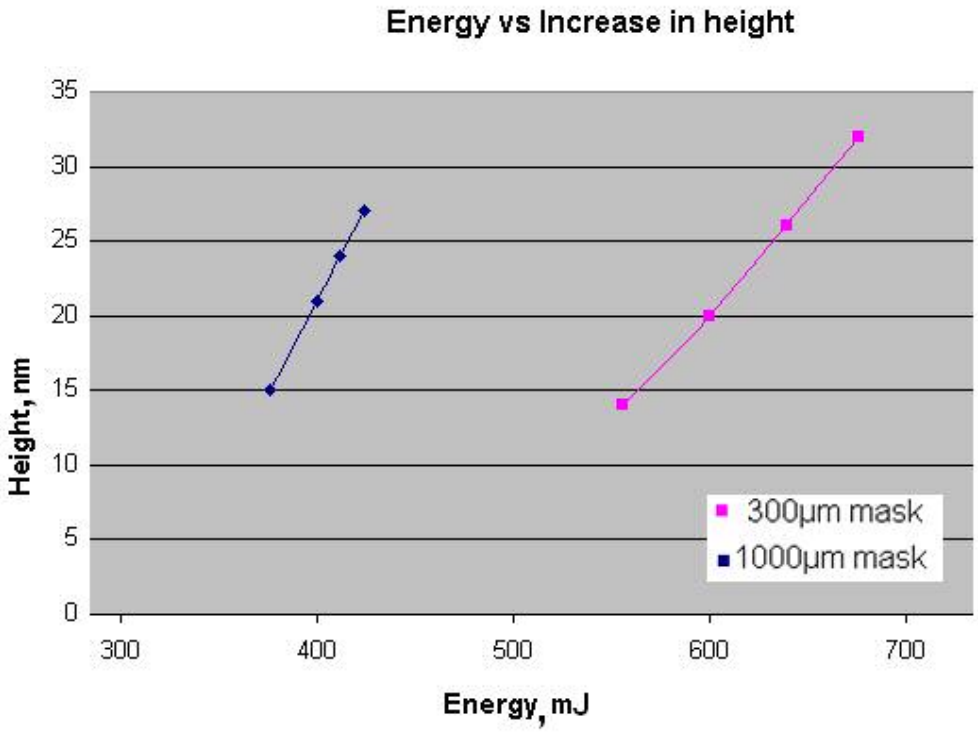

Fig 8.13 Variation of height with energy for two sizes of mask used.

3. Another interesting feature is observed when the numbers of loops are increased and the energy is kept constant. Experiments are conducted on borosilicate glass in air, under water, salt, sugar and methanol solution. For a fixed energy, the numbers of loops are increased and the response on borosilicate glass is observed.

It is observed that regardless of the medium, with increase in the number of loops the height increases. This process takes place till a fixed height is reached and then ablation starts taking place. The number of loops required for the material to get ablated decreases with increase in energy. For example, in dry machining with 1000 μm mask three loops are required for a material to get ablated at an energy of 376 mJ where as two loops are sufficient for an energy of 424 mJ.

Figures 8.14 to 8.16 show the surface of the material in air when subjected to one to three loops at energy of 376 mJ. At this energy, the height increases from 15 to 19 nm as the loops increase from one to two and then cracks start to develop. Also, improvement in surface finish is also observed. Figures 8.17 and 8.19 show similar process for energy of 424 mJ. The height observed for the first loop is 27 nm and cracks are formed for the second loop. This happens because with increase in number of loops, more photon energy is concentrated at the same spot and increased thermal ablation takes place. Another thing of importance is the height obtained. For the first loop at 376 mJ, it is 15 nm whereas the height obtained for 424 mJ energy is 27 nm. This is because higher energy means more amount of laser beam reaches the substrate resulting in faster built up and removal.

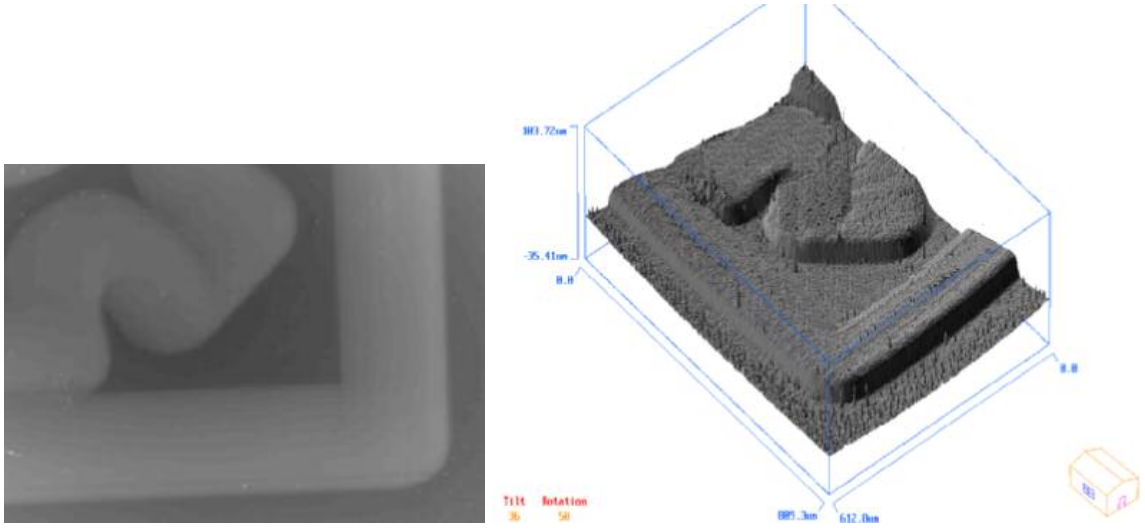

(a) (b)

Fig 8.14 (a) Top view (b) 3 D solid model of borosilicate glass subjected to energy of 376 mJ in air using 1000 µm mask for 1 Loop. Height formed is 15 nm.

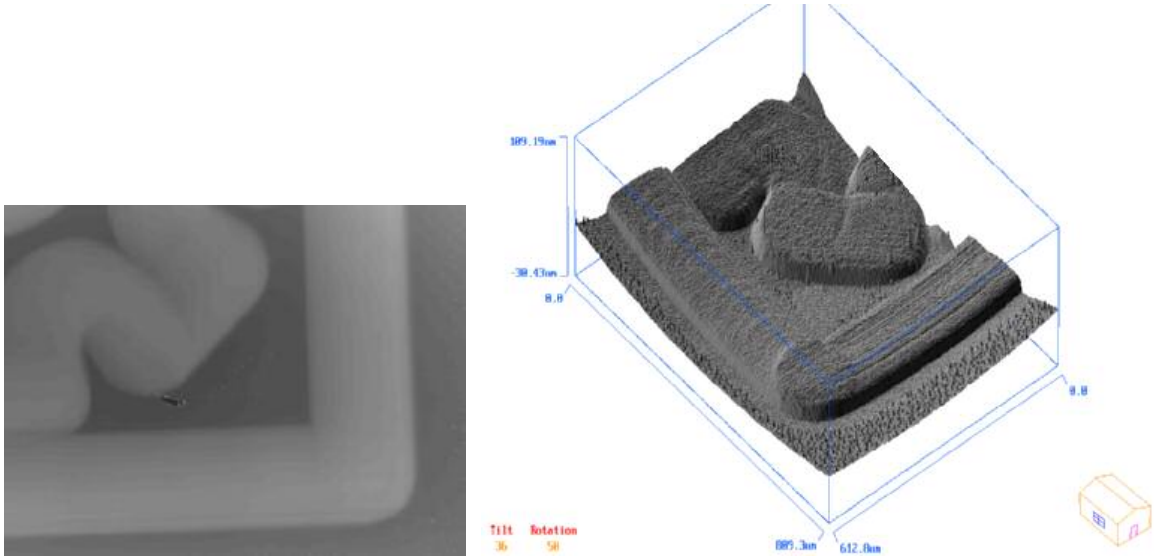

(a) (b)

Fig 8.15 (a) Top view (b) 3 D solid model of borosilicate glass subjected to energy of 376 mJ in air using 1000 µm mask for 2 loops. Height formed is 19 nm.

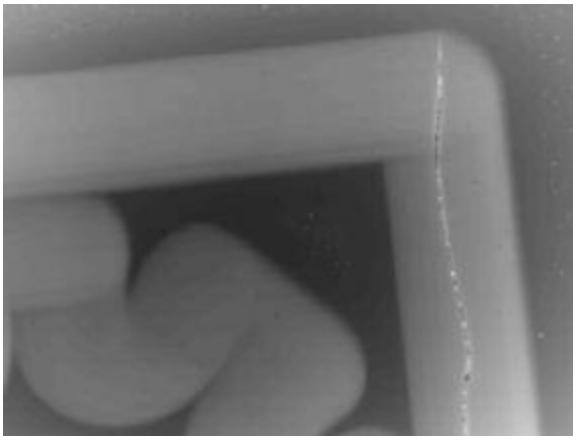

(a)

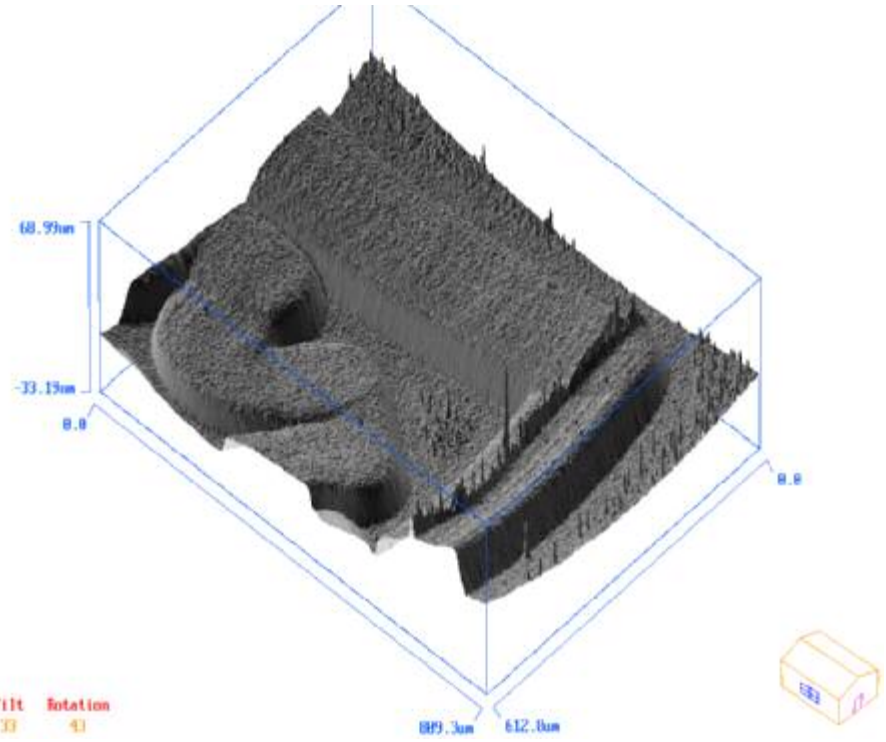

(b)

Fig 8.16 (a) Top view (b) 3 D Solid Model of borosilicate glass subjected to energy of 376 mJ in air using 1000 μm mask for 3 loops. Height formed is 19 nm with cracks.

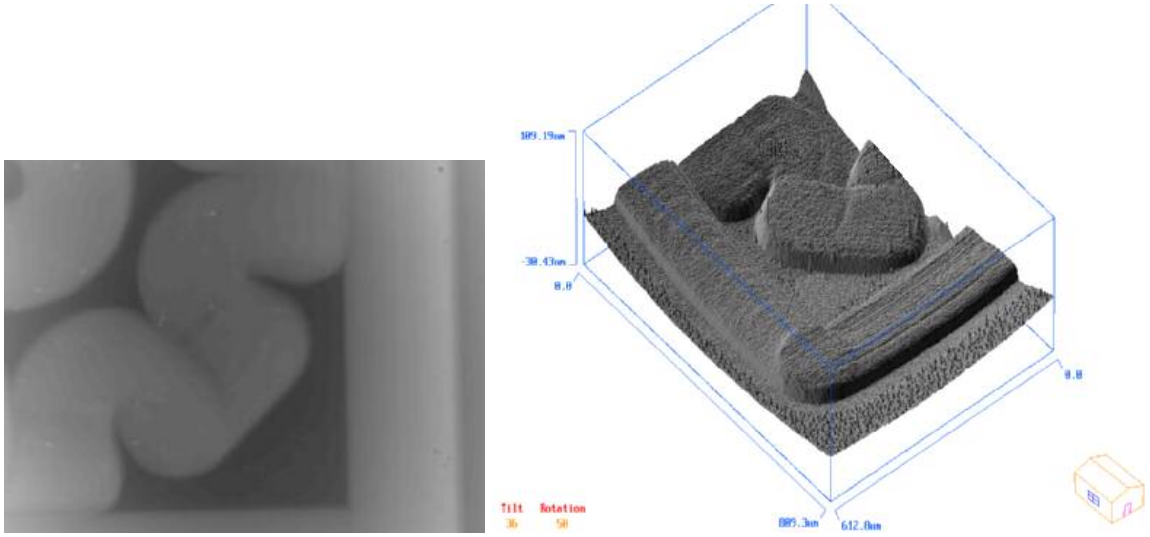

(a) (b)

Fig 8.17 (a) Top view (b) 3 D solid model of borosilicate glass subjected to energy of 424 mJ in air using 1000 µm mask for 1 loop. Height formed is 27 nm.

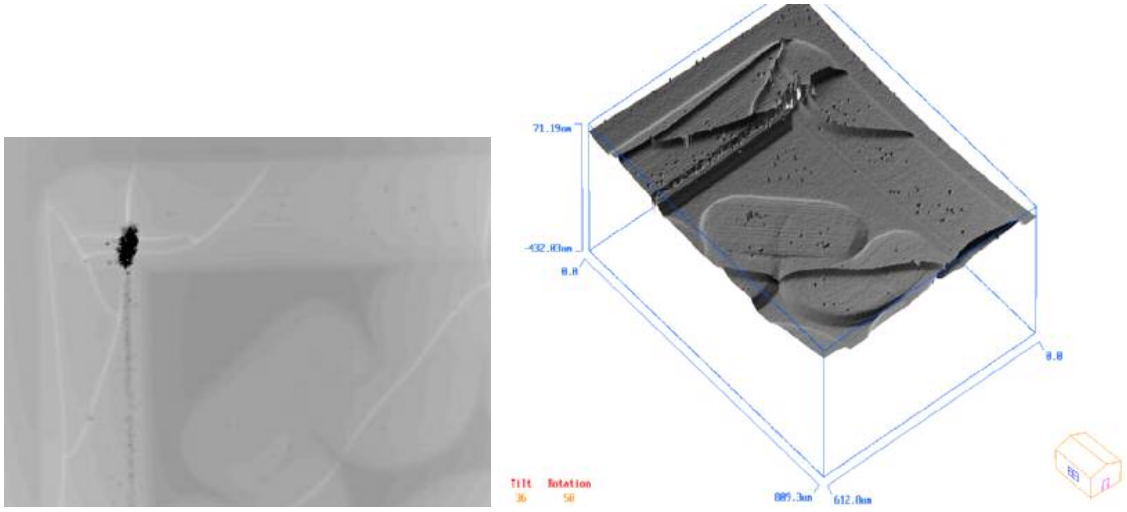

(a) (b)

Fig 8.18 (a) Top view (b) 3 D solid model of borosilicate glass subjected to energy of 424 mJ in air using 1000 µm mask for 2 loops. Height formed is 27 nm with cracks.

The results obtained are similar when the medium is replaced by distilled water. Figures 8.19 to 8.21 show the material built up t an energy of 436 mJ and Figures 8.22 to 8.25 show at energy of 480 mJ. For energy of 436 mJ, the height obtained in the first loop was 5 nm and it increased to 12 and 19 nm in the second and third loops. One thing that could be clearly observed is a very low built up height when the medium is water. The built up height at 436 mJ energy was 5 nm whereas in air, (with the other parameters same), the built up height obtained was 27 nm. This is because of the higher absorption properties of water. Laser beam gets absorbed by the water molecules before reaching the glass substrate. Thus lesser amount of beam reaches the substrate resulting in lesser built up height. Also, at 436 mJ energy no cracks are formed for a run of three loops where as cracks are observed for the same number of loops at 480 mJ energy. The reason for this is the increase in energy. At 480 mJ higher energy reaches the glass substrate resulting in a higher built up surface and cracks. These surfaces formed are uniform without any irregularities and could be extremely beneficial to the nano industry.

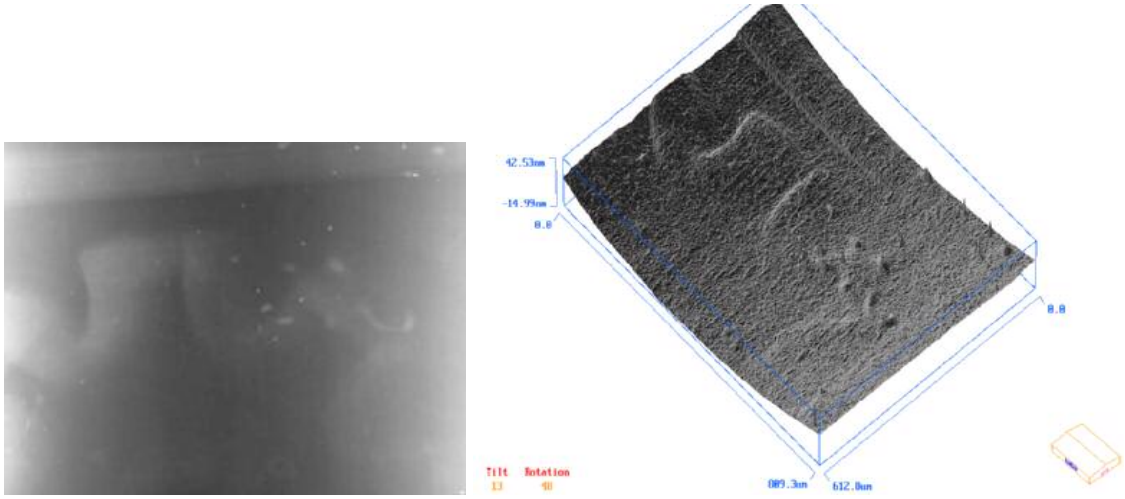

(a) (b)

Fig 8.19 (a) Top view (b) 3 D solid model of borosilicate glass subjected to energy of 436 mJ in distilled water using 1000 µm mask for 1 loop. Height formed is 5 nm.

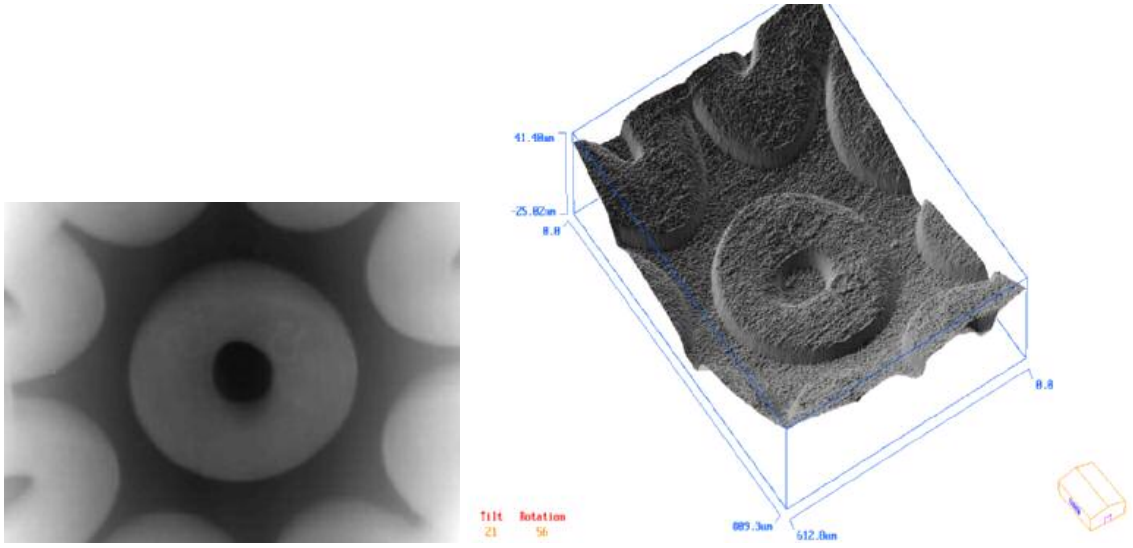

(a) (b)

Fig 8.20 (a) Top view (b) 3 D solid model of borosilicate glass subjected to energy of 436 mJ in distilled water using 1000 µm mask for 2 loops. Height formed is 12 nm.

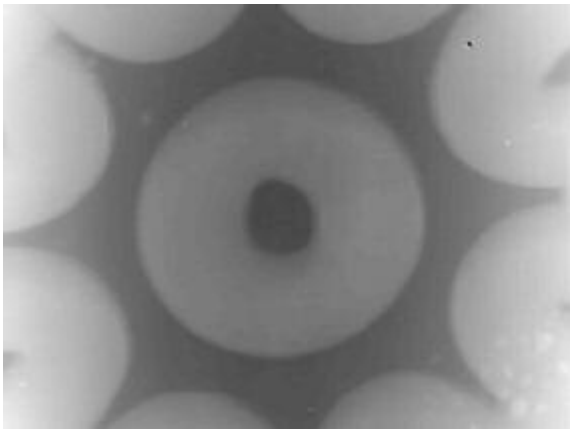

(a)

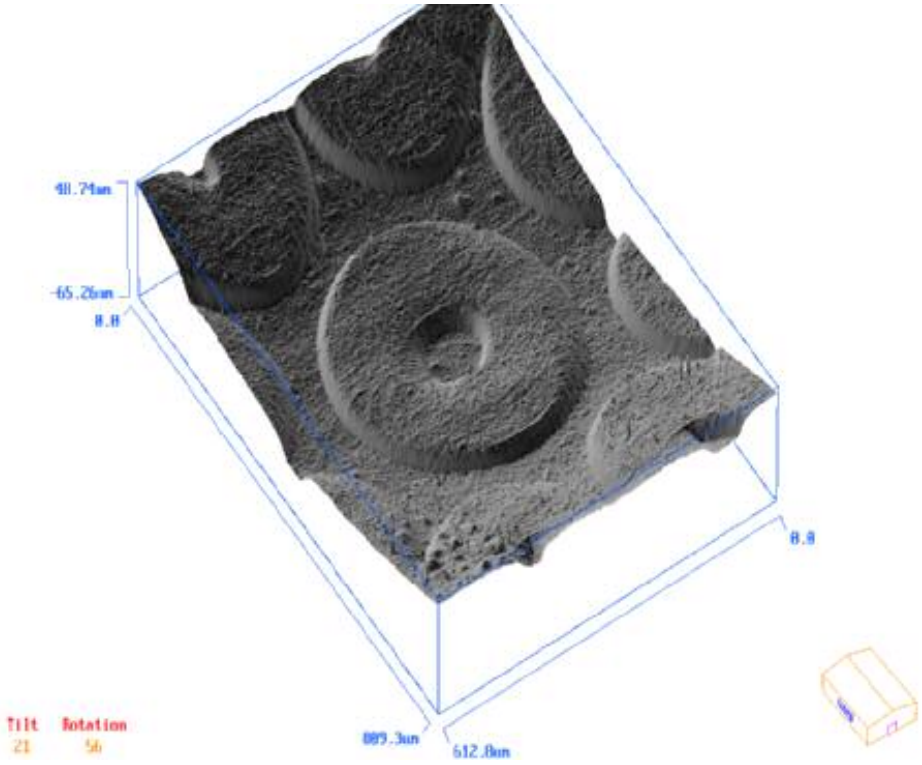

(b)

Fig 8.21 (a) Top view (b) 3 D solid model of borosilicate glass subjected to energy of 436 mJ in distilled water using 1000 µm mask for 3 loops. Height formed is 19 nm.

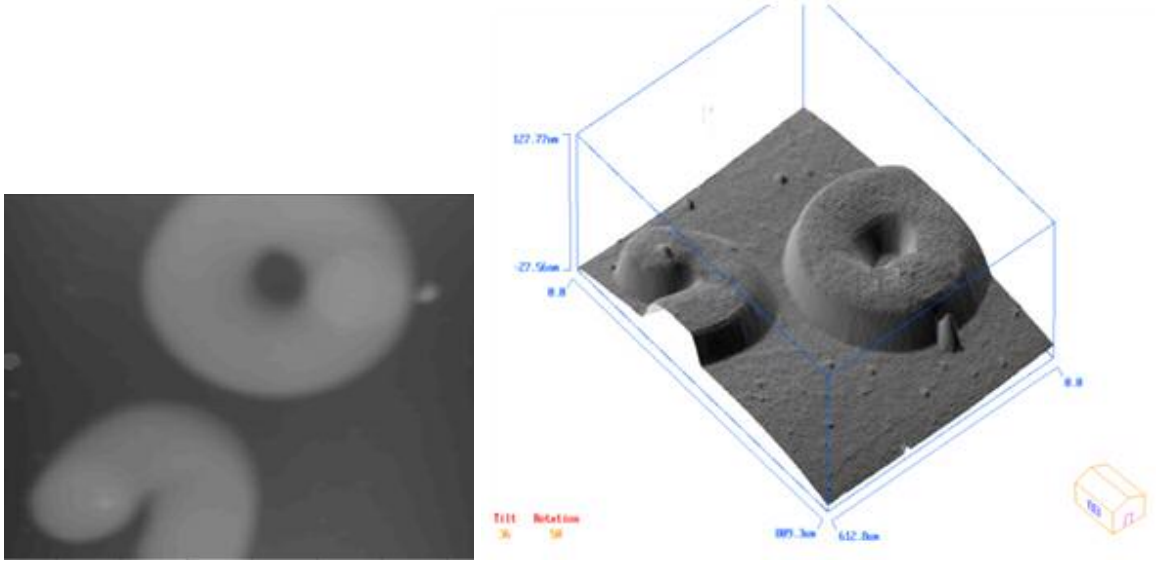

(a) (b)

Fig 8.22 (a) Top view (b) 3 D solid model of borosilicate glass subjected to energy of 480 mJ in distilled water using 1000 µm mask for 1 loop. Height formed is 18 nm.

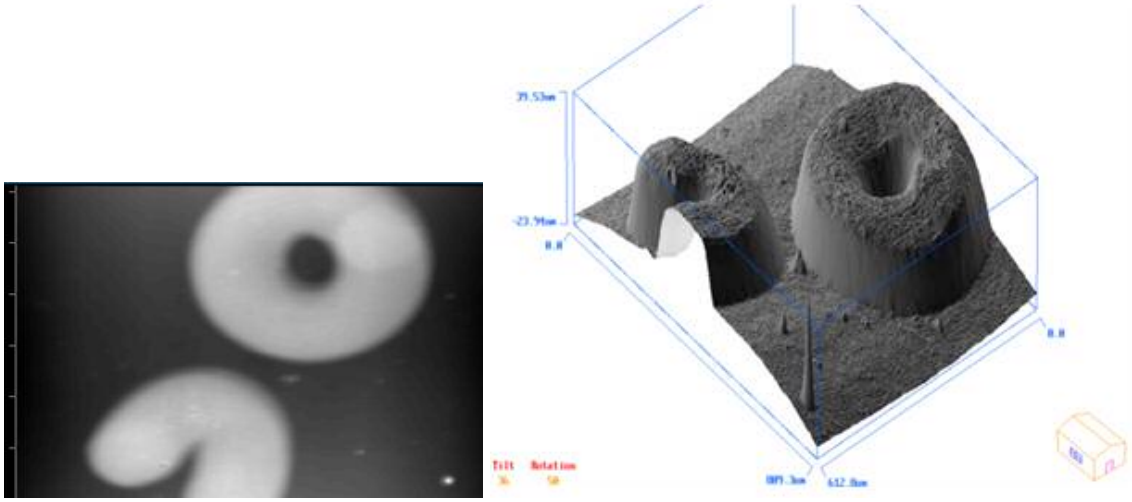

(a) (b)

Fig 8.23 (a) Top view (b) 3 D solid model of borosilicate glass subjected to energy of 480 mJ in distilled water using 1000 µm mask for 2 loops. Height formed is 24 nm.

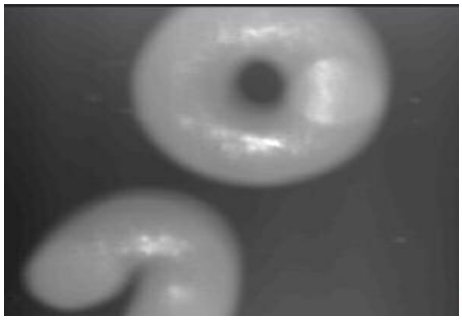

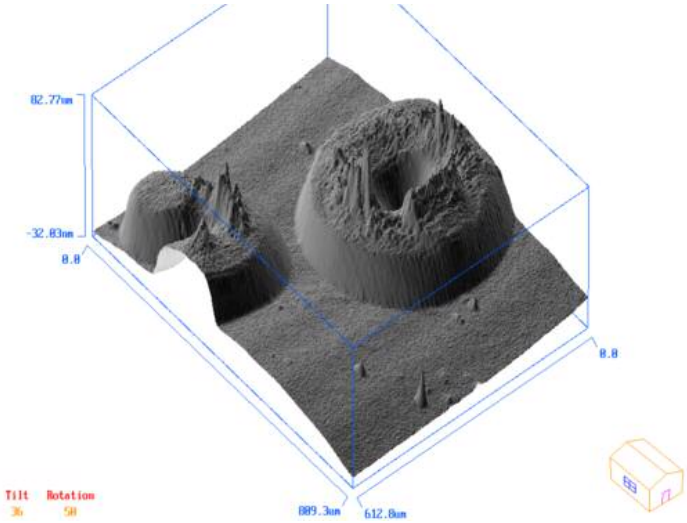

Fig 8.24 (a) Fig 8.24 (b)

Fig 8.24 (a) Top view (b) 3 D solid model of borosilicate glass subjected to energy of 480 mJ in distilled water using 1000 µm mask for 3 loops. Cracks just started.

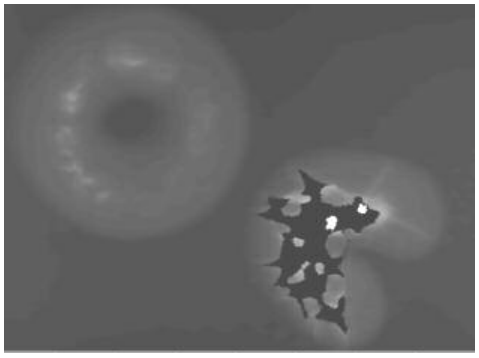

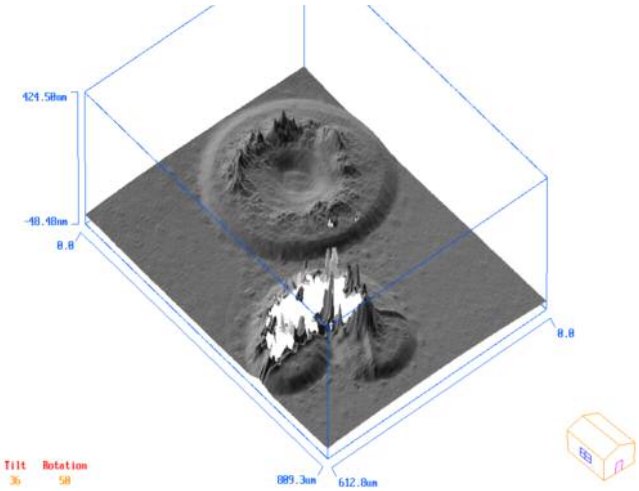

Fig 8.25 (a) Fig 8.25 (b)

Fig 8.25 (a) Top view (b) 3 D solid model of borosilicate glass subjected to energy of 480 mJ in distilled water using 1000 µm mask for 4 loops. Cracks observed.

The formation of smooth and uniform built up surfaces prompted a series of experiments in other media. Experiments are carried out by changing the medium to salt, sugar, and methanol solution. Figures 8.26 to 8.28 show the surface built up for one to three loops for salt solution (NaCl). In case of salt solution, the height of the built up surface at energy of 480 mJ is 15 nm compared to 18 nm of water. The reason for this is the presence of salt molecules present in the water. These molecules also absorb the laser energy in addition to the water molecules thus resulting in lesser built up height. Also the presence of salt molecules causes irregularities on the surface of the substrate and the obtained surface is not uniform compared to other media. This is because salt has a tendency to crystallize on the surface. Cracks start appearing from the second loop itself because of the crack formation tendency of salt solution. When salt dissolves in water, the salt molecules get split up into sodium and chlorine ions. Because of the higher corrosive nature of the chlorine ions, cracks result earlier in case of salt solution.

Figures 8.29 to 8.32 show the surface built up for sugar solution. In case of sugar solution, the height of the surface at energy of 480 mJ is 12 nm. The reason for the low height is the presence of sugar molecules. Since sugar do not change their molecular makeup in water, unlike the salt molecules, higher amount of laser beam falling on the substrate is absorbed leading to a lesser formed height. The topography of the substrate in the sugar solution is considered not as uniform as that of distilled water, but is smoother than that of salt solution.

When the medium is 25% methanol solution the built up surface is initially non uniform and uneven. The height obtained is 10 nm indicating higher absorption

properties of methanol. With increase in the number of loops, a uniform surface with a flat top surface is formed. This is because of the absence of any dissolved particles in the solution. Thus depending on the industrial application and energy available, built up surface as a result of under water or using methanol solution could be used. Figures 8.33 to 8.36 show the material built up for loops from one to four in case of methanol solution.

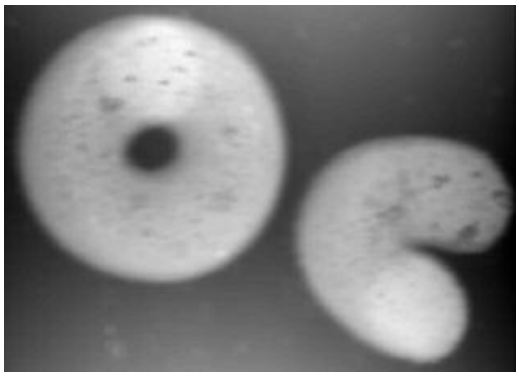

(a)

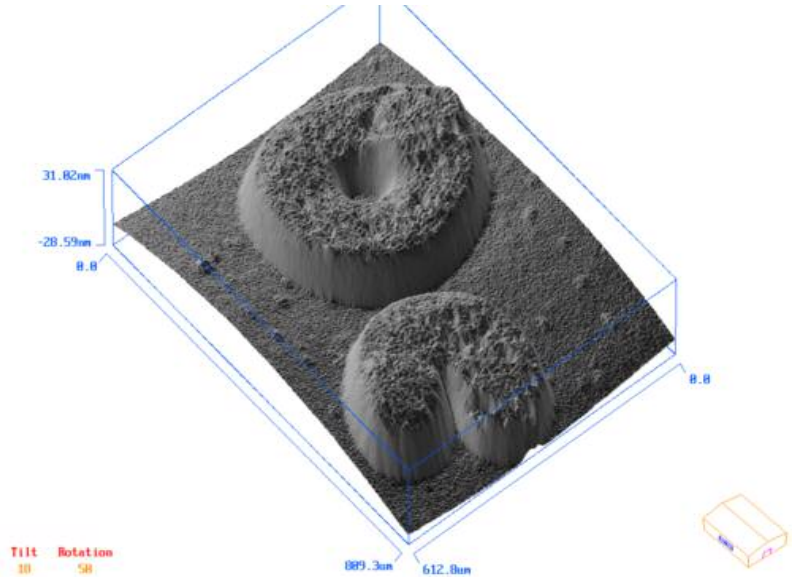

(b)

Fig 8.26 (a) Top view (b) 3 D solid model of borosilicate glass subjected to energy of 480 mJ in salt solution using 1000 µm mask for 1 loop. Height formed is 15 nm.

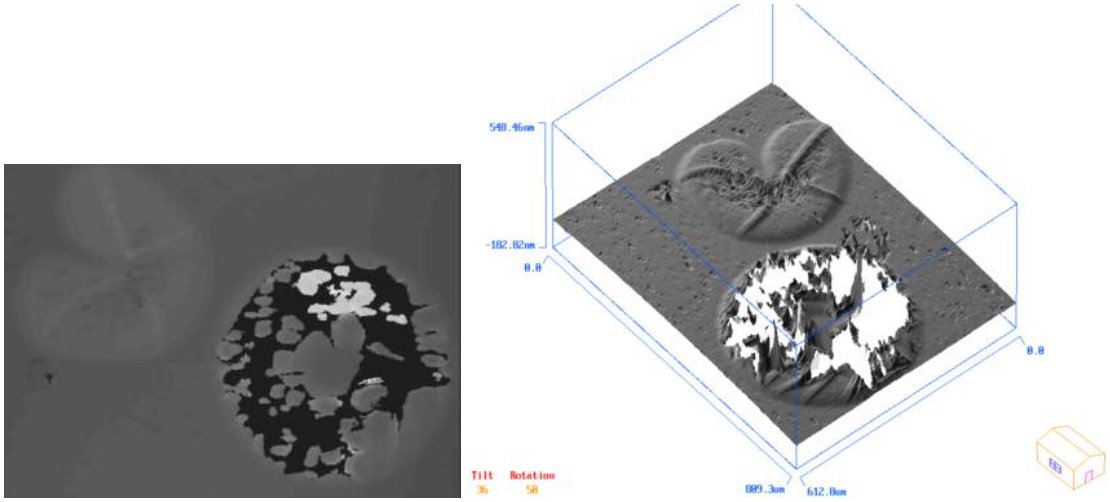

(a) (b)

Fig 8.27 (a) Top view (b) 3 D solid model of borosilicate glass subjected to energy of 480 mJ in salt solution using 1000 µm mask for 2 loops. Cracks Started.

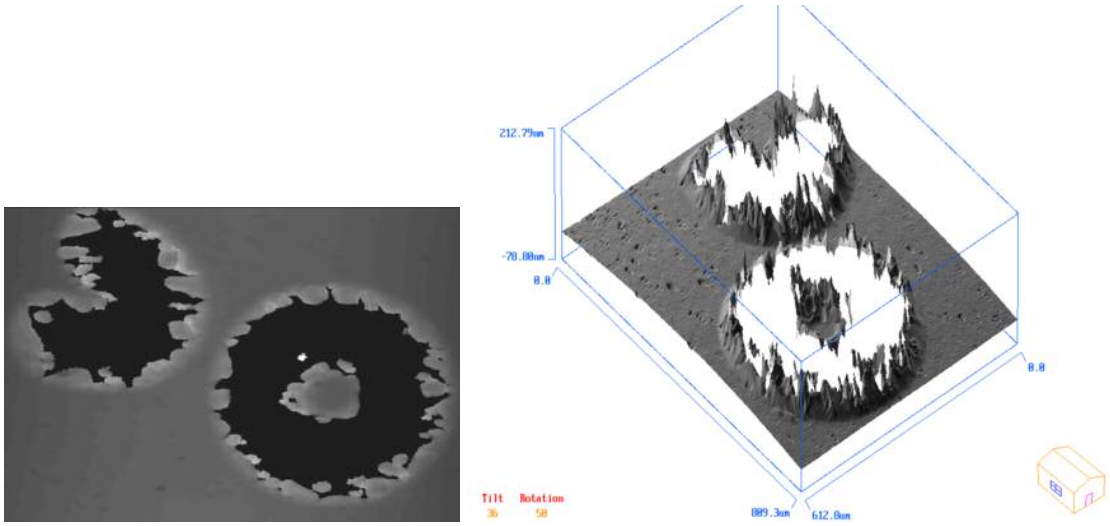

(a) (b)

Fig 8.28 (a) Top view (b) 3 D solid model of borosilicate glass subjected to energy of 480 mJ in salt solution using 1000 µm mask for 3 loops. Cracks Observed.

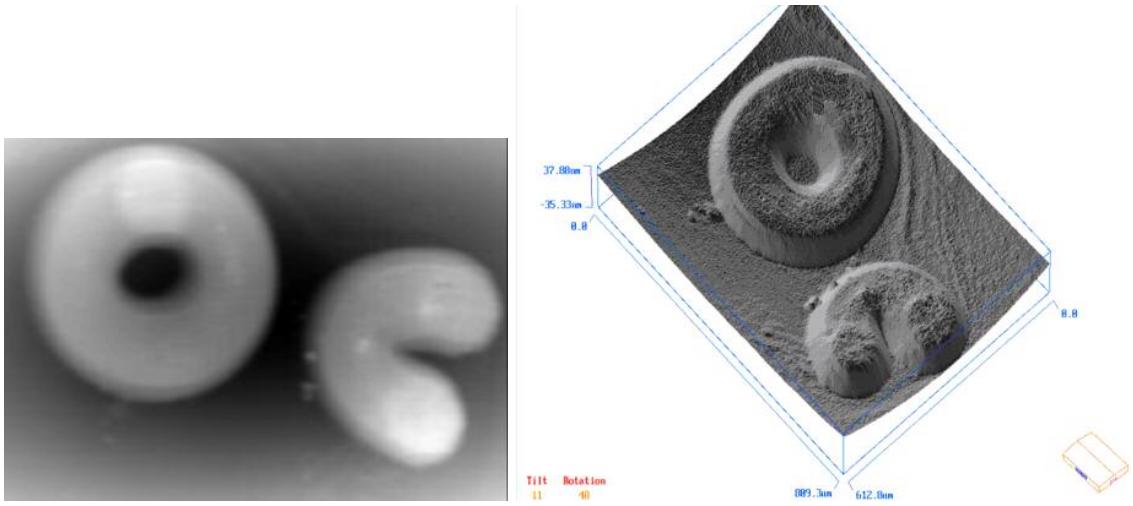

(a) (b)

Fig 8.29 (a) Top view (b) 3 D solid model of borosilicate glass subjected to energy of 480 mJ in sugar solution using 1000 µm mask for 1 loop. Height formed is 12 nm.

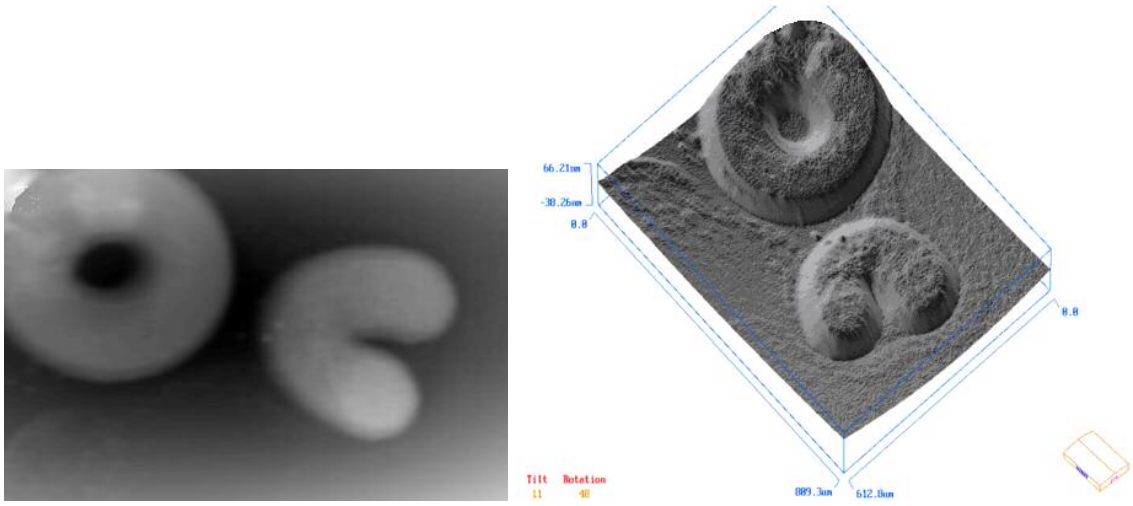

(a) (b)

Fig 8.30 (a) Top view (b) 3 D solid model of borosilicate glass subjected to energy of 480 mJ in sugar solution using 1000 µm mask for 2 loops. Height formed is 18 nm.

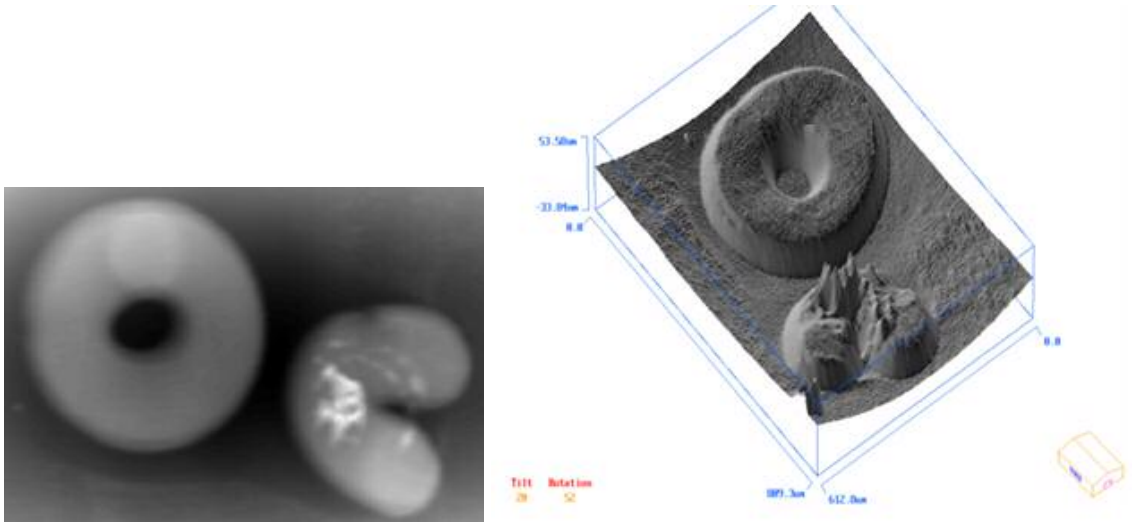

(a) (b)

Fig 8.31 (a) Top view (b) 3 D solid model of borosilicate glass subjected to energy of 480 mJ in sugar solution using 1000 µm mask for 3 loops. Cracks just started.

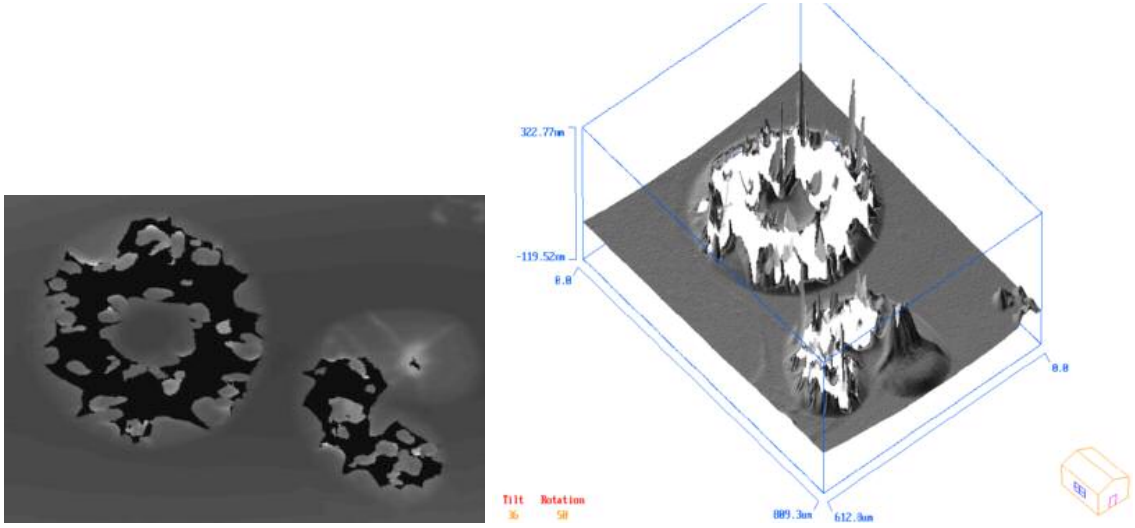

(a) (b)

Fig 8.32 (a) Top view (b) 3 D solid model of borosilicate glass subjected to energy of 480 mJ in sugar solution using 1000 µm mask for 4 loops. Cracks Observed.

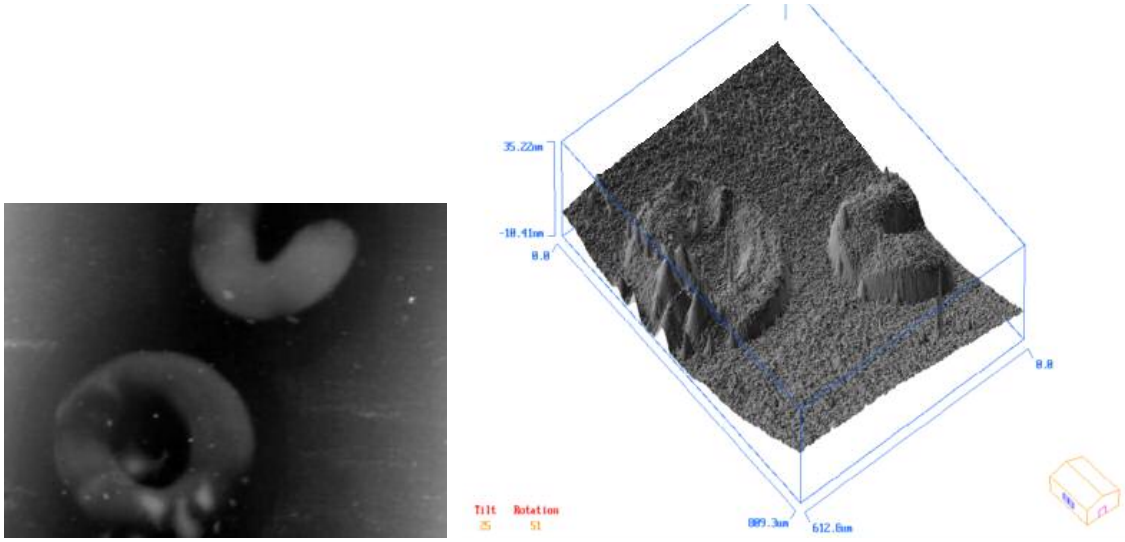

(a) (b)

Fig 8.33 (a) Top view (b) 3 D solid model of borosilicate glass subjected to energy of 480 mJ in methanol solution using 1000 µm mask for 1 loop. Height formed is 10 nm.

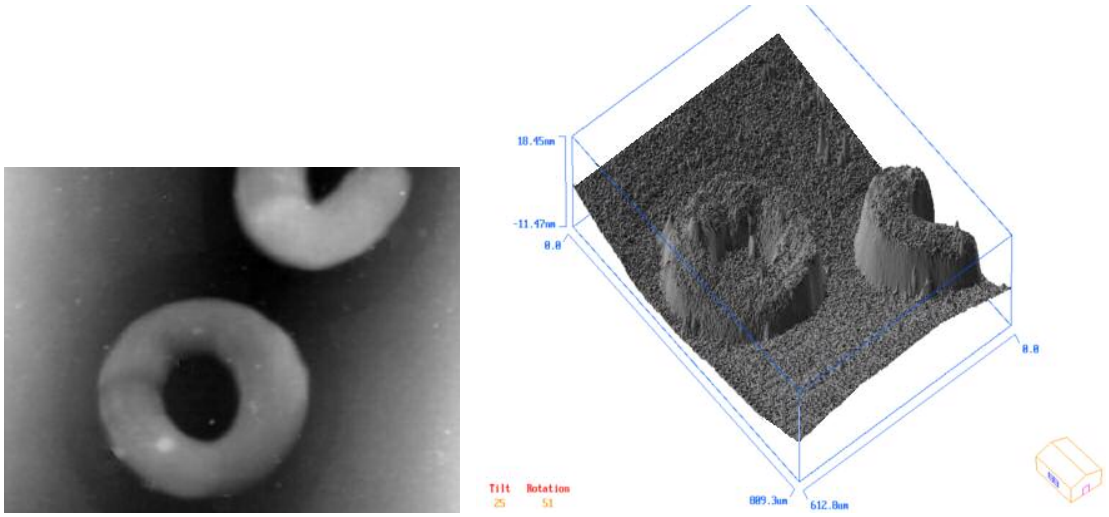

(a) (b)

Fig 8.34 (a) Top view (b) 3 D solid model of borosilicate glass subjected to energy of 480 mJ in methanol solution using 1000 µm mask for 2 loops. Height formed is 16 nm.

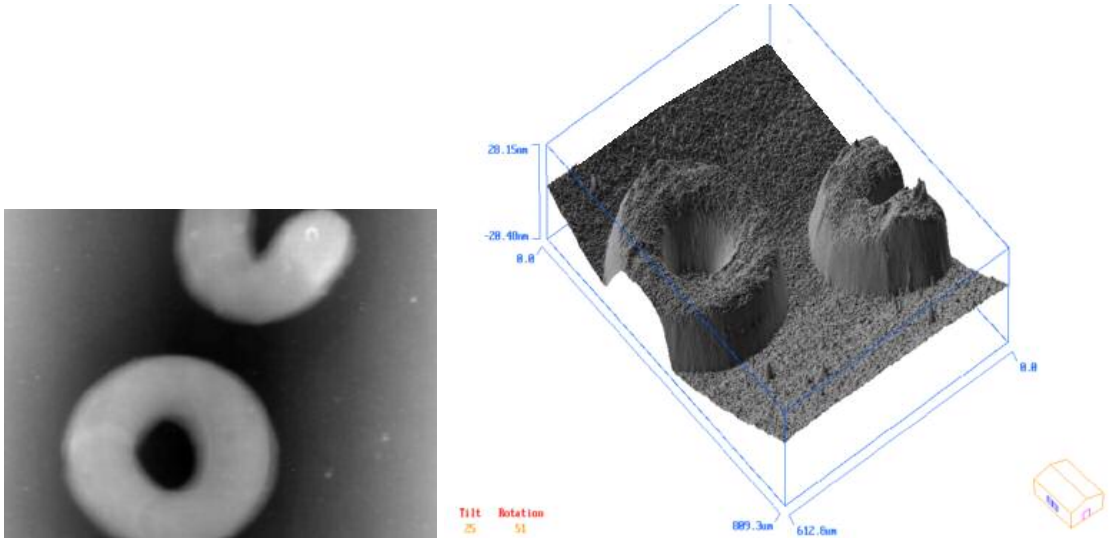

(a) (b)

Fig 8.35 (a) Top view (b) 3 D solid model of borosilicate glass subjected to energy of 480 mJ in methanol solution using 1000 µm mask for 3 loops. Height formed is 24 nm.

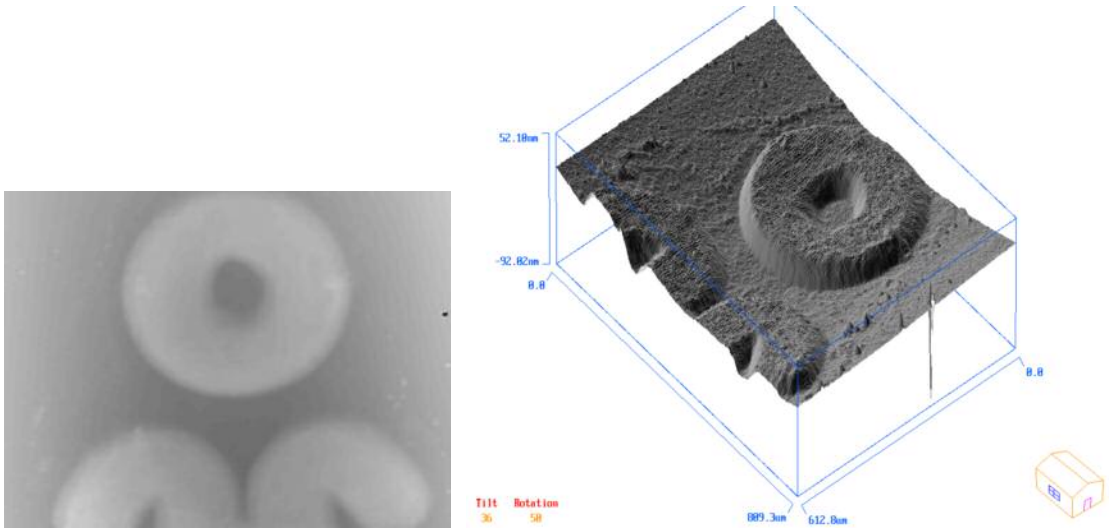

(a) (b)

Fig 8.36 (a) Top view (b) 3 D solid model of borosilicate glass subjected to energy of 480 mJ in methanol solution using 1000 µm mask for 4 loops. Height formed is 26 nm.

Table 8.1 Summary on the effect of various laser parameters on the built up surface of borosilicate glass for different media.

Type of medium	Energy Involved(mJ)	Number of loops	Height in nm
Air	376	1	15
		2	19
		3	19 with cracks
	424	1	27
		2	28 with cracks
Underwater	436	1	4-6
		2	12
		3	19
	480	1	18
		2	24
		3	Cracks started
25% methanol + 75% distilled water	480	1	10
		2	16
		3	24
		4	26
Under salt water	480	1	15
		2	Cracks started
		3	cracks
Under sugar water	480	1	12
		2	18
		3	Cracks started

The following observations can be made from Table 8.1. First, we can see that the energy required for the built up surface is lesser in air compared to other media. This is because of lower absorption properties of air compared to other media. Another thing that can be observed is the amount of built up height. Air, distilled water, and methanol have

built up surfaces ~25 nm whereas in salt and sugar solutions the built up observed is ~10 nm. One more thing that is evident is the crack formation. In methanol solution cracks did not form even when the number of loops are run from 1 to 4 whereas in salt solution the cracks are formed in the second loop itself. This indicates that methanol solution absorbs higher amount of laser energy and less amount reaches the substrate. The reason for the cracks in the salt solution is the presence of chlorine ions which gives an etching effect on the base material.

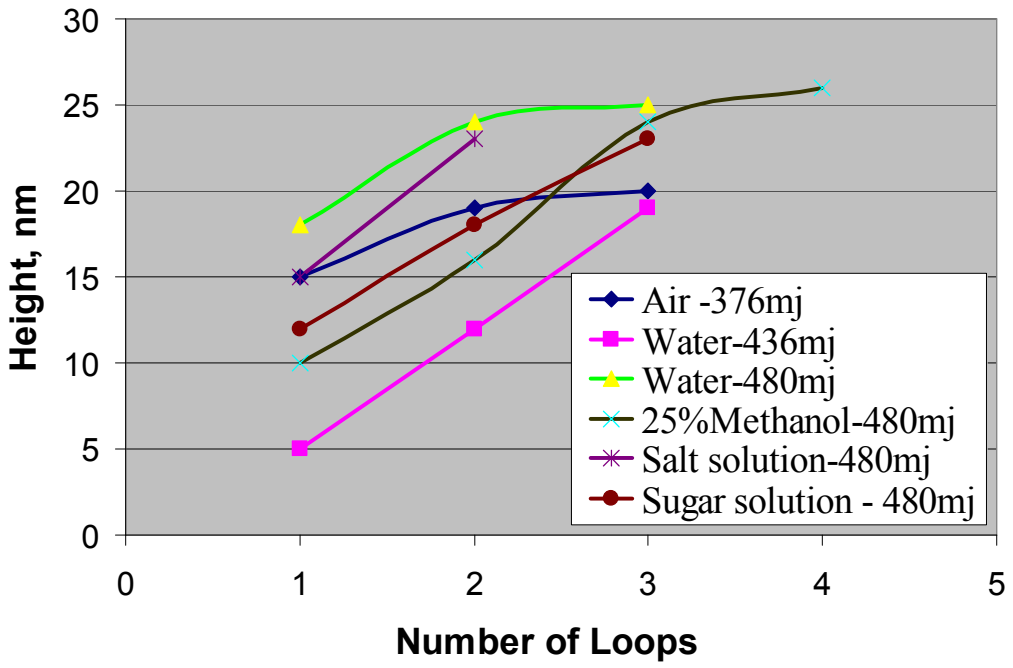

Fig 8.37 Increase in Loops vs. Height for different media.

Figure 8.37 shows an increase in height when the number of loops is increased for different media. The main thing that needs to be observed is the increase in height with the increase in number of loops. In some cases a linear increase in height is observed whereas in other cases the increase in height decreases with the number of loops. This decrease in height with the increase in number of loops indicates that the material has

reached that point and no further built up surface can be built by varying the parameters. Thus the increase in height first decreases and then rapid decrease in height is observed with the start of ablation.

Fig 8.38 shows the variation in height for different media at a constant energy of 480 mJ. It can be seen that at 480 mJ the built up height in nanometers is highest in case of water followed by salt, sugar and methanol solution. Thus, the effect of laser is higher in the case of water compared to the other media. Therefore, the process of surface built up followed by material removal takes place first in water prior to other media.

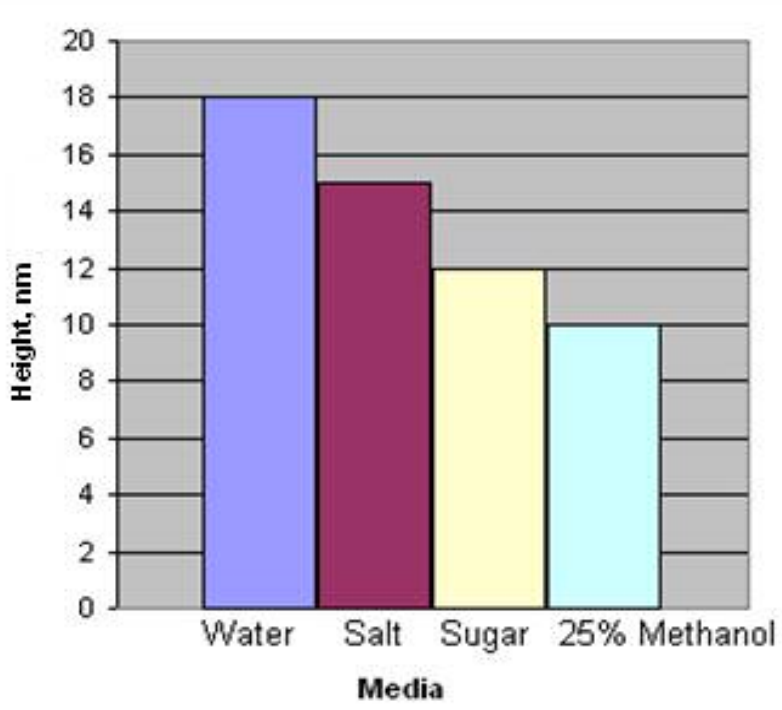

Fig 8.38 Variation of height for different media at constant energy (480 mJ)

CHAPTER 9

MICROMACHINING ON BOROSILICATE GLASS USING AN EXCIMER LASER

9.1 Introduction

Micromachining is the name given for the techniques used to produce structures and moving parts of microengineered devices. Silicon and glass micromachining have the most prominence, because micromachining has been applied to these materials more than other materials. Excimer lasers are used for micromachining because of their ability to micromachine a number of materials without heating them. Borosilicate glass generally results in cracks during conventional micromachining because of its brittle nature. Hence, care should be taken such that cracks resulting from this are negligible.

The experimental procedure used is similar to the one discussed in Chapter 8. The main difference is pulse energy and numbers of loops are higher for this case. Since micromachining follows material build-up, the energy and the number of loops are increased such that the material built up process is completed and micromachining takes place. Micromachining on borosilicate glass is also carried out in different media, such as air, under water, and polymer. The results and observations resulting from them are discussed in the following.

9.2 Results and Observations

First, borosilicate glass is subjected to excimer laser beam in air using a 1000 µm mask with energy of 536 mJ for 6 and 10 loops. The process is observed and Figures 9.1 and 9.2 show the interaction of the laser beam on glass. It can be observed that the periphery of the machined surface extends in the form of spikes. These spikes are on the order of a few hundred nanometers and not beneficial in the MEMS industry. Figures 9.1 and 9.2 show micromachining of borosilicate glass in air for 6 and 10 loops, respectively.

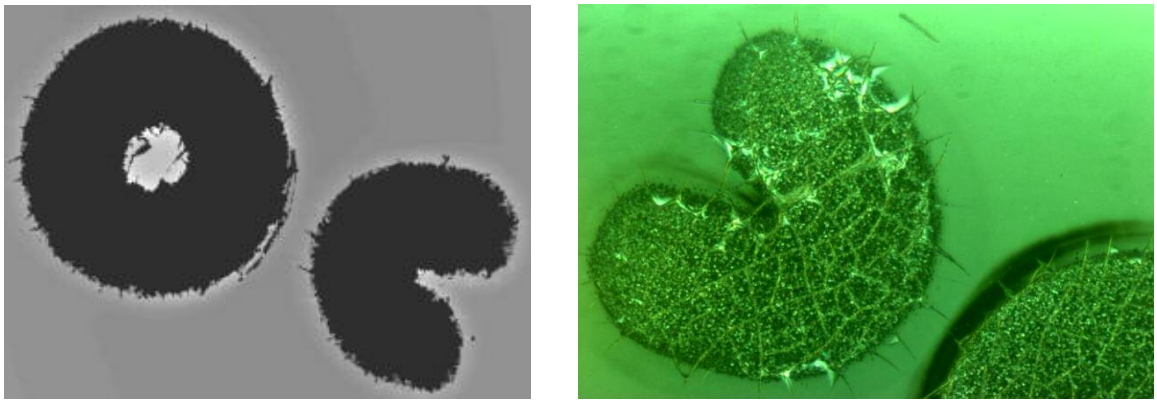

(a)

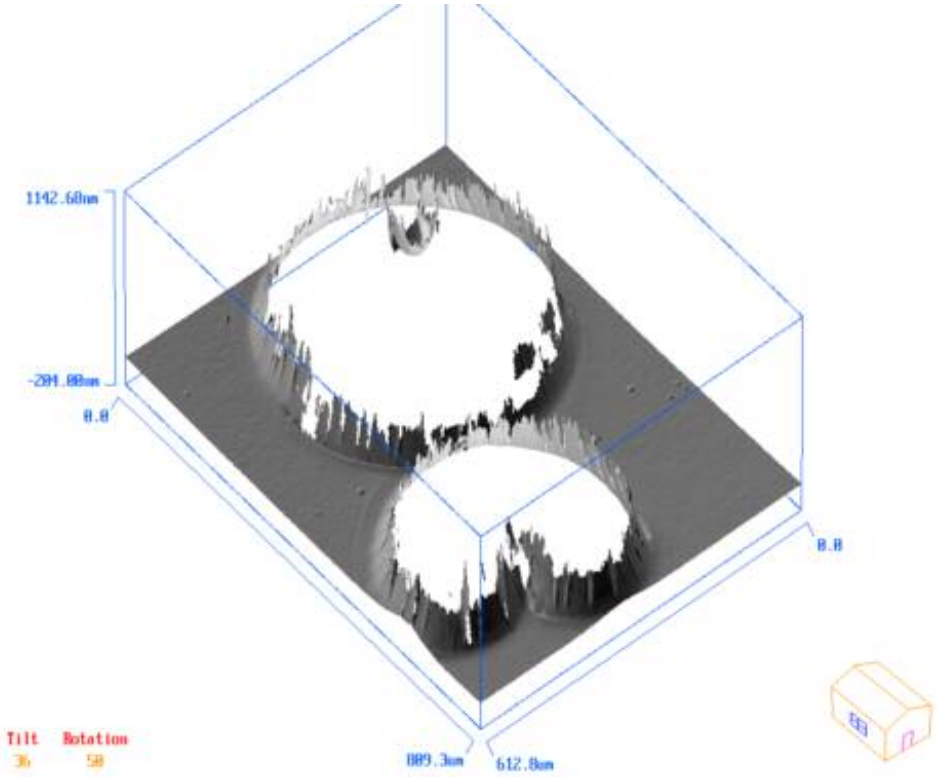

(b)

Fig 9.1 (a) Top view (b) 3 D solid model of borosilicate glass subjected to an energy of 536 mJ in air using 1000 µm mask for 6 loops.

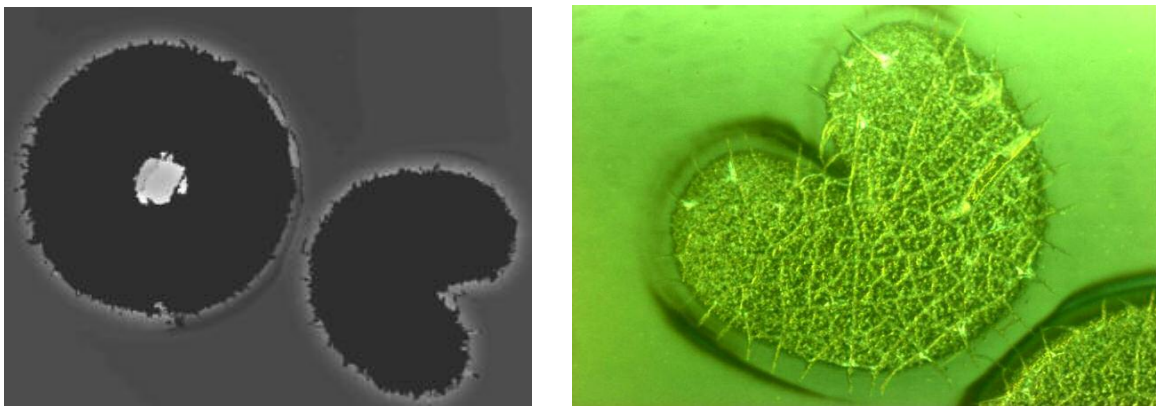

(a)

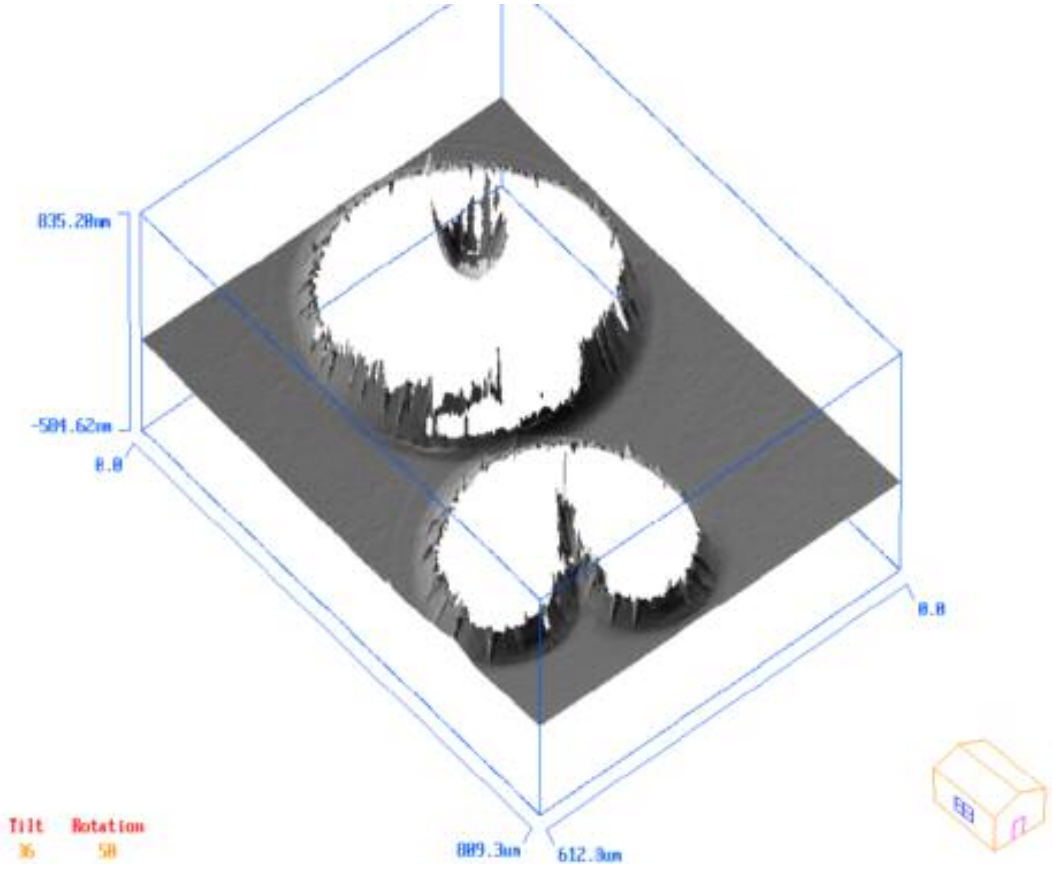

(b)

Fig 9.2 (a) Top view (b) 3 D solid model of borosilicate glass subjected to an energy of 536 mJ in air using 1000 µm mask for 10 loops.

Since micromachining of borosilicate glass in air results in the formation of spikes on the periphery, this process was extended to under water and under polymer. Figures 9.3 and 9.4 show micromachining of borosilicate glass under water. It can be seen that under water micromachining results in considerable cracks. The reason for the cracks is the tendency for crack formation and propagation in presence of a liquid media. Figure 9.3 shows micromachining of borosilicate glass under water for 10 loops.

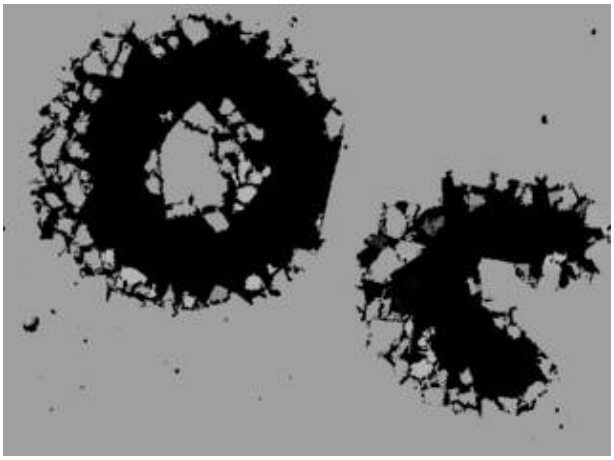

(a)

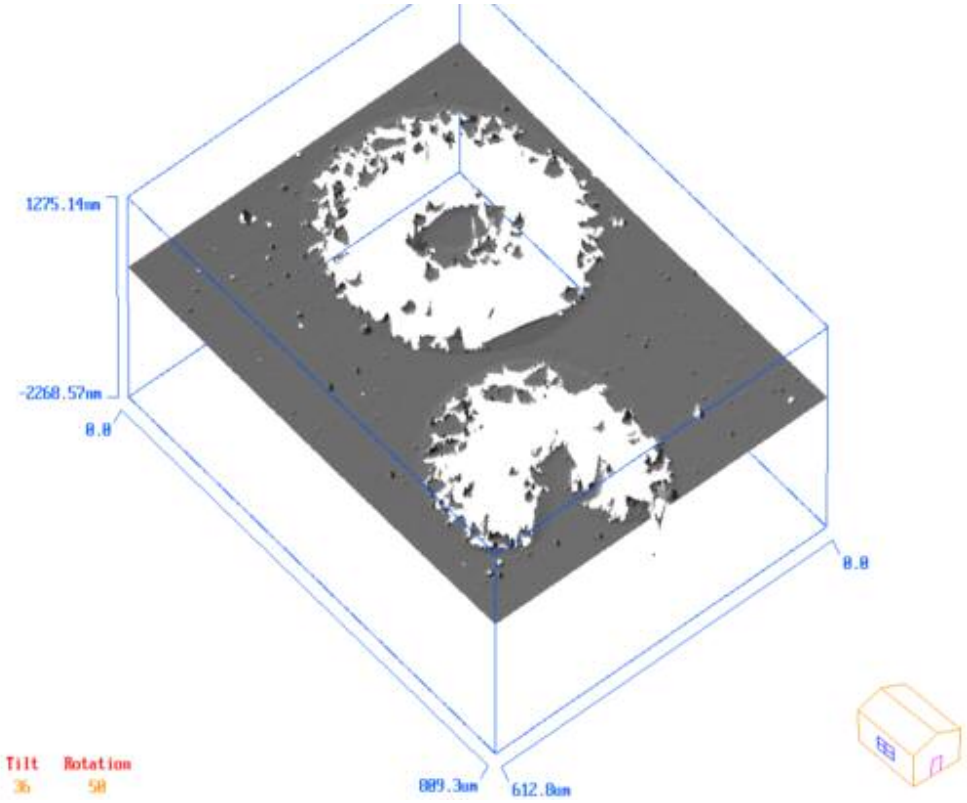

(b)

Fig 9.3 (a) Top view (b) 3 D solid model of borosilicate glass subjected to an energy of 536 mJ under water using 1000 µm mask for 10 loops.

In this process micromachining is performed on borosilicate glass by placing a polymer (OHP sheet) on top of it. The schematic of the experimental setup is shown in Fig 9.4.

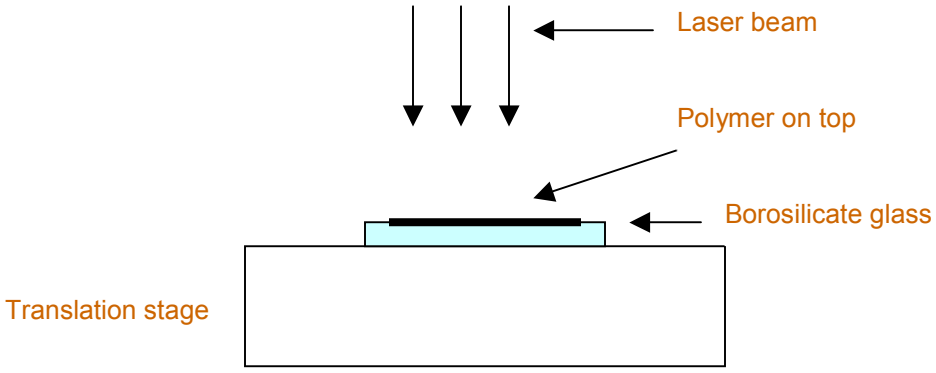

Fig 9.4 Schematic of the setup for micromachining underwater

Figure 9.5 shows micromachining of borosilicate glass under polymer. It can be seen that the number of spikes in the case of air and cracks in the case of water are absent in the case of micromachining under the polymer. Thus machining under a polymer is beneficial in the MEMS industry.

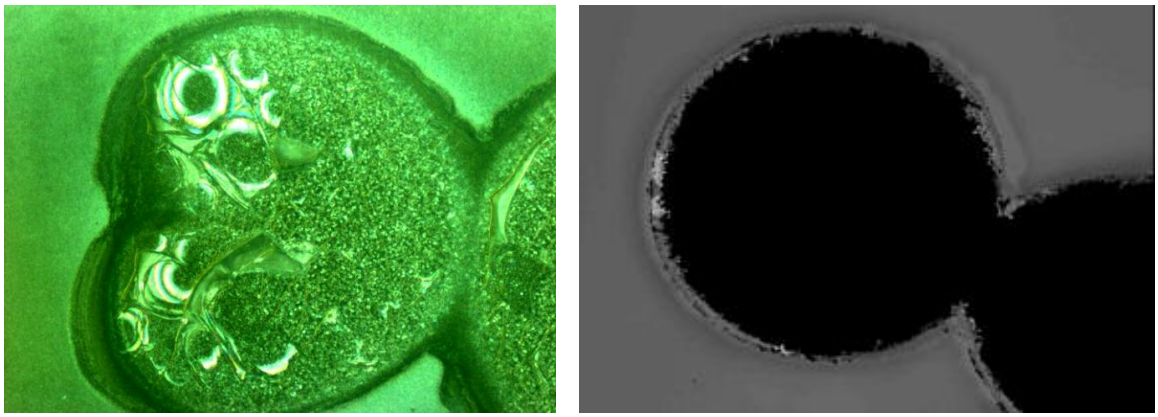

(a)

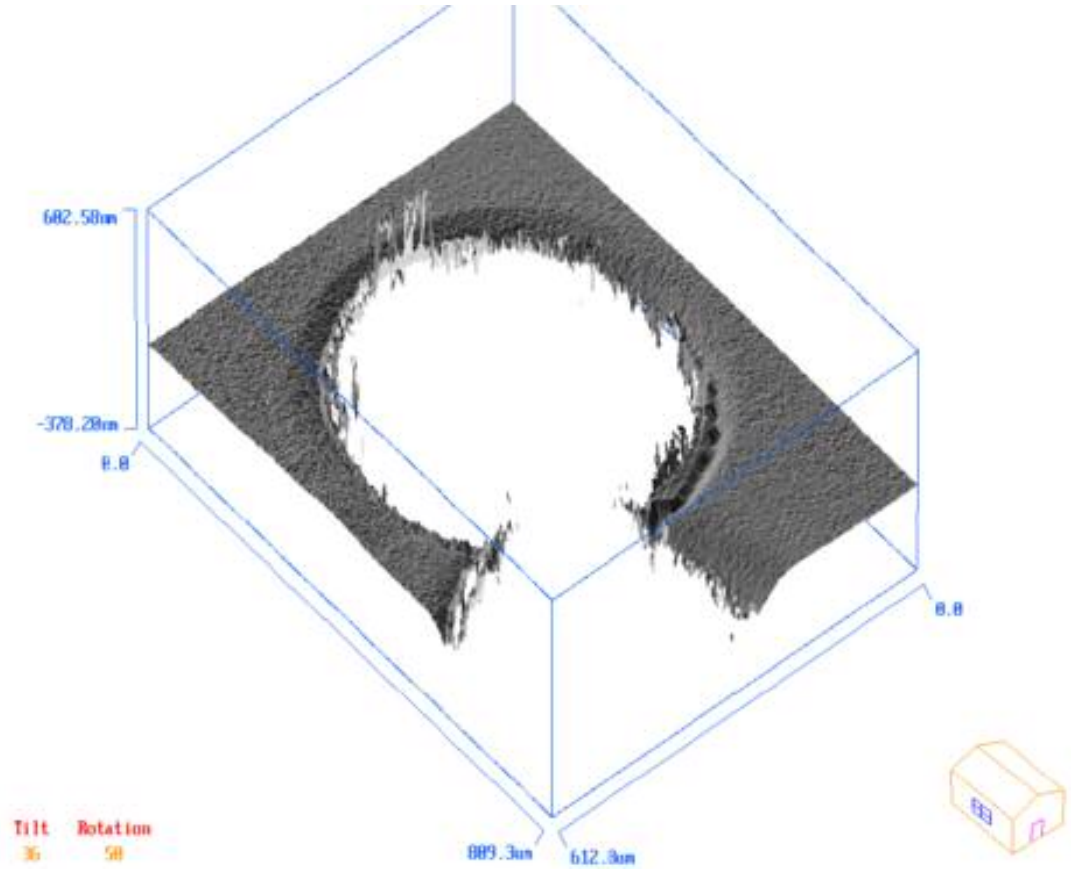

(b)

Fig 9.5 (a) Top view (b) 3 D solid model of borosilicate glass subjected to an energy of 536 mJ under polymer using 1000 μm mask for 10 loops.

Figures 9.6 to 9.9 show different circuits of MEMS which are fabricated by micromachining using an excimer laser on different materials.

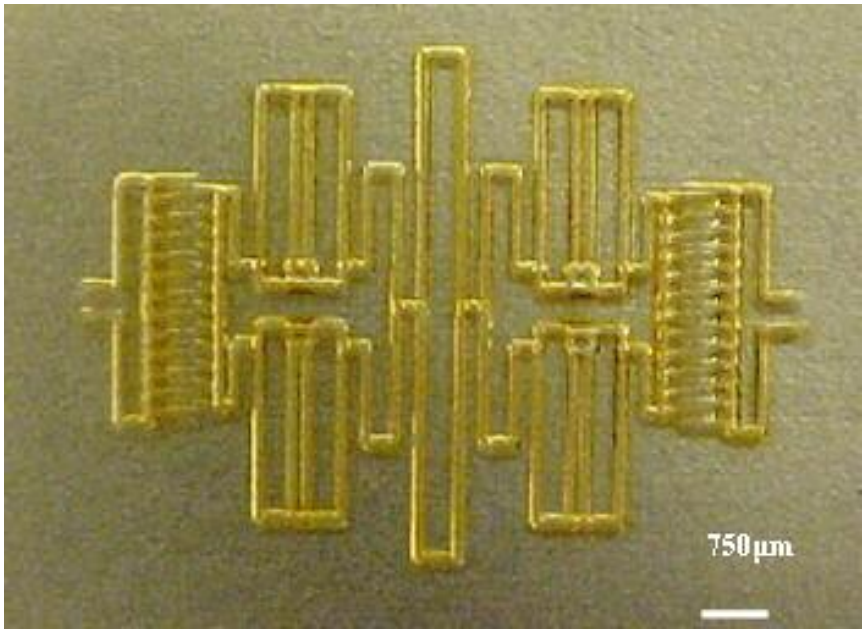

Fig 9.6 Surface machined for micro electro mechanical filter on PMMA polymer

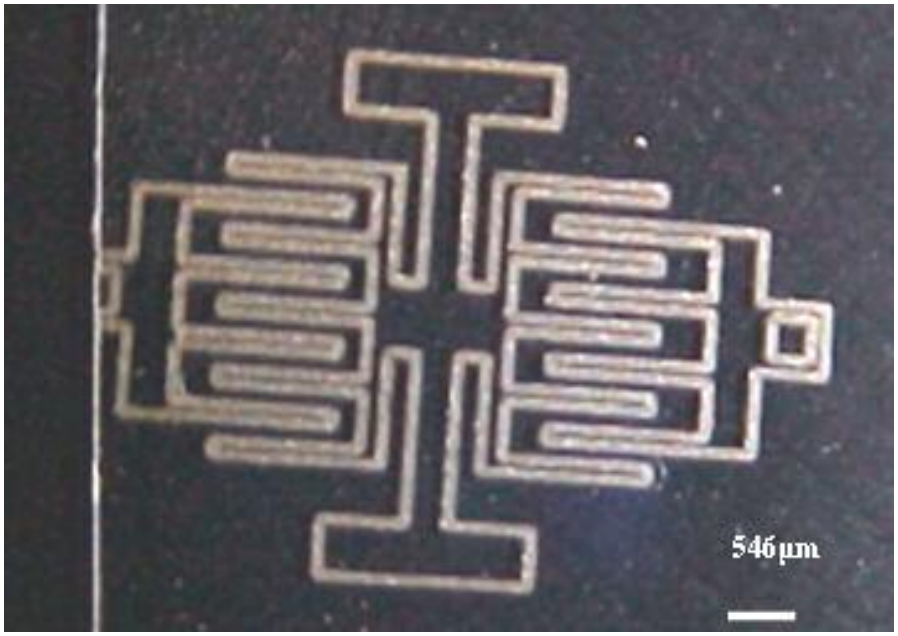

Fig 9.7 Layout of a lateral resonator on borosilicate glass

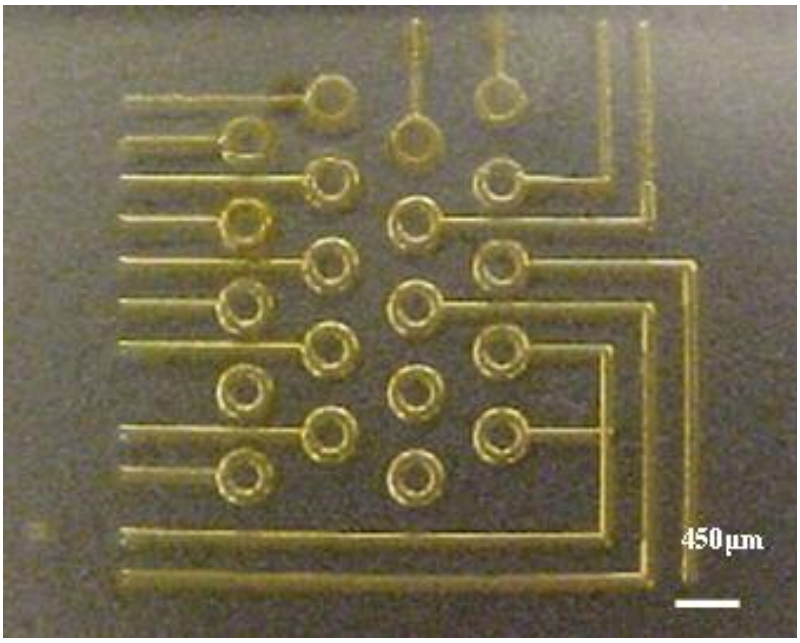

Fig 9.8 Integrated circuit on PMMA polymer

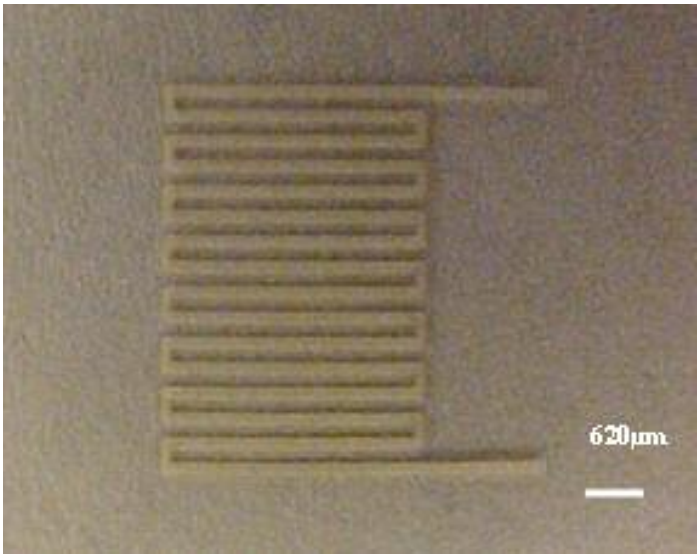

Fig 9.9 Temperature sensor on polymer (OHP sheet)

CHAPTER 10

CONCLUSIONS AND FUTURE WORK

10.1 Conclusions

The objective of this investigation is to obtain a material removal or material build up devoid of any cracks or deformation on different materials. Such a surface can be obtained by controlling various input parameters, such as the size of the mask, input energy, and media. Experiments were conducted on different geometries and the following are the main conclusions resulting from the experiments.

1. The final surface formed on borosilicate glass can be build up or material removal. The depth or height, thickness and uniformity of this surface can be controlled by various parameters, such as the size of the mask, input energy or pulse energy, different media, or number of loops.

2. Increasing the input energy increases the intensity of the laser thus facilitating a faster or higher material removal of the substrate.

3. By keeping the other parameters, such as energy, media and the work material constant, increasing the size of the mask allows for larger area of laser beam to fall on the substrate thus resulting in larger surface getting displaced but at a lower rate.

4. Increasing the number of loops results in laser impacting on the same place multiple times. The results obtained are similar to that of laser beam impinging with higher energy.

5. The thermal damage present in the case of air is almost absent when the micro machining process is conducted under different media solutions.

6. Debris resulting in case of micromachining is absent or carried away when machining under liquid solution.

8. Distilled water results in better material built up compared to water with sugar or salt dissolved in it.

9. Methanol, acetone, or toluene requires higher pulse energy for the built up process to take place.

10. Various circuits used in microelectromechanical systems (MEMS) are fabricated on glass and polymer surfaces.

10.2 Future work

This process of surface generation (material build up) is investigated taking borosilicate glass as the substrate. Further investigation can be done by extending it to different types of glasses and polymers. Different sizes of mask can be used to obtain a wider or more complex geometry. Also, the effect of different solutions can be investigated.

Laser deposition on samples, such as glass can be performed using pulse laser deposition (PLD) followed by micromachining

REFERENCES

1. Maiman, T.H., "The Laser Odyssey**,"** Laser Press, California (2000).
2. Townes, C.H., "How the Laser Happened," Oxford University Press, New York (2002).
3. Einstein, A., "Zur Quantentheorie der Strahlung" Physikalische Gesellschaft Zurich Mitteilungen Nr. 16(18) (1916) 47-62; an English translation appears in B.L. van der Waerden, ed., "Sources of Quantum Mechanics." North Holland, Amsterdam (1967).
4. Simon, Z., and K. Marvin, "Material Removal Rates of Biocompatible Polymers During Laser Ablation" Tamarack Scientific Co., California
5. Dyer, P. E. and J. Sidhu, "Excimer Laser Projection Micromachined Free-Standing Polymer Films," Dept. Appl. Phys. 6 (1985) 67-77.
6. Lutz, N. and M. Geiger, "Micromachining of ceramics with Excimer Laser Radiation," J. European Ceramic Society. 12 (1993) 315-321.
7. Lim, S. Y. and C.R. Chatwin, "Spatial Chaos Aspects of Laser Material Interaction," Optics and Lasers in Engineering. 20 (1994) 341-356.
8. Seddon, B. J., Shao, Y., Fost, J. and H. Girault, "The application of Excimer Laser Micromachining for the fabrication of disc microelectrodes," Electrochimica. 39 (6) (1994) 783-791.
9. Lutz, N., and S. Biermann, "Glass surface treatment with excimer and CO_2 lasers," Appl. Surf. Sci. 46 (1990) 430-434.
10. Zimmer, K., Hirsh, D., and F. Bigl, "Excimer laser machining for the fabrication of analogous microstructures," Appl. Surf. Sci. 96-98 (1996) 425-429.

11. Ihlemann, J., “Excimer laser ablation of fused silica,” Appl. Surf. Sci. 54 (1992) 193-200.

12. Fujii, T., Gotoh, Y. and S. Kuroyanagi, “Fabrication of micro diaphragm pressure sensor utilizing micro machining,” Sensors and Actuators A. 34(1992) 217-224.

13. Lutz, N., “Ablation of silicate glasses by laser irradiation: modeling and experimental results,” Appl. Surf. Sci. 54 (1992) 187-192.

14. Ihlemann, J. and B. Wolff-Rottke, “Excimer laser micro machining of inorganic dielectrics,” Appl. Surf. Sci. 106 (1996) 282-286.

15. Tseng, A. A., Chen, Y. T. and K. J. Ma, “Fabrication of high aspect ratio microstructures using excimer laser,” Optics and Lasers in Engineering 41 (2004) 827-847.

16. Ding, X., Kawaguchi, Y., Sato, T., Narazaki, A., Kurosaki, R. and H. Niino, “Micron- and submicron sized surface patterning of silica glass by LIBWE method,” Journal of photochemistry and photobiology A: Chemistry 166(2004) 129-133.

17. Zimmer, K., Braun, A. and R. Bohme, “Etching of fused silica and glass with excimer laser at 351nm,” Appl. Surf. Sci. 208-209 (2003) 199-204.

18. Zimmer, K. and R. Bohme, “The influence of the laser spot size and the pulse number on laser-induced backside wet etching,” Appl. Surf. Sci. 247 (2005) 256-261.

19. Zimmer, K. and R. Bohme, “Precise etching of fused silica for micro optical applications,” Appl. Surf. Sci. 243 (2005) 415-420.

20. Dyer, P. E., Karnakis, D.M., Key, P.H. and J.P. Tait, “Excimer Laser ablation of low and high index polymers,” Appl. Surf. Sci. 96-98 (1996) 596-600.

21. Jackson, S.R., Methiringham, W.J. and P.E. Dyer, “Excimer laser ablation of Nd: YAG and Nd:glass,” Appl. Surf. Sci. 86 (1995) 223-227.

22. Dyer, P. E., Farley, R.J., Giedl, R. and D.M. Karnakis, “Excimer Laser ablation polymers and glasses for grating fabrication,” Appl. Surf. Sci. 96-98 (1996) 537-549.

23. Chen, Y. T., Ma, K.J., Tseng, A.A. and P.H. Chen, “Projection ablation of glass based single and arrayed microstructures using excimer laser,” Optics and Laser Technology 37 (2005) 271-280.

24. Sanchez, F., Aguiar, R., Serra, P., Varela, M. and J.L. Morenza, “Study of material emission in ArF and KrF excimer laser ablation of yttria stabilized zirconia single crystals,” Thin Solid Films 317 (1998) 108-111.

25. Laurens, P., Bouali, M. O., Meducin, F. and B. Sadras, “Characterization of modifications of polymer surfaces after treatments below the ablation threshold,” Appl. Surf. Sci. 154-155 (2000) 211-216.

26. Laude, L.D., Martinez, D., Dicara, Cl., Hanus, Fr. and K. Kolev, “The ablation of polymers under excimer laser irradiation: the physics of the process and the polymer structure,” Nuclear Instruments and Methods in Physics Reseacrh B 185 (2001) 147-155.

27. Suzuki, M., Yamaguchi, M., Ramonat, L. and X. Zeng, “Effect of polymer addition and temperature on the structure of silicon-based polymer fimls deposited by excimer laser ablation of hexaphenyldisilane,” Journal of photochemistry and photobiology A: Chemistry 145(2001) 223-228.

28. Kruger, J., Niino, H. and A. Yabe, “Investigation of excimer laser ablation threshold of polymers using a microphone,” Appl. Surf. Sci. 197-198 (2002) 800-804.

29. Vanagas, E., Mizuyama, A., Koshihara, S. and H. Misawa, “Glass cutting by femtosecond pulsed irradiation,” Journal of Microlithography, Microfabrication, and Microsystems, Volume 3 Issue 2, April 2004 Pages 358-363.

30. Keiper, B., Horst, E., Udo, L. and K. Thomas, “Drilling of glass by excimer laser mask projection technique,” Journal of laser applications, Volume 12 Number 5, October 2000, Pages 189-193.

31. Ben-Yakar, A. and R.L. Byer, "Femtosecond laser ablation properties of borosilicate glass," Journal of Applied Physics, Volume 96 Number 9, November 2004, Pages 5316-5323.

32. Ben-Yakar, A. and R.L. Byer, "Morphology of femtosecond-laser-ablated borosilicate glass surfaces," Applied Physics Letters, Volume 83 Number 15, October 2003, Pages 3030-3032.

33. Yue, T.M., Mei, S.M. and K.C. Chan, "Excimer laser ablation of glass fiber in reinforced polymer" Materials and Manufacturing Processes , Volume 17 Number 6, 2002, Pages 783-788.

34. Zhang, J., Sugioka, K. and K. Midorikawa, "Micromachining of glass materials by laser-induced plasma-assisted ablation (LIPAA) using a conventional nanosecond laser" Proceedings of SPIE, the international society for optical engineering, Volume 3618, 1999, Pages 363.

35. Choo, K.L., Ogawa, Y., Kanbargi, G., Otra, V., Raff, L.M. and R. Komanduri, R "Micromachining of silicon by short pulse laser ablation in air and under water," Materials science and Engineering A 372 (2004) 145-162.

36. Kopitkovas, G., Lippert, T., David, C., Wokaun, A. and J. Gobrecht, "Fabrication of micro-optical elements in quartz by laser induced backside wet etching," Microelectronic Engineering 67-68 (2003) 438-444.

37. Vass, Cs., Hopp, B., Smausz, T. and F. Ignacz, "Experiments and numerical calculations for the interpretation of the backside wet etching of fused silica," Thin Solid Films 453-454 (2004) 121-126.

38. Boulmer-Leborgne, C., Hermann, J. and B. Dubreuil, "Plasma formation resulting from the interaction of a laser beam with the solid metal target in an ambient gas," Plasma Sources Sci. Technol.2 (1993) 219-226.

39. Balandin, Yu, V., Otte, D., and O. Bostanjoglo, "Thermocapillary Flow Excited by Focused Nanosecond Laser Pulses in Contaminated Thin Liquid Iron Films," J. Appl. Phys. 78 (1995) 2037-2044.

40. Estler, R. C., and N. G. Nogar, "Mass Spectroscopic Identification of Wavelength Dependent UV Laser Photoablation Fragments From Polymethylmethacrylate," Appl. Phys. Lett. 49 (18) (1896) 1175-1177.

41. Ho, J. R., Grigoropoulos, C.P., and J.A.C. Humphrey, "Computational Study of Heat Transfer and Gas dynamics in the Pulsed Laser Evaporation of Metals," J. of Applied Physics 78(7)(1995) 4696-4709.

42. Kim, D., and C. P Grigoropoulos., "Phase Change Phenomenon and Acoustic Transient generation in Pulsed Laser Induced Ablation of Absorbing Liquids," App. Surf. Sci. 127-129 (1998) 53-58.

43. Navarrete, M., Muniz, M. V., Ponce, L., and T. Flores, "Photoacoustic Detection of Microcracks induced in BK7 Glass by Focused Laser Pulses," Optics and Lasers in Engg 40 (2003) 5-11.

44. Peyre, P., Fabbro, R., Merien, P. and H. P. Lieurade, "Laser Shock Processing of Aluminum Alloys. Application to High Cycle Fatigue Behavior," Mat. Sci Eng. A A210 (1996) 102-113.

45. Brannon, J. H., Lankard, J. R., Baise, A. I., Burns, F., and J. Kaufman, "Excimer Laser Etching of Polyimide," J. Appl. Phys. 58 (5) (1985) 2036-2043.

46. Wang, J., Niino, H., and Akira Yabe, "Micromachining of Transparent Materials with Super-heated Liquid generated by Multiphotonic Absorption of Organic Molecule," App. Surf. Sci 154-155 (2000) 571-576.

47. Li, C., and S.Nikumb, "Optical Quality micromachining of Glass with Focused Laser-produced Metal Plasma Etching in the Atmosphere," Applied Optics 42 (2003) 2383-2387.

48. Peyre, P., Berthe, L., Scherpereel, X., Fabbro, R., and E. Bartnicki, "Experimental Study of Laser-Driven Shock Waves in Stainless Steel," J. Appl. Phys. 84 (1998) 5985-5992.

49. Guthrie, R. I. L., and T. Iida, "Thermodynamic Properties of Liquid Metals," Mater. Sci. Eng. A A178 (1994) 35-41.

50. Choo, K.L, "Micromachining using an Excimer (248 nm) laser," MS thesis, School of Mechanical and Aerospace Engineering, Oklahoma State University, Stillwater, OK (2004).

51. Kanbargi, G, "Micromachining of Borosilicate Glass and Laser Induced Backside Wet Etching of Quartz using an Excimer Laser (248 nm)," MS thesis, School of Mechanical and Aerospace Engineering, Oklahoma State University, Stillwater, OK (2005).

52. "The UNIDEX 500 Motion Controller and Windows Software Operation & Technical Manual," Version 1.2, Aerotec, Inc.

53. "The ATS 100 Series Position Stages Instruction Manual," Version 1.0, Aerotech, Inc.

54. Corman, T., Enoksson, P., and G. Stemme, "Deep wet etching of borosilicate glass using an anodically bonded silicon substrate as mask," Journal of Micromechanics and Micro engineering. 8 (1998) 84-87.

55. Bien, D.C.S., Rainey, P.V., Mitchell, S.J.N., and H.S. Gamble, "Characterization of masking materials for deep glass micromachining," Journal of Micromechanics and Micro engineering. 13 (2003) S34-S40.

56. Argument, M., Tsui, Y., Fedosejevs, R., Li, J., and P. Herman, "Drilling and Micromachining of Glasses with UV and VUV Laser Pulses," Department of Electrical and Computer Engineering, University of Alberta, Edmonton, AB T6G 2V4, Canada.

57. Chung, C.K., Lin, Y.C., and G.R. Huang, "Bulge Formation and improvement of the polymer in CO_2 laser micromachining," Journal of Micromechanics and Micro engineering. 15 (2005) 1878-1884

58. Jensen, M.F., Kruhne, U., Christensen, L.H., and O. Geschke, "Refractive microlenses produced by excimer laser irradiation of poly (methyl methacrylate)," Journal of Micromechanics and Micro engineering. 15 (2005) 91-97

59. Yang, C., Hsieh, Y., and G. Hwang, "Refractive microlenses produced by excimer laser irradiation of poly (methyl methacrylate)," Journal of Micromechanics and Micro engineering. 14 (2004) 480-489

60. Ghantasala, M.K., Hayes, J.P., Harvey, E.C., and D.K. Sood, "Patterning, electroplating and removal of SU-8 moulds by excimer laser micromachining Journal of Micromechanics and Micro engineering. 11 (2001) 133-139

61. Li, J., and G.K. Ananthasuresh, "A quality study on the excimer laser micromachining of electro-thermal-compliant micro devices. 11 (2001) 38-47

62. Winburn, D.C., "What Every Engineer should know about Lasers," Marcel Dekker, Inc., New York (1987).

63. Hecht, J. and D. Teresi, "Laser, Supertool of the 1980's," Ticknor and Field, New York (1982).

64. Hecht, J., "Understanding Laser," Howard W. Sam & Company Hayden Books, California (1990).

65. Chryssolouris, G., "Laser Machining: Theory and practice," Springer – Verlag, New York (1991).

66. Ready, J.F., "Lasers in Modern Industry," Society of manufacturing Engineering, Dearborn, Michigan, (1979).

67. McGeough, J.A., "Advanced Methods in Machining," Chapman and Hall, London and New York (1988).

68. Waver, L.A., "Machining and Welding Applications," Laser Applications Vol. 1, Academic Press, New York and London (1971) 579-602.

69. Carlaw, H.S., and J.C. Jaeger, "Conduction of Heat in Solids," 2nd edition, Oxford university Press, Oxford (1959).

70. Ready, J.F. and D.F. Farson, "LIA Handbook of Laser Material Processing," 1st edition, Laser Institute of American (2001).

71. Phillipe, B., C., William and S. Ali, "Introduction to Micromachining Handbook," Version 2.2, Clark-MXR, Inc. (2001).

VITA

Jilludimudi Surya Supradeep

Candidate for the Degree of

Master of Science

Thesis: MICROMACHINING AND SURFACE BUILD-UP ON BOROSILICATE GLASS USING EXCIMER LASER

Major Field: Mechanical Engineering

Biographical:

Personal data: Born in Visakhapatnam, Andhra Pradesh, India, on August 10, 1981, the son of Prasad Rao and Dhanalakshmi Jilludimudi.

Education: Received Bachelor of Technology degree in Mechanical Engineering from Jawaharlal Nehru Technological University, Hyderabad, India in August 2002.Completed the requirements for the Master of Science degree with a major in Mechanical and Aerospace Engineering at Oklahoma State University in December 2005.

Experience: Graduate Research Assistant in the School of Mechanical and Aerospace Engineering, Oklahoma State University, Stillwater, Oklahoma, Feb 2004 - present

Name: Jilludimudi Surya Supradeep Date of Degree: December, 2005

Institution: Oklahoma State University Location: Stillwater, Oklahoma

Title of Study: MICROMACHINING AND SURFACE BUILD-UP ON BOROSILICATE GLASS USING EXCIMER LASER

Pages in Study: 107 Candidate for the Degree of Master of Science

Major Field: Mechanical Engineering

Scope and Method of Study:

Micromachining is advancing rapidly for numerous nanotechnology applications. It is an enabling technology for the production of micro-electro-mechanical-systems (MEMS). Borosilicate glass, owing to its several desirable properties, such as electrical insulation, resistance to many chemicals, and transparency at certain wavelengths finds a number of applications in microsensor and microactuator technologies. The main feature this glass requires now is ability to be shaped for MEMS components to the required size and surface finish. Since conventional machining techniques result in microcracks in such brittle materials as borosilicate glasses, in this investigation, laser micromachining is used. Material build-up and material removal result when an excimer laser beam impinges a borosilicate glass surface. The material build up features are studied by systematic investigating various input parameters, such as input energy, size of the mask and the media used to obtain desirable shape and quality. In surface machining (material removal) of borosilicate glass experiments were conducted such that the cracks formed on the periphery of the machined surface are minimal. Also, several geometries used in MEMS applications on glass and polymers were fabricated.

Findings and Conclusions:

The machined surfaces and the surfaces formed are examined using optical and laser interference microscopes (MicroXam). It can be concluded that the resultant surface on borosilicate glass could either be a built up or ablated surface. The type of surface observed depends mainly on the input energy provided from the excimer laser. Various other factors that effect the material built up are the mask, media and the number of loops. Good material built-up, on the order of 25 to 35 nm was obtained for 1 mm mask when tests were conducted in air, distilled water, and methanol. Thus by controlling of various parameters, material built up of uniform height was obtained. It is also found that borosilicate glass results in fewer number of cracks when machining under polymer compared to machining in air, or under water. Thus it can be concluded that good surface finish with minimal number of cracks can be obtained in micromachining under polymers.

ADVISOR'S APPROVAL: Dr. Ranga Komanduri